Title
The Role of Landscape Heterogeneity in Urban Runoff Generation, Modeling, and Management

Author
Sytsma, Anneliese

Publication Date
2021

Peer reviewed|Thesis/dissertation

The Role of Landscape Heterogeneity in Urban Runoff Generation, Modeling, and Management

by

Anneliese Sytsma

A dissertation submitted in partial satisfaction of the

requirements for the degree of

Doctor of Philosophy

in

Landscape Architecture and Environmental Planning

and the Designated Emphasis

in

Global Metropolitan Studies

in the

Graduate Division

of the

University of California, Berkeley

Committee in charge:

Professor G. Mathias Kondolf, Chair
Professor Sally Thompson
Professor Iryna Dronova
Professor John Radke

Spring 2021

The Role of Landscape Heterogeneity in Urban Runoff Generation, Modeling, and Management

Abstract

The Role of Landscape Heterogeneity in Urban Runoff Generation, Modeling, and Management

by

Anneliese Sytsma

Doctor of Philosophy in Landscape Architecture and Environmental Planning

and the Designated Emphasis in

Global Metropolitan Studies

University of California, Berkeley

Professor G. Mathias Kondolf, Chair

Urban areas – often characterized by their impervious surfaces – have a disproportionate impact on the hydrologic regimes of associated river systems and their water quality. Over the past century, enormous amounts of scientific research and funding has been allocated towards the effective management of urban runoff. Despite these investments, however, it continues to confound engineering solutions, causing pollution, flooding, and habitat destruction. These challenges are compounded by the need to plan for non-stationarity in climate, shifts in hydrologic regimes and land use, and inter-dependencies between ecological, hydrological, and human systems. The first chapter of the dissertation provides relevant background on the challenges associated with effectively managing the hydrologic impacts of urbanization. These challenges arise from some of the assumptions that have driven management decisions over the past century, namely: (1) that production of urban runoff is dominated by overland flow across impervious surfaces; and (2) that overland flow in urban areas is controlled by the total quantity of impervious surfaces, rather than their patterns with interspersed previous areas, and characteristics of these pervious areas.

The second chapter of the dissertation explores the first of these assumptions, and asks: What are the implications of different hydrologic processes for the production of urban stormwater and its management? The assumption that runoff in urban areas is driven by impervious surfaces has dominated our understanding and management of urban catchments for decades. Through a literature review and theoretical framework, this chapter identifies the range and drivers of hydrologic processes in urban settings, characterizes their associated spatial and temporal scales, and shows how a mismatch in process and management scales

can lead to unintended outcomes. It offers guidance for adaptation of the current 'risk-based' approach for managing urban runoff across the different runoff processes and scales.

The third chapter of the dissertation explores the second assumption, and asks: How does landscape variability impact the spatial production of urban runoff? This chapter uses a combination of hydrologic modeling, machine learning, and geospatial analysis to determine the extent to which different landscape factors moderate runoff contribution from impervious areas. Results show that impervious surface contribution to runoff (or, 'hydrologic connectivity of impervious areas', HCIA), is controlled by spatial variability of pervious area characteristics and temporal variability in pervious area conditions and rainfall. To enable such analysis in practice and for urban planning purposes, this chapter presents a geospatial tool for estimation of HCIA at watershed scales.

The fourth chapter of the dissertation explores the implications of the second assumption for the predictive accuracy of semi-distributed hydrologic models, and asks: How do land cover characteristics and climate variability impact calibration and predictive accuracy of semi-distributed runoff models? Semi-distributed models represent landscape heterogeneity, such as pervious and impervious patterns, with unobservable effective parameters. Through comparative 'virtual experiments', this chapter demonstrates that the predictive accuracy of a widely used urban hydrological model (SWMM) can be affected by calibrated parameter dependence on soil, storm, and landcover characteristics. The inter-dependencies between the forcing parameters and calibration parameters can result in significant prediction error when a calibrated model is applied to predict runoff from novel climate and landcover conditions.

The research presented in this dissertation will help municipalities and flood managers identify applicable policies, design standards, and planning mechanisms for urban runoff management. It also points to a need for a better understanding of the process (or processes) by which runoff is generated, the effects of human alteration and management on these processes, and the sensitivity of such processes to ongoing changes in climate, land use, and management.

To my fiance John Van Citters

Thank you for supporting me, going on rain walks with me, and loving the cat I adopted while you were out of town

Contents

List of Figures

List of Tables

Acknowledgments

There are so many people to thank for their support throughout this journey. First and foremost, thank you to my advisor Matt Kondolf, for being there to guide the soul searching experience that this PhD has been over the past few years. Despite the million things you juggle, you always make time to review drafts, brainstorm ideas, and provide general guidance. A huge thank you to Sally Thompson, my master's advisor and outside committee member. Your energy and commitment to your students is truly inspiring and greatly appreciated. Thank you for your support and generosity over the years. Thank you to Iryna Dronova, who provided much needed support in my first year as a PhD student, and has continued to be a terrific mentor over the years. Last but definitely not least, thank you to John Radke, for your enthusiasm and assistance, particularly in my second year as my Qualifying Exam committee chair.

To William Eisenstein, who has provided support, guidance, and funding (!) over the past four years: I cannot thank you enough for meeting with me in my first year of my PhD, and for continually going to bat for me to obtain research funding. I do not know if I would have made it without your support. To Terri Hogue at Colorado School of Mines: thank you for your support and collaboration, for extending resources and assistance, and for adopting me into your lab.

To all my colleagues and collaborators I've have the privilege to meet during my PhD. At Colorado School of Mines, everyone I've met through Terri - Colin Bell, Katie Spahr, Chelsea Panos, Jordyn Wolfand, and others - thank you for accepting me into your research lab, for your emotional and technical support, and for being there to make this a fun process (and for SCRAM!). To my lab mates in River Lab and other friends in LEAP PhD program – thank you for your shoulders, camaraderie, motivation, support, and critical reviews. I am excited to see you on the other side!

Chapter 1

Introduction

While urban areas occupy only about 2-3% of the world's land surface (Liu et al., 2014), they are home to half of the worlds population (United Nations, 2018) and have a disproportionate impact on the hydrologic regimes of associated river systems and their water quality. Replacing permeable areas with impervious surfaces, such as roads, parking lots, and rooftops, reduces infiltration of rainwater through soil, and results in increased runoff from urban areas (Leopold, 1968). These increased flows cause erosion of stream beds and banks (Booth & Jackson, 1997; Gillies et al., 2003; Walsh et al., 2005). Pollutants accumulate on these urban surfaces, and combine with runoff to flow directly (untreated) into receiving lakes, bays, and streams as non-point-source pollution (Arnold & Gibbons, 1996a; Burns et al., 2010; Leopold, 1968; Simmons & Reynolds, 1982). Despite the enormous amount of scientific research, regulation, and administration related to urban runoff management over the past few decades, it continues to confound engineering solutions, causing pollution, flooding, and habitat destruction (Karvonen, 2011; Patterson et al., 2013).

These ongoing issues in urban runoff management are compounded by large uncertainty in future climate and development conditions (Gober et al., 2010). Urban runoff management is confronted with the need to plan for non-stationarity in climate, shifts in hydrologic regimes and land use, and inter-dependencies between ecological, hydrological, and human systems (Penny et al., 2020a; Martin et al., 2017; Milly et al., 2008; Wagener et al., 2010). Such planning problems (i.e., those that hinge on major uncertainty and inter-dependencies) are 'inherently wicked', having neither clear missions nor solutions (Patterson et al., 2013). Wicked problems – characterized by an incomplete or contradictory knowledge, a large number of stakeholders and opinions involved, a large economic burden to solve it, and inability to intervene without impacting something else (Rittel & Webber, 1973) – cannot be easily solved using rational, technological approaches (Karvonen, 2011).

The wicked problem presented for urban runoff management is perpetuated, in part, by the failure to recognize hydrological processes in urban areas as unique from each other and derived from their physiographic and climatic contexts. While imperviousness of urban

areas is indeed a major defining characteristic of urban areas, it is not the *only* characteristic. Indeed, the extreme spatial variations in land cover in urban areas (e.g., grass, pavement, trees, gardens, and bare ground juxtaposed over short distances) can complicate underlying hydrologic mechanisms, affecting the temporal interactions between precipitation and catchment response (Robinson & Sivapalan, 1997). Urban water infrastructure, which may, for example, promote rapid infiltration of stormwater, can also result in scale-dependent changes in process importance, where flow is routed into the subsurface (Miles & Band, 2015; Salvadore et al., 2015; Cristiano et al., 2017). The assumption that imperviousness is the defining hydrological characteristic of urban hydrologic process has led to a hydrologic classification of urban areas as 'other' and inherently different from 'natural' catchments, and consequently, a rather limited understanding of urban hydrologic processes (Fletcher et al., 2013).

To address the mounting environmental issues posed by urban runoff under an uncertain future, urban runoff management must be based on an understanding of the process (or processes) by which runoff is generated, the effects of human alteration and management on these processes, and the sensitivity of such processes to ongoing changes in climate, land use, and management. An approach to urban runoff management that considers these aspects requires a close look at some of the assumptions that have driven management decisions over the past century, namely: (1) that production of urban runoff is dominated by overland flow across impervious surfaces; and (2) that overland flow in urban areas is controlled by the total quantity of impervious surfaces, rather than their patterns with interspersed previous areas, and characteristics of these pervious areas.

1.1 Background

Runoff mechanisms

Knowing which runoff process(es) predominate in a watershed is critical for the success of hydrological management. Hydrologists have historically categorized three primary runoff processes: infiltration excess overland flow (IEOF) (i.e., Hortonian overland flow (Horton, 1939)), saturation excess overland flow (SEOF) (i.e., Dunnian flow (Dunne & Black, 1970)), and shallow groundwater flow (SGWF) (Whipkey, 1965). At the catchment scale, the extent to which one of these three runoff generation processes dominates is known to depend on feedbacks between 'static' surface and subsurface properties (e.g., vegetation, saturated hydraulic conductivity, depth to groundwater or bedrock Dunne & Leopold (1978)) and 'dynamic' forcing (e.g., precipitation, climate). Consequently, each of these runoff processes defines a unique hydrologic system, e.g., relevant flow paths, scales, and boundaries, which form the basis of hydrologic analysis and planning. Misattributing hydrological outcomes to particular runoff processes can cause a mismatch of management actions to this system, undermining the success of management.

Because of the prevalence of impervious surfaces in urban areas, runoff production is often

assumed to occur as IEOF, which occurs when the rainfall rate exceeds the rate at which the land surface can infiltrate (Horton, 1939, 1933). This simple conceptual model has dominated our understanding and management of urban runoff for decades (Schwartz & Smith, 2014), defining management policies, planning approaches, and methods of evaluation (Stewart et al., 2019). While this assumption – and the management approaches it has defined – is broadly defensible in major cities or areas with dense urban development, the fact that urban areas span a wide range of climates, topographies, and geologies, suggests a range of possible runoff processes.

In SEOF and SGWF dominated regions, surface water flows and groundwater flows can interact, resulting in complex processes that might challenge the effectiveness of urban stormwater infrastructure (Schwartz & Smith, 2014). The question of whether our current approach to urban runoff management, developed under the assumption of IEOF, still applies in areas that exhibit SEOF and SGWF has not been adequately explored. Advancing our understanding of urban hydrologic processes, including the spatial and temporal scales that define them, may help municipalities and flood managers identify more appropriate and effective policies, design standards, and planning mechanisms (Voter & Loheide, 2018; Miles & Band, 2015).

Spatial metrics

In urban areas, replacement of natural soils and vegetation with impervious surfaces with decreased permeability (such as roads, roofs, and driveways) has long been recognized as a major cause of environmental degradation, stemming from changes to water balance factors, e.g. decreased infiltration and increased runoff (Burns et al., 2010; Leopold, 1968; Simmons & Reynolds, 1982). Consequently, two of the most common spatial metrics in urban areas are related to impervious surface: total impervious surface, and directly connected impervious surface.

Total impervious area (TIA) – the total area occupied by impervious surfaces – is often used as an indicator of the degree of urbanization and consequent effects of urbanization on hydrologic conditions. However, TIA does not distinguish between impervious areas that are 'directly connected' to streams (being adjacent or connected via stormwater pipes) from those that are distant and whose runoff flows over pervious surfaces (Boyd et al., 1993) and thus is limited in its ability to predict runoff at local scales (McGrane, 2016; Crompton et al., 2019; Fletcher et al., 2013; Lim, 2016; Y. Zhang & Shuster, 2014). The directly connected impervious area (DCIA) metric was introduced to measure impervious areas that are physically connected to the stormwater network or stream channel (e.g., Hwang et al., 2017; Lee & Heaney, 2003a; Seo et al., 2013).

Despite their potential to describe heterogeneous landscapes, there are a number of challenges to using landscape pattern metrics – such as TIA and DCIA – for predicting runoff. Chief among these is the fact that landscape pattern metrics are static and are therefore unable to capture dynamic changes in hydrologic pathways that can occur over time or space (Bracken et al., 2013; Bracken & Croke, 2007; Lexartza-Artza & Wainwright,

2009). More nuanced metrics are needed in urban areas that capture the impacts of variable climates, slope gradients, soils conditions, and heterogeneous flow paths on impervious surface connectivity.

Hydrologic models

Hydrologic models are used to predict changes to runoff and infiltration in response to hydrologic forcing (e.g., changes in precipitation or climate patterns). Urban hydrologic models often fall into one of two major categories: distributed or semi-distributed.

Distributed models, such as RHESSYS (Tague & Band, 2004) and ParFLOW.CLM (Maxwell & Miller, 2005), simulate processes 'everywhere' in space. Many of the distributed models are 'process-based', that is, they are based on governing equations of physics such as the 2-D Saint Venant Equation to simulate overland flow routing. Such models are typically computationally intensive and require a large number of input parameters (Sun et al., 2014), making them impractical for many applications in urban settings.

Semi-distributed models, such as SWMM, CANOE or MOUSE, aggregate heterogeneous parameters (e.g., soil hydraulic conductivity, topography, land covers) to coarser - e.g., subcatchment – scales and produce aggregated results at this scale (Carpenter & Georgakakos, 2006a; Golden & Hoghooghi, 2018). Such models make catchment-scale hydrologic predictions by simulating overland flow and water quality in each subcatchment independently, and then linking subcatchments by a drainage network to allow for conveyance of water and pollutants across the watershed.

Lumping hydrologic parameters increases model efficiency, but also necessitates 'effective' parameters representing emergent hydrological behavior (Petrucci & Bonhomme, 2014) rather than physical processes. Effective parameters are inherently impossible to measure or estimate directly and must be calibrated to obtain a good fit between observed and modeled hydrological data. Calibrating effective parameters generates a number of well known problems, including a demand for accurate calibration and validation data (Sorooshian & Gupta, 1995), selecting which parameters to calibrate and defining functions that measure model performance (Khatami et al., 2019).

However, calibrating models for rapidly changing urban environments brings up further, even more basic issues: the optimal parameter values may vary with forcing conditions (e.g., rainfall, land cover). While there is a wide literature dealing with non-stationarity in hydrologic predictions (e.g., Clarke, 2007; Klemeš, 1983; Koutsoyiannis, 2006), the ability of existing models to cope with this non-stationarity is questionable (Wagener et al., 2010) and is a largely unaddressed problem particularly for urban hydrological modeling (Fry & Maxwell, 2018). If optimal calibration parameters are sensitive to changing conditions, urban hydrological predictions for future climate and landcover conditions may be subject to unquantified error.

1.2 Problem statement

This dissertation aims to improve understanding of urban runoff processes by exploring how spatial patterns of impervious and pervious surfaces influence urban runoff when subject to varied rainfall and soil conditions, and to create frameworks which make such relationships relevant to policy and planning (Figure 1.1). I focus my research on three primary questions:

1. What are the implications of different hydrologic processes for the production of urban stormwater and its management?
2. How do local landscape patterns, land cover characteristics, and climate variability impact the spatial production of urban runoff?
3. How do land cover characteristics and climate variability impact calibration and predictive accuracy of semi-distributed runoff models?

1.3 Overview of chapters

To answer the first question (Chapter 2), I conduct a literature review to characterize the range of challenges posed by presence of SEOF and SGWF for management of urban runoff. I discuss the range and drivers of potential hydrologic responses in urban settings and the implications these runoff processes on urban runoff management approaches. Finally, I offer a heuristic framework for adaptation of 'risk-based' approach for managing urban runoff arising from SEOF and SGWF.

To answer the second question (Chapter 3), I use a combination of hydrologic modeling, machine learning, and geospatial analysis to develop spatially-explicit estimates of hydrologically connected impervious areas (HCIA) in ungauged urban catchments that accounts for variability in hydrologic pathways that result from variability in soil types, pervious and impervious areas, rainfall events and soil moisture conditions. I present a method and geospatial tool for estimating hydrologically relevant landscape metrics across varied soils and climate conditions.

To answer the third question (Chapter 4), I explore the implications of calibration parameter sensitivity to changes in model forcing for urban hydrological prediction. I demonstrate that sensitivity of calibration parameters to changes in model forcing can be identified through the use of virtual model experiments, similar to previous studies that explore hillslope controls on connectivity (Hopp & McDonnell, 2009), runoff from heterogeneous land surfaces (Crompton et al., 2019), and climatic and landscape controls on runoff partitioning (C. Li et al., 2014). These virtual experiments identify the limits of calibration parameter applicability across distinct environmental and climatic conditions.

Finally, Chapter 5 concludes by summarizing the findings of these three chapters in response to the three guiding questions, and discusses the importance of this research in the context of rapidly changing urban environments.

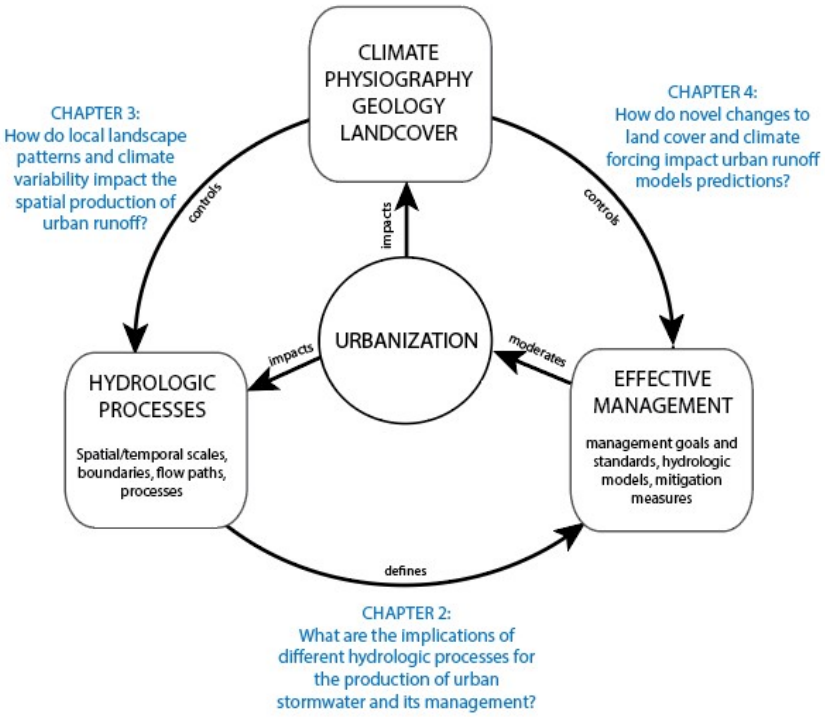

Figure 1.1. Conceptual overview urban hydrologic systems under change. Natural landscape and climate factors control hydrologic processes, which are impacted by urbanization. Knowledge of urban hydrologic processes should be used to define effective management approaches that moderate the impacts of urbanization. At the same time, changes in urbanization interact with changes in natural landscape and climate factors, which exert controls on the effectiveness of these management approaches.

Chapter 2

Managing urban sogginess: implications of saturation excess and shallow groundwater flow for management of urban runoff

Abstract. Changes in runoff characteristics following urbanization are often attributed to infiltration excess overland flow (IEOF) generated across impervious surfaces. The assumption of IEOF in urban areas has dominated the understanding and management of urban runoff for decades. It forms the basis of definitions of risk and the subsequent policy, management, and infrastructure that intend to mitigate this risk. Yet even early hydrology literature has recognized that urban runoff mechanisms are significantly more complex than suggested by the simple conceptual model of IEOF. This complexity derives from the presence of non IEOF hydrological responses, which may arise from either the remaining pre-development hydrologic mechanisms, from human interventions in the landscape and runoff management infrastructure, or from the interaction of the two. The resulting runoff mechanism may vary from IEOF in terms of relevant processes, spatial scales, and temporal scales, which can challenge the effectiveness of the current IEOF-based management paradigm and the consequent management infrastructure it defines. In this paper, we (i) describe how - and why - the current management paradigm is based on the assumption of IEOF; (ii) compare the hydrologic processes, spatial scales, and temporal scales of other runoff mechanisms to those of IEOF; and (iii) offer guidance for adaptation of the 'risk-based' approach for managing urban runoff across these different runoff generation mechanisms. We highlight the value of process-based approach (compared to the current approach based on the assumption of IEOF) to guide effective management of the wide range of hydrologic processes that can arise in urban areas.

2.1 Introduction

Different watersheds exhibit distinct hydrologic regimes and respond differently to different management approaches. The differences in runoff regimes are understood to arise from differences in topography, soils, land cover, groundwater dynamics, climate and weather (Dunne & Leopold, 1978; H.-Y. Li et al., 2014; Budyko, 1977; Buchanan et al., 2018). For the purposes of surface hydrology, these differences are often interpreted through the lens of the dominant runoff (or streamflow) generation mechanisms (Lyon et al., 2006; Saadi et al., 2020; Tilahun et al., 2016; Buchanan et al., 2018; Dunne & Leopold, 1978; K. Beven, 2006a).

Runoff generation mechanisms are often classified into three major types: infiltration excess overland flow (IEOF) (i.e., Hortonian overland flow sensu Horton (1939)), saturation excess overland flow (SEOF) (i.e., Dunnian flow sensu Dunne & Black (1970)), and shallow groundwater flow (SGWF) (in low-relief, high groundwater regions sensu Zimmer & McGlynn (2017) cf. in steep, humid regions sensu Whipkey (1965)). The contribution of these mechanisms to runoff in a specific watershed remains challenging to identify *a priori* and can fluctuate seasonally and with the degree of storage in the basin. The role of these mechanisms in producing runoff can change also over longer timescales – sometimes referred to as a change in hydrologic regime – due to water abstraction (Kinal & Stoneman, 2012), land use or land cover change (Penny et al., 2020a), drainage infrastructure (Foufoula-Georgiou et al., 1969a), or climate change (Milly et al., 2008).

The different runoff mechanisms are associated with distinct processes, which have characteristic spatial and temporal scales. Here, the term scale refers to a characteristic region in space or period in time at which a process occurs (Salvadore et al., 2015; Blöschl & Sivapalan, 1995). For example, groundwater flow processes can occur over large spatial scales ($\sim 10^4$m) and fluctuate on seasonal time scales, while IEOF processes can arise at smaller scales corresponding to landcover permeability ($\sim 10^1$m) and fluctuate rapidly with changes in rainfall.

A knowledge of the mechanisms and associated processes by which rainfall becomes runoff is central to effective management of any landscape as it informs the potential types and scales of hydrological challenges and appropriate methods for prediction (Leopold, 1968). Among other things, incomplete knowledge of hydrological processes and feedbacks can lead to institutional or planning frameworks for management that are not aligned with hydrological systems, and that can be detrimental to the ecological systems they support (Borgström et al., 2006; Folke et al., 2007; Cumming et al., 2006). Mismatches in scale can also arise through unexpected or long term change to underlying dynamics and processes (Cumming et al., 2006; Scheffer & Carpenter, 2003), e.g., in the case of hydrological regime shifts, which presents other major management challenges (Ehret et al., 2014).

Because it is difficult to identify the dominant runoff mechanism in a catchment a priori, and therefore to predict such hydrologic regime shifts, planners, engineers, and hydrologists are required to make generalizations and assumptions about runoff mechanisms and processes. While often essential for practical reasons, these generalizations can also result in misattribution of hydrological outcomes to particular runoff mechanism,

resulting in inaccurate predictions and ineffective management (Lyon et al., 2006).

In urban areas, almost all prediction and management support tools embed the assumption that runoff is generated via IEOF, influencing definitions of risk, policies, management practices, and design guidelines (Stewart et al., 2019; Schwartz & Smith, 2014). Indisputably, urbanization is associated with increases in impervious surface area which promotes local IEOF (Leopold, 1968). Yet the physiographic and climatic context of urban areas is highly variable. A simple global analysis shows that approximately 40% of major urban areas are situated over shallow bedrock or high groundwater (Figure 2.1), conditions promoting SEOF or SGWF. Indeed, recent analyses of US catchments suggests that for most of the US – including in urbanized catchments – evaporation-controlled soil moisture, rather than extreme precipitation events, is a primary control on flooding (Berghuijs et al., 2016), and that antecedent wetness is as important as impervious area in explaining variations in runoff ratio (flow per unit rainfall) (Saadi et al., 2020). Of course, while such coarse global scale analyses indicate that SEOF and SGWF runoff may occur in urban areas, management of runoff must be implemented at much smaller scales (e.g., city, catchment, or site-scales); runoff mechanisms at these scales may be more variable than implied by global analyses. For example, analytical modeling indicates that a given urban area may transition between producing IEOF and SEOF under different storm characteristics (Stewart et al., 2019), while in several urban areas characterized by high groundwater, the importance of IEOF versus SGWF varies with annual groundwater hydrograph (C. J. Ocampo et al., 2013).

In such areas where multiple runoff generation mechanisms co-exist, their processes can interact, generating complex variations in the volume and timing of runoff production that can challenge the effectiveness of urban stormwater infrastructure (Schwartz & Smith, 2014; Lim & Welty, 2017). Urban water infrastructure, which may, for example, promote rapid infiltration of stormwater, can also result in scale-dependent changes in processes, where IEOF is generated at small spatial scales (e.g., across impervious surfaces such as sidewalks and driveways), but infiltration from stormwater infrastructure and permeable areas promote subsurface flows at larger scales (e.g., to regional groundwater tables) (Miles & Band, 2015; Salvadore et al., 2015; Cristiano et al., 2017).

Many conventional hydrologic models do not resolve multiple, interacting runoff processes (Buchanan et al., 2018). Since the dominant runoff process can vary with different forcing conditions (Stewart et al., 2019), the use of simplified process descriptions can lead to large changes in the validity of model calibration between different forcing conditions (Sytsma et al., 2021; K. Beven & Binley, 1992). Conversely, models tailored to a specific runoff generation process - for example TOPMODEL-like SEOF models (K. J. Beven & Kirkby, 1979), infiltration-driven IEOF models (Smith et al., 1995) or water-table simulating SGWF process models (Fleckenstein et al., 2010), embed process-specific conceptualizations, equations, and process parameters. Unsurprisingly, therefore, incorrectly specifying the dominant runoff process inhibits the quality and utility of predictions made by hydrologic models (Easton et al., 2007; Bhaskar et al., 2015), and in policy or infrastructure responses. Similarly, failure to recognize a hydrologic regime shift

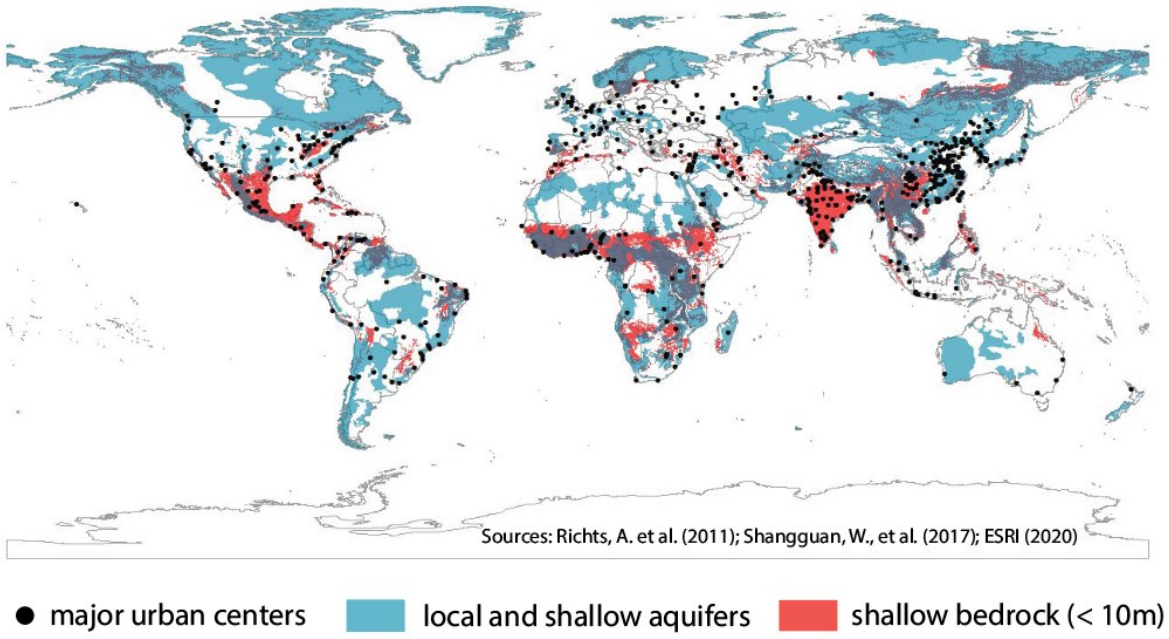

Figure 2.1. Global map of shallow/perched groundwater aquifer (from Richts et al., 2011), shallow bedrock (from Shangguan et al., 2017), and major urban centers (from ESRI, 2020)

can lead to large uncertainty and error in hydrological predictions that continue to rely on past observations.

Thus, while IEOF is produced across impervious surfaces, many urban areas also exhibit SEOF and SGWF processes that dominate or interact with IEOF. This variation in runoff generation mechanism likely brings the validity of predictive and management approaches dependent on IEOF into question. This twofold argument raises numerous questions for management, namely:

1. How is the current runoff management paradigm based on IEOF? Why did it develop?
2. How do SEOF and SGWF processes, spatial scales, and temporal scales compare to those of IEOF?
3. What are the implications of different spatial and temporal scales for urban runoff management?

The answers to these questions will help municipalities and flood managers identify applicable policies, design standards, and planning mechanisms for urban stormwater (Voter & Loheide, 2018; Miles & Band, 2015). This synthesis focuses on hydrological aspects of these questions (i.e., on the volume of runoff generated, its flow paths, velocity

and timing) to (1) discuss the underlying reasons for the reliance of management on IEOF (Section 2.2); (2) investigate how the hydrologic controls and spatio-temporal scales of IEOF compare to other runoff mechanisms (Section 2.3); and (3) describe the implications of these different spatial and temporal scales for runoff management (Section 2.4). We then apply this assessment to offer guidance for adaptation of the current approach to urban runoff management (Section 2.5). The closely related challenges of water quality in urban runoff are not addressed directly but are referred to when the implications of different runoff generation mechanisms for management of urban stormwater volume/timing are particularly relevant for common water quality management practices.

2.2 How (and why) does the current runoff management paradigm hinge on the assumption of IEOF?

IEOF processes and scales

Proposed initially by Robert Horton in 1933, infiltration excess overland flow (IEOF) is initiated when the rate of water inputs (typically precipitation) exceeds the infiltration capacity of the soil (Horton, 1939, 1933) (Figure 2.2). The infiltration capacity represents a maximum rate of vertical water flow into the soil, which is controlled by the unsaturated water potential in the soil and depth of the wetting front (H. W. Green & Ampt, 1911), and typically decreases as soils become wetter until it approaches the saturated hydraulic conductivity (Philip, 1969). IEOF production is therefore strongly influenced by rainfall characteristics and the land surface hydraulic properties. It is prevalent in locations characterized by impermeable surfaces including urban areas (Leopold, 1968), areas with exposed rocks and bedrock (montane regions), or areas exhibiting crusted or sealed bare soil surfaces such as drylands and bare agricultural land (Assouline, 2004).

IEOF responds quickly to rainfall, often on the order of minutes; streamflow it generates is 'flashy', with short lag times, and steep rising and recession limbs (Figure 2.2a). Often, streams in IEOF dominated landscapes are ephemeral, with channels that lie above the groundwater reservoir at all times, and which flow only in direct response to rainfall. Because IEOF runoff is driven by rainfall intensity and soil infiltration capacity, relevant spatial scales for IEOF are closely related to spatial scales over which these controls vary. While rainfall can vary across small scales, it is often considered to be constant across a catchment. Thus, the primary factor that defines spatial scales relevant for IEOF is the spatial variation in soil infiltration capacity. In a catchment dominated by IEOF with uniform soils, Horton's mechanism implies time to ponding occurs at the same time everywhere and (for a storm of sufficient duration) the entire catchment contributes to flow at the outlet (Figure 2.2d,e). Catchment morphology under such conditions is therefore irrelevant, except in so far as it affects routing of the runoff and the timing of the hydrograph (K. J. Beven et al., 1988).

For a catchment with spatially variable soils, however, IEOF occurs at spatial scales that correspond to the variability in soil infiltration capacity, sometimes referred to as partial area IEOF (sensu Betson, 1964).

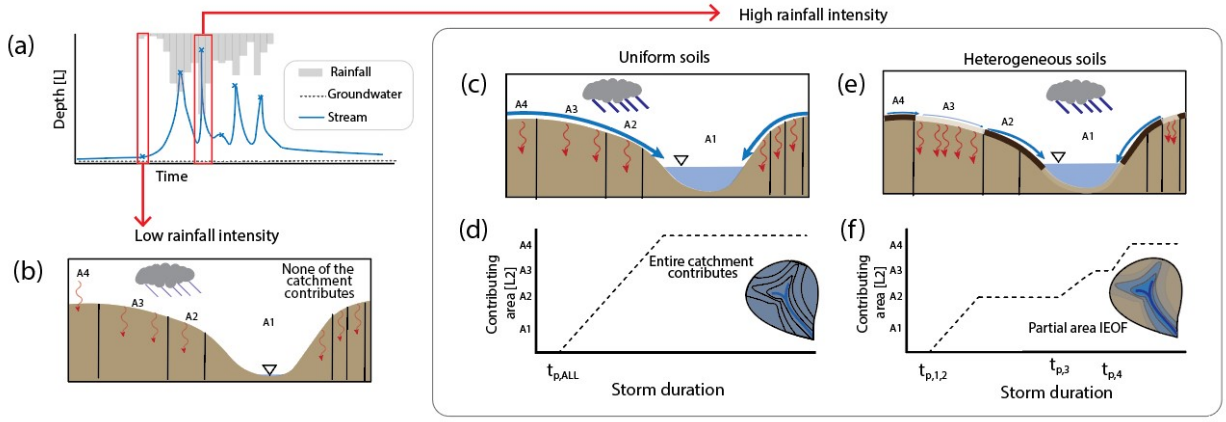

Figure 2.2. Conceptual schematic of infiltration excess overland flow temporal and spatial scales. Under IEOF conditions, the stream often flows in direct response to rainfall (a). If rainfall intensity is less than the infiltration capacity, however, all rainfall infiltrates and no overland flow is produced (b). For a catchment of uniform soils (c), all areas contribute to overland flow simultaneously (d). For a catchment with variable soils (e), partial area IEOF is produced only in areas where the precipitation intensity exceeds the infiltration capacity (f).

IEOF was the first runoff generation mechanism of runoff to be discovered. It enabled simple, process-driven approaches for hydrological predictions (K. Beven, 2004; K. J. Beven et al., 1988) and – for at least a decade after its definition – was assumed (by Horton and others) to be globally occurring (K. Beven, 2006a). Observations by Hursh & Brater (1941) of stream flow without overland flow challenged the universality of IEOF, and indicated that water of subsurface origin is often a major component of storm runoff. Mechanistic experiments in the 1960s and 1970s revealed additional runoff generation mechanisms: saturation excess overland flow (SEOF) (Dunne & Black, 1970), and shallow groundwater flow (SGWF) (Whipkey, 1965). These processes, described in detail in Section 2.3, are unlike IEOF in that they are controlled by the accumulation and flow of water in the subsurface.

The story of how hydrology moved from a paradigmatic assumption of global IEOF occurrence to the more complex picture of runoff generation mechanisms prevailing today is well known (see, e.g., K. Beven, 2006a). Yet the legacy of that historical paradigm lingers in some areas of practice. As we outline below, the assumption that runoff production arises from IEOF - not without justification - underpins the history and contemporary practice of urban runoff management.

Urban runoff management hinges on IEOF assumption

Despite a detailed, observation-derived insight into many hydrologic processes (K. Beven, 2004), Horton remains best known for proposing a simple model of IEOF production, which he likely developed in support of engineering applications (K. Beven, 2004; Klemeš, 1986; Yevjevich, 1968). The conceptual model of IEOF dominated hydrologic research, including urban hydrology and urban water management, for many years (K. Beven, 2004). It informed the development of methods of prediction, design, management tools and management approaches. Because urban water management has evolved from this background, the presumption of IEOF is implicit in the management of urban runoff.

The operational paradigm for managing runoff in urban areas is to link runoff characteristics to adverse outcomes (environmental or social); to specify a risk tolerance for how often these adverse outcomes might occur; and to design infrastructure or management regimes that satisfy the specified tolerance. IEOF influences this operational paradigm in two important ways (Figure 2.3). First, the presumption that IEOF is the most important driver of runoff responses leads to the widespread (indeed, near universal) use of event-scale rainfall extreme value distributions to provide the basis for specifying tolerance and risk within urban stormwater designs. Secondly, many of the methods used to relate rainfall extreme value distributions to flow characteristics – and thus to infrastructure design or management – are based on an underlying presumption of IEOF.

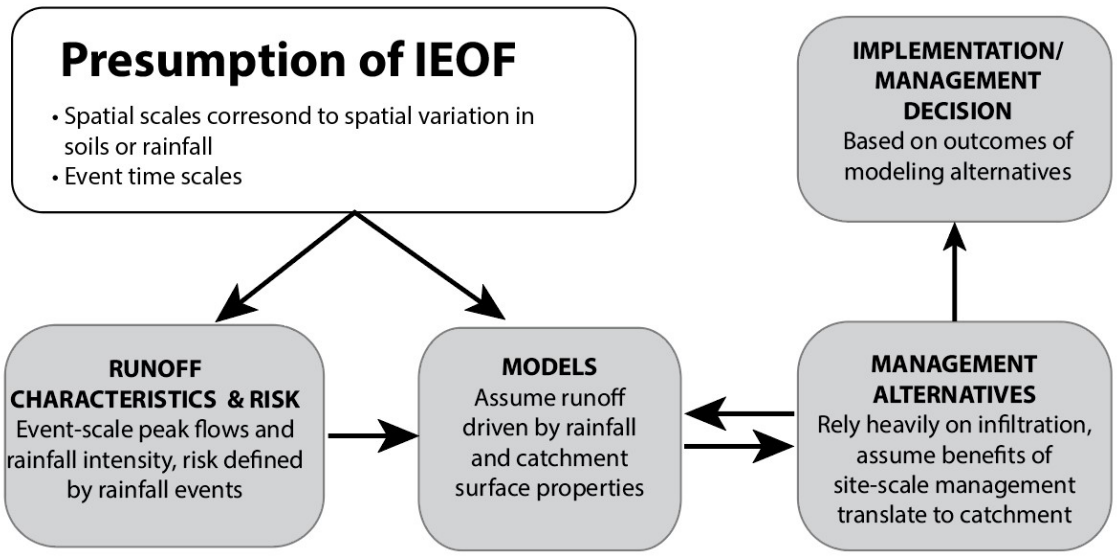

Figure 2.3. Operational paradigm for managing runoff in urban areas is dependent on the assumption of IEOF

Runoff characteristics and risk

The flow characteristics that often define urban runoff management are peak flows and runoff volumes. Traditional urban water management focused on mitigating flood risk, typically by sizing conveyances and drainage systems to accommodate flood flows associated with specific risk levels (Burian et al., 1999). As the implications of urban runoff on ecological systems have become better understood, protecting flow characteristics (e.g., flow durations, volumes) relevant to these systems (sufficient to ensure that e.g., bankfull scouring floods occur frequently enough to maintain channel health and function) have become a priority for urban water management (Booth & Jackson, 1997; Poff et al., 1997).

Risk levels are determined using intensity - duration - frequency (IDF) curves based on rainfall extreme value distributions, an approach to rainfall characterization that dates back to 1899 (Burian et al., 1999). IDF curves cover a range of timescales that broadly correspond to typical timescales of rainfall events (e.g., 72 hours, or three days, is a common upper limit in IDF curve durations), and give estimates of rainfall average annual exceedance probabilities and return intervals. Central to this approach is the assumption of homogeneity (i.e., that all flood peaks are independent and drawn from the same probability distribution) and stationarity (i.e., that the probability distribution of flood peaks does not change over time) (Struthers & Sivapalan, 2007). In other words, the rainfall distribution is treated as independent of the hydrological or physical state of the catchment. Joint probability methods that account for heterogeneity (e.g., of event characteristics and variably saturated area extent), or conditional probability methods that account for non-stationarity in event characteristics (e.g., event characteristics conditional on time periods when soils are frozen, or season) are not usually developed - likely for practical reasons. The result is that the probabilistic drivers used for urban stormwater management are primarily based on event-scale precipitation - consistent with an IEOF assumption, but, as we describe below in Section 2.3, not necessarily consistent with SEOF or SGWF processes.

Hydrologic models

IDF curves and the design rainfall they produce are then applied in rainfall-runoff models to produce estimates of flooding, which are assumed to have the same probability of occurrence as the design rainfall. Rainfall-runoff routing and/or hydrological modeling forms a huge body of work in the discipline of hydrology, which certainly encompasses modeling approaches which are appropriate to SEOF and SWGF as well as IEOF. Here, however, we focus on the tools most widely used and available to urban stormwater managers, which do continue to be biased towards IEOF (Dunne & Leopold, 1978).

Traditional runoff routing tools such as the Rational Method, the unit hydrograph method, and curve number methods are either explicitly or implicitly predicated on assumptions of IEOF (Walter & Shaw, 2005; Bartlett et al., 2016; Schneiderman et al., 2007). For example, the Rational Method (Kuichling, 1889) embeds the assumption that runoff rate is proportional to rainfall rate, and as such implicitly assumes IEOF

(McPherson, 1969)[1]. Fundamentally, the Rational Method and other traditional methods share a common set of limitations in their inability to directly represent how interactions between catchment state and rainfall properties control flow behavior: because these models lack a description of the spatial variability of runoff within a watershed, they consequently assume a homogeneous watershed with a spatially uniform runoff processes (Bartlett et al., 2016). Given how central these interactions are to SEOF and SWGF, these methods are most reasonable when considering IEOF. Nevertheless, these methods continue to be applied to landscapes that do not exhibit IEOF, the consequences of which have been identified in number of studies. For example, Bartlett et al. (2016) attributes the poor performance of the curve number methods in rangeland and forested sites to the fact that these sites are dominanted by subsurface flow rather than IEOF. Consequently, a nontrivial body of scientific research has focused on modifying simple routing methods to account for factors they omit, e.g., spatial variability of contributing areas (Bartlett et al., 2016; Schneiderman et al., 2007; Steenhuis et al., 1995) and space or time-dependencies in loss coefficients (Baiamonte, 2020; Froehlich, 2016).

Contemporary urban hydrologic models incorporate more complex rainfall-runoff routing algorithms, yet many of them - e.g., SWMM (James et al., 2010a), CANOE (Boutaghane & Ouerdachi, 2012), and MOUSE (Dhi, 2017) models - continue to base these algorithms on IEOF. For example, the only land cover classification relevant to runoff production in SWMM relates to presence of permeable or impermeable surfaces; the model assumes synchronous production of runoff on all surfaces where rates of rainfall exceed infiltration, and water, once infiltrated, is "lost" from the system and cannot further influence its runoff generation behavior. Perhaps because measuring what happens to infiltrated water is difficult, its potentially complex fate (e.g., re-emergence downslope or contribution to perched aquifers) is usually ignored (Stewart et al., 2019) and it is commonly assumed to have simply recharged the aquifer (Newcomer et al., 2014).

Many of these contemporary models are spatially 'lumped', aggregating inputs (i.e., pervious surfaces, soil moisture, topography) at subcatchment scales, and produce aggregated results at the same scales (Carpenter & Georgakakos, 2006b). There are no generally applicable rules to perform this aggregation; the resulting model structure is usually a function of the modeler's hydrological understanding of the area (Wagener, 2003). In the case of urban areas, this is typically an understanding based on the assumption of IEOF. These contemporary methods are distinct from the traditional lumped methods described above in that, for a given catchment, rather than aggregating parameters across the entire catchment, they aggregate parameters into smaller subcatchments within the catchment. These scales of aggregation may be smaller than the traditional lumped methods described above; still, this aggregation means that contemporary models simulate spatially uniform runoff processes within the subcatchments. These models only address the role of spatial variability of catchment properties and processes in so far that modelers

[1]Although Kuichling (1889) did recognize this limitation, calling for further research on the impacts of antecedent soil moisture on the relationship between peak runoff rate, rainfall rate, and drainage area.

chose a subcatchment scale in accordance with these properties. Even more challenging issues arise when such models are used to estimate pollutant loads because they neglect to account for potentially important pollutant contributions and transformations across permeable areas, assuming that pollutant transport occurs solely as overland flow across impermeable surfaces (Arnold & Gibbons, 1996b; Tuomela et al., 2019). Each of these features embeds IEOF assumptions into the model.

While it is undoubtedly true that the expansion of impervious areas results in an increase in the occurrence of IEOF, the reliance of urban hydrologic models on IEOF assumptions places modelers at a distinct disadvantage in many real-world situations in which more than one runoff generation mechanism operates, where surface and groundwater interact in complex ways, and where calibration of parameters must compensate for poor process representation in models (Sytsma et al., 2021). The widespread and continual use of IOEF-based models in the face of these limitations likely reflects the influence of model legacy and modeler preference (Addor & Melsen, 2019), which may be perpetuated by IEOF-centric foci in urban hydrology planning/engineering courses. From a practical perspective, too, such models are attractive: the dependence of IEOF on surface properties (e.g., topography, infiltration capacity) means that IEOF-based models have relatively simple data requirements that can be readily observed or measured.

Stormwater management controls

Unsurprisingly, given the traditional focus on IEOF in urban areas, conventional, or 'first generation' stormwater management controls aim to to reduce peak flows and runoff volumes. These stormwater controls are typically centralized, located within or proximal to surface waterway, and rely on detention and release of runoff. Such detention-based stormwater controls (e.g., stormwater ponds and retention basins) focus almost entirely on surface flow, and as such align closely with IEOF assumptions (Burns et al., 2012; Hamel et al., 2013; Jefferson et al., 2017). However, these types of stormwater controls are increasingly considered to be problematic, sometimes exacerbating flood risks (Emerson et al., 2005) and requiring large tracts of land, which make them challenging to implement in high density urban areas (Karvonen, 2011).

These challenges inspired a new generation of stormwater infrastructure in the 1990s, variously termed Water Sensitive Urban Design, Low Impact Development, or Green Stormwater Infrastructure (henceforth referred to as Water Sensitive Urban Design, or WSUD). In contrast to centralized stormwater controls, WSUD relies on engineered nature-based solutions (such as green roofs, bioretention, infiltration basins and trenches, and cisterns) to retain hydrologic functions at smaller, site scales (e.g., housing development site) as a means of restoring hydrologic function at a watershed scale (Karvonen, 2011; Poff et al., 1997; Fletcher et al., 2013; Roy et al., 2008; Jefferson et al., 2017; Petrucci et al., 2013). Because they are sized to manage runoff from smaller areas, WSUD require less area than centralized stormwater controls, making them better suited for densely populated urban areas. WSUD often incorporate vegetation and aim to not

only mitigate peak flows and flow velocities but to also provide water quality treatment (Bell et al., 2016; Hamel et al., 2013; Jefferson et al., 2017). While WSUD often encourage a range processes – e.g., infiltration, evapotranspiration, groundwater recharge, or storage – the current planning, modeling, and policy emphasis is focused on infiltration (Clark & Pitt, 2007).

Despite having objectives that are inclusive of a broad range of potential hydrologic outcomes, WSUD design, planning, and modeling are engrained within a system predicated on the assumption IEOF. Risk-based design standards are based on event time scales, apply across municipal scales, and implemented at site scales; the models used to size and plan WSUD are based on IEOF; and WSUD preference for infiltration assumes that infiltrated water does not contribute to runoff response. Their effectiveness in meeting their objectives and any given urban area is therefore contingent on the degree to which the urban area is controlled by IEOF. While this assumption is widely defensible in many urban areas (e.g., in dense cities with high impervious surface coverage), runoff processes other than IEOF can occur in urban areas, particularly where underlying geology, topography, and soil conditions promote subsurface flows. In these areas, application of WSUD and IEOF-based management paradigm may be problematic. For example, conditions that promote subsurface flows in Baltimore, Maryland (USA) and Perth, Western Australia (AU) have raised concerns regarding the use of infiltration-centric stormwater management approaches such as WSUD (Miles & Band, 2015; Lim, 2016; Bhaskar et al., 2015; Groffman et al., 2004; C. Ocampo et al., 2017; Claydon et al., 2020).

Given the ongoing and impending investment in WSUD infrastructure globally (Jefferson et al., 2017), there is an urgent need to critically assess their application, and the current paradigm on which they depend, to areas with runoff processes that challenge the assumptions of this paradigm. In the following sections, we describe first how the spatial and temporal scales of SEOF and SGWF differ from IEOF (Section 2.3) and secondly what these differences mean for effectiveness of the current IEOF management paradigm (Section 2.4).

2.3 How do SEOF and SGWF processes and scales compare to those of IEOF?

Unlike IEOF, both SEOF and SGWF runoff mechanisms depend on subsurface processes. Controls on these subsurface processes generally act over larger spatial scales and longer temporal scales than do the controls on surface processes relevant for IEOF (Figure 2.4). Below, we compare the processes, controls, spatial scales, and temporal scales associated with SEOF and SGWF to those of IEOF.

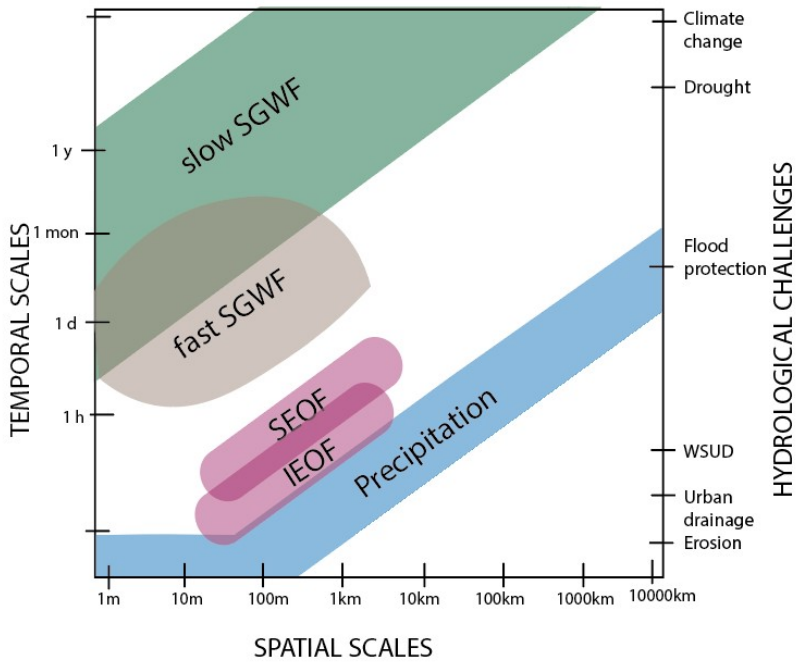

Figure 2.4. Spatial and temporal scale variability of hydrological processes, adapted from (Blöschl & Sivapalan, 1995; Salvadore et al., 2015; Cristiano et al., 2017).

SEOF processes and scales

For SEOF to occur, soil must become saturated in some locations before storm events can produce a runoff response. These variably saturated areas, or 'variable source areas' (first termed by Hewlett & Hibbert, Alden (1966)), can vary through space and time as a function of soil moisture and topographic controls (Dunne & Leopold, 1978; Hewlett & Hibbert, Alden, 1966). SEOF occurs as a combination of return flows from the subsurface and precipitation on these saturated areas. This type of runoff often arises in humid, forested, well-vegetated and hilly areas (Dunne & Leopold, 1978), particularly where bedrock, restrictive layers, or shallow water tables result in limited available storage for water in the subsurface.

One way to understand the controls on the space and timescales associated with SEOF is therefore to consider the controls on soil saturation. In a simplified, one dimensional analysis, Porporato et al. (2004) show that the probabilistic behavior of soil moisture depends on a set of dimensionless ratios (Figure 2.5a): $\gamma = w_o/\alpha$, the ratio of the maximum available soil water storage in a 1D soil column (w_o [mm]) to the average storm depth α [mm]; and λ/η, the ratio of the storm frequency λ [day$^-$1] to the frequency with which the soil column is dried by evapotranspiration occurring at potential (maximum) rates, $\eta = w_o/ET_{max}$. Porporato

et al. (2004) found that soils are skewed towards saturated conditions when $\gamma \leq \frac{\lambda}{\eta} - 1$. Physically, these conditions arise when the frequency and depth rainfall relative to available storage is enough that the rainfall tends to 'refill' the soils faster than evapotranspiration can deplete them. Conversely, soils are skewed towards dry conditions where $\lambda/\eta \leq 1$, i.e., when soils are refilled by rainfall more slowly than they are dried by evapotranspiration. Soil moisture distributions are more uniform (and thus variable) for climate and soil conditions intermediate to these values.

While simplified, this argument immediately highlights the potential complexity of SEOF in terms of time and spatial scales. For climates and soils where $\lambda/\eta \leq 1$, SEOF would be unlike IEOF (Figure 2.5b). SEOF would likely be localized to areas such as hillslope breaks, riparian zones or regions of shallow soil (Dunne & Black, 1970; Hewlett & Hibbert, Alden, 1966; McDonnell, 2003; Bhaskar et al., 2015), with saturation in these areas being dependent on process occurring across entire hillslopes. Overland flow would occur infrequently, and would be significantly controlled by the coincidence of antecedent wetness and storm characteristics. These conditions are more likely to result in runoff processes with longer temporal scales and more variability spatial scales than IEOF.

Conversely, for very humid climates and thin/shallow soils $\gamma \leq \frac{\lambda}{\eta} - 1$ (soils are shallow, rainfall is frequent and deep), SEOF would often resemble IEOF (Figure 2.5c). In extreme cases, SEOF could be prevalent throughout a whole catchment, and its runoff behavior would be largely dictated by storm characteristics. Under these conditions, the current management regime based on IEOF would likely still apply. However, it is likely that attempts to urbanize catchments with in conditions such as these (i.e., where soils are saturated most of the time) would rely on methods to drain, fill, or otherwise alter the saturated areas to make the catchment amenable for urban development (e.g., Claydon et al., 2020).

Adding to this complexity, variations in rainfall and evaporation rates can change over time (between events and seasonally) and soil storage can change over space (between locations within a given catchment) (Figure 2.6). These changes impact the wetness of a catchment, leading to transitions between 'wet' and 'dry' conditions and consequently to transitions in runoff response (Western et al., 1999; Penna et al., 2011). Temporally, seasonal variation in rainfall depth and frequency can shift a SEOF landscape from 'dry' or 'intermediate' conditions to 'wet' conditions (see Figure 2.6c). Spatially, *where* the saturation (and thus SEOF) occurs within the landscape also depends the lateral rate of water flowing into an area relative to the lateral rate of water flowing out of the area (i.e., the topographic wetness index). An area with a high lateral inflow rate (such as lowland areas and valleys) would, theoretically, shift the threshold for wetness to a lower λ/η value (as shown in blue in Figure 2.6d). This lower threshold means that these areas are more likely to become saturated compared to upland areas (with low lateral inflow rates). Even when a landscape as a whole is considered 'dry', lowland areas at the bottom of hillslopes could produce overland flow responses frequently (Figure 2.6e).

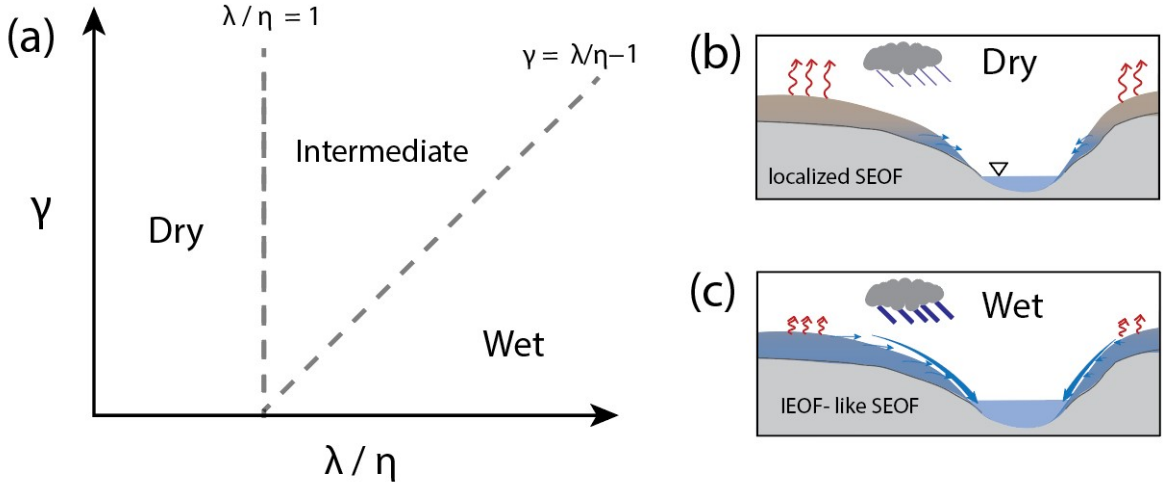

Figure 2.5. Classification of soil water balance as a function of the two governing parameters, γ (the ratio of the maximum available soil water storage to the average storm depth) and λ/η (the ratio of the frequency of rainfall to the frequency with which the soil could be dried by evapotranspiration) (a). Soils are skewed towards dry conditions where $\lambda/\eta \leq 1$, leading slower and localized SEOF (b). Soils are skewed towards wet conditions when $\gamma \leq \frac{\lambda}{\eta} - 1$, leading to IEOF-like SEOF conditions (c).

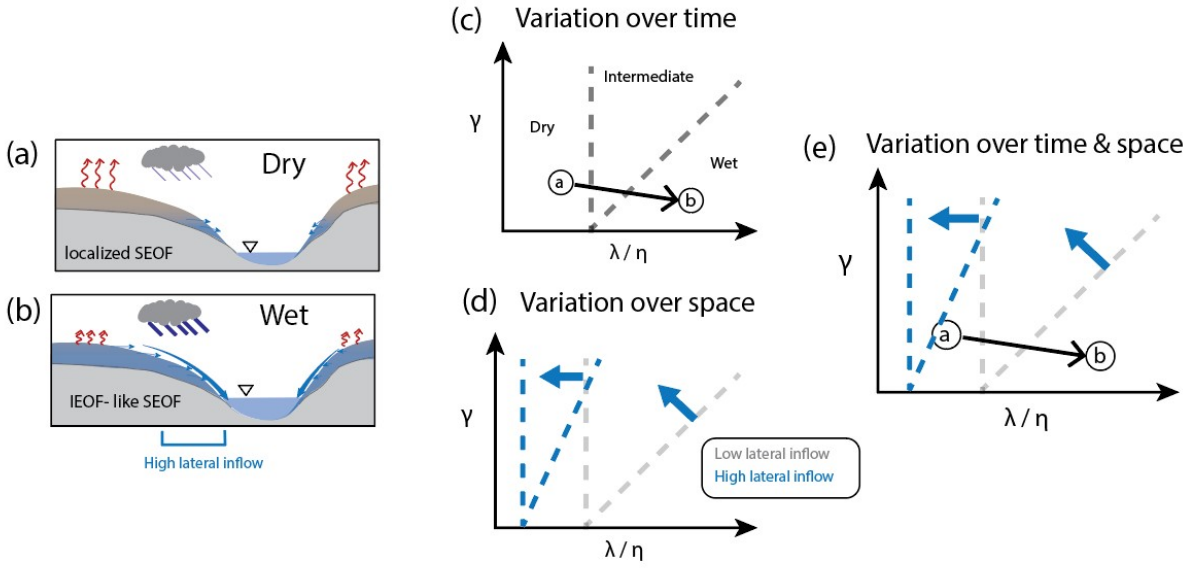

Figure 2.6. Conceptual schematic of saturation excess overland flow under 'dry' (a) and 'wet' (b) conditions. These different conditions can arise due to seasonal variations in climate, leading to a shift in catchment state (c). Spatial variability in saturated areas requires modifications to the Porporato framework to account for lateral inflow (d). Thus, for an area with high lateral inflow, the threshold for 'wet' and 'dry' conditions would shift such that the area is likely to be in 'wet' conditions even when the landscape as a whole is considered 'dry' (e).

This variability – in both time and space – lengthens the characteristic response timescales of SEOF relative to IEOF both between storms, due to seasonal variations in antecedent wetness (S. Godsey et al., 2004; Whiting & Godsey, 2016), and within storms, due to the fragmented and changing nature of the variably saturated area (Dunne & Black, 1970; K. J. Beven et al., 1988; Day, 1983). The temporal scales and spatial scales of runoff in SEOF dominated systems therefore tightly linked to each other, and depend on the temporal and spatial scales of soil saturation: runoff is event-based and similar to IEOF after soils are saturated (Lim, 2016; McMillan, 2020) but is more limited in volume and extent of production under drier conditions.

SGWF processes and scales

SGWF occurs when the primary source of stormflow production in channels or receiving bodies is the lateral movement of groundwater itself. This movement may be facilitated by highly permeable soils, the presence of preferential or macropore flow pathways, or by the rapid propagation of pressure signals from a rising water table to the riparian aquifer (Dunne & Leopold, 1978; Whipkey, 1965; Hursh & Brater, 1941; Jencso & McGlynn, 2011). In this research, we consider two types of SGWF - 'fast' SGWF, and 'slow' SGWF - which arise under different conditions.

Fast SGWF

Fast SGWF is well known to be a dominant runoff generation mechanism in steep, humid forested areas, where where water tables become perched on less transmissive layers. In these conditions, soils remain very wet most of the time and relatively small rainfall inputs can rapidly activate pressure, macropore, or riparian-aquifer driven runoff responses (McGlynn et al., 2002; Harr, 1977; Montgomery D.R. & Dietrich W.E., 1988; R. C. Sidle et al., 2000; Dunne, 1990; Tromp-Van Meerveld & McDonnell, 2006; Woods & Rowe, 1996; Graham et al., 2010; Sklash & Farvolden, 1979; Sklash et al., 1986; Whipkey, 1965; Mosley, 1979). Fast SGWF can also promote SEOF when groundwater saturates the soil column, meaning that it is common for SEOF and fast SGWF to occur concurrently during wet periods.

Like SEOF, the controls on fast SGWF can be understood through controls on soil saturation. For climates and soils where $\lambda/\eta \leq 1$, SGWF may not produce substantial runoff (Figure 2.7a). These conditions are more likely to result in runoff processes with longer temporal scales and more variability spatial scales than IEOF. Conversely, for very humid climates and thin/shallow soils $\gamma \leq \frac{\lambda}{\eta} - 1$, fast SGWF response to rainfall on steep slopes could very rapidly produce streamflow on event timsecales (Whipkey, 1965; Mosley, 1979; Sklash et al., 1986; McGlynn et al., 2002; Harr, 1977) (Figure 2.7b). This can lead to temporary conditions of rapid flow associated with connectivity of saturated zones (and consequently in SEOF) in the hillslope–riparian– stream system (Woodward et al., 2016). However, this type of rapid SGWF is unlikely to occur in urban areas, since urban

development is usually built on shallow slopes (Miles & Band, 2015) (which typically do not promote fast SGWF).

Slow SGWF

Compared to groundwater in humid areas, groundwater in mesic catchments may be recharged more slowly by rainfall events (due to longer travel paths and greater evapotranspiration rates in the unsaturated zone), and are less likely to produce a water table rise that intersects with channels or the land surface to produce surface runoff via SEOF. In such cases, and where the unsaturated zone has sufficient capacity to conduct the infiltrated water to the stream channel, the flow path lies entirely below the ground surface (Dunne, 1990). Slow SGWF of this sort can be a major contributor to runoff in arid and mesic regions (Hardie et al., 2012), in areas of high permeability and low porosity (e.g., in fractured bedrock landscapes Montgomery et al., 1997; Hahm et al., 2019; Rempe & Dietrich, 2018; Graham et al., 2010), as well as in low relief landscapes with sedimentary areas with deep soils and regional water tables (Zimmer & McGlynn, 2017; Devito et al., 2005). While slow SGWF is an essential contributor to baseflow in many areas and can be remarkably invariant over long periods of time (Hornberger et al., 2014), seasonal variation of groundwater levels is often on the order of meters (Dunne & Leopold, 1978; Gribovszki et al., 2010). These seasonal changes in groundwater levels drive variability in spatial and temporal scales for slow SGWF landscapes.

The spatial extent of shallow groundwater aquifers can vary from local scales (e.g., hillslope, $\sim 10^1 m$), to regional scales (e.g., groundwater flow systems spanning $\sim 10^4$m) (Toth, 1963). Groundwater from regional flow systems may be discharged in regional low points, e.g., streams or wetlands (Hornberger et al., 2014) (Figure 2.7c). In contrast, where local or sub-regional systems exist local groundwater systems can develop and result in groundwater discharge in local topographic lows (Figure 2.7d). Because peak groundwater levels (maximum elevation of the phreatic surface crest) can lag the peak of the rainy season, the greatest potential for peak runoff generation in slow SGWF environments arises from the combination of a high water table with a large rainfall event. These conditions can also give rise to SEOF where the water table is close to the ground surface (Dunne & Black, 1970; Dunne, 1990; Dunne & Leopold, 1978) (e.g., footslopes and in valley bottoms).

Mismatch of process drivers, spatial and temporal scales

In short, due their dependence on subsurface processes and more specifically on whether or not watersheds enter a particular hydrological state that favor their occurrence, SEOF and SGWF (fast and slow) tend to be more heavily influenced by slow hydrological processes than is IEOF. Similarly, because spatial patterns in saturation often emerge on hillslope scales, while regional water tables can respond over scales of many square kilometers, SEOF and SGWF also tend to have large characteristic length-scales relative to IEOF - particularly in urban landscapes where surface soil properties are heterogeneous on length-scales of $\approx 10^1$m.

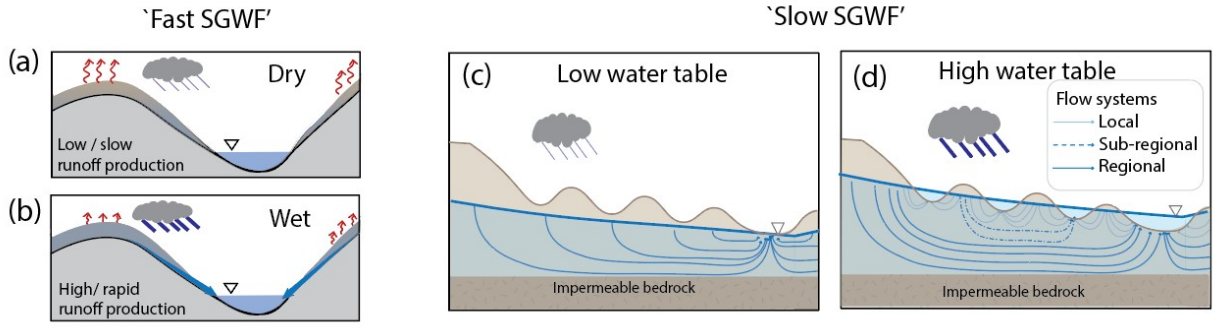

Figure 2.7. Conceptual schematic of two types of SGWF and controls on their spatial and temporal scales. Scales of 'fast' SGWF is controlled by soil moisture, similar to SEOF: soils skewed towards dry conditions ($\lambda/\eta \leq 1$) may produce minimal or no SGWF (a), whereas soils skewed towards wet conditions (when $\gamma \leq \frac{\lambda}{\eta} - 1$) and lead to IEOF-like SGWF conditions (c). Sales of 'slow' SGWF depend on the water table. Under low water table conditions, regional groundwater systems dominate, and flows remain below the surface (c). Under high water table conditions, regional, local, and subregional systems interact and contribute to streamflow, and the high water table can intersect with the ground surface, leading to local saturation (d).

The mismatch in spatial and temporal scales that can arise between SEOF and SGWF to those of IEOF means that: (1) the process of urbanization in areas previously dominated by SEOF and SGWF introduces opportunities for wide variation in space and time scales of urban runoff production; and (2) there is a corresponding mismatch between the scales of SEOF and SGWF and scales of the current management paradigm defined by IEOF.

2.4 What are the implications of different spatial and temporal scales for urban runoff management?

The effectiveness of the IEOF-based management paradigm is compromised in areas whose runoff processes occur at different spatial and temporal scales, and arise from subsurface processes (Figure 2.8). In this section, we focus on the implications of current approach to urban runoff management for (1) SEOF landscapes, and (2) slow SGWF landscapes. We omit further discussion of fast SGWF landscapes because, as discussed above, these landscapes generally less amenable for urbanization in the first place.

Mis-specification of flow characteristics and design storms

Under the current IEOF paradigm, design storms with a given probability of occurrence (produced from event-scale rainfall extreme value distributions) are generally expected to

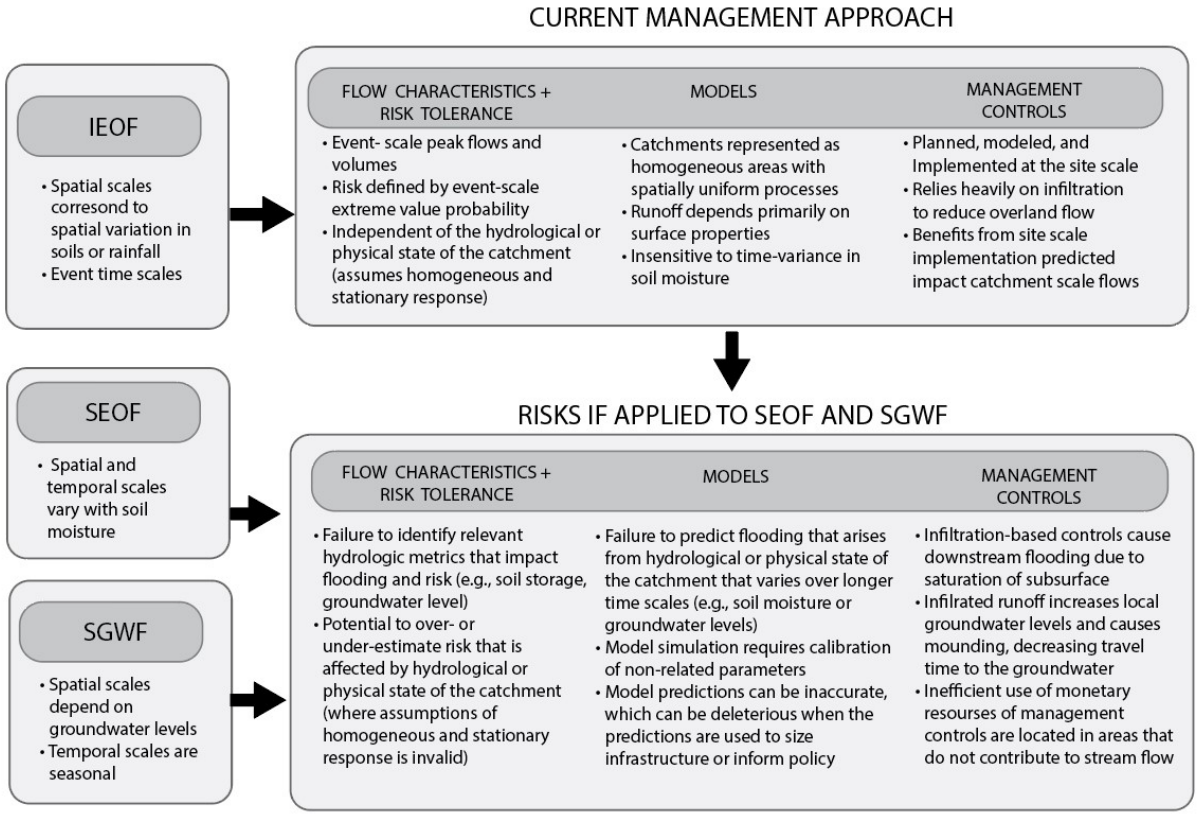

Figure 2.8. Applicability of IEOF-based management approach to SEOF and SGWF settings.

produce floods of the same probability (Singh, 2013; Struthers & Sivapalan, 2007). The assumption that a design rainfall probability matches that of the flooding it produces is generally valid for IEOF processes, where the production of runoff depends directly on rainfall timescales. However, is likely to be invalid for SEOF and SGWF processes, where runoff is sensitive to temporal variability in catchment conditions.

For SEOF and SGWF landscapes, therefore, event-scale rainfall does not translate directly to flood risk: the 'worst case' rain event does not necessarily correspond to the 'worst case' flood under SEOF and SGWF conditions. For example, the highest flood risk for a catchment dominated by SGWF may occur when the groundwater level reaches the land surface (see Figure 2.7b); in these cases, flooding itself may arise from groundwater levels and be largely independent of event rainfall (Singh, 2013; Fürst et al., 2015; Rolls et al., 2012). This type of flooding occurs long after storms have passed and persists for weeks or months (Cobby et al., 2009). In SEOF catchments, agreement between the probability of a design storm event and the resulting flood event depends on the soil saturation at the onset of the storm: for example, under extremely 'wet' conditions (see Figure 2.6b), the

'worst case' storm event may indeed produce a 'worst case' flood. If the same storm event occurred when the catchment was in 'dry' conditions (e.g., early in the season) (see Figure 2.6a), however, the resulting flood could have a much higher exceedance probability (and lower return period) than the rain event. Indeed, antecedent soil moisture can be more important than rainfall in predicting modest flooding events (Case et al., 2021) and can sustain and/or intensify impacts of extreme flood events, as in the case of e.g., the North Atlantic Tropical Cyclone Erin, which dramatically intensified over west-central Oklahoma due to soil saturation (Evans et al., 2011; Case et al., 2021).

Where flood risk is dependent on factors other than rainfall, therefore, the traditional statistical methods for event-based rainfall analysis are unsuited, and could lead to development of design storms with exceedance probabilities that do not align with the flooding they produce. In many cases, the use of design storms based on event rainfall would tend to overestimate corresponding floods peaks in SEOF catchments. For example, Hill et al. (1998) demonstrated - for ten catchments in Australia - that use of design events that did not account for initial losses resulted in overprediction of the 10% annual exceedance probability flood (10-year return interval) by an average of 47% when compared to analysis of recorded peak flows. In SGWF catchments, where peak groundwater levels can lag peak rainfall events, design storms could either over- or under-estimate peak flooding. This is particularly problematic since groundwater flooding is generally not considered in flood maps or policies, and groundwater flood risk mapping has not been well developed (Hughes et al., 2011).

In short, event-based approaches suffer from a fundamental limitation when applied to SEOF and SGWF landscapes, namely that the initial conditions of the catchment – e.g., soil moisture, initial losses, and groundwater levels – must be specified exogenously. That is, they must be derived from data and procedures separate from the event analysis. The flood simulation process then needs to allow for the joint probability of initial states of the catchment and rainfall conditions, whose distributions may be correlated or independent of each other. Obtaining data on catchment initial conditions may be a significant problem in areas where gauged data are scarce (Kuczera et al., 2006). In these cases, design events from rainfall data must be specified such that they account for these processes. For example, Maréchal et al. (2008) proposed a cumulative 25-day rainfall could be used to predict the occurrence of groundwater flooding in karst systems, and in Western Australia, the 72-hour, 50% annual exceedance probability event (2-year return interval) is recommended for design purposes in shallow groundwater sites (IEWEA, 2016). Where gauged data are available, however, continuous hydrologic models can be used to characterize catchment conditions through calibration, which can then applied to determine the flood that corresponds with a given design rainfall.

Mismatch of model structure and hydrologic processes

The most common hydrologic models applied in urban areas are, however, also predicated on the assumption of IEOF (see Section 2.2) and are therefore poorly suited to characterize

important catchment conditions that are required for accurate estimation of SEOF and SGWF runoff.

Because IEOF-based hydrologic models lack explicit methods for characterizing runoff pathways across and between scales relevant to SEOF and SGWF – e.g., changes in soil moisture, runoff generating areas (Easton et al., 2007), or individual storm runoff pathways (Buchanan et al., 2012) – calibrating such models in SEOF and SGWF catchments depends on tuning model parameters that do not represent relevant SEOF and SGWF processes. Hydrologic predictions in SEOF and SGWF catchments based on a IEOF-based model are therefore invariably subject to statistical bias and underestimation of uncertainty. In the context of urban runoff management, such uncertainty can have major consequences for infrastructure and flood risk estimates. Design of a culvert intended to convey large events (e.g., 1 to 2% annual exceedance probability) could result catastrophic flooding and damage if its design based on inaccurate runoff predictions. For more common design storms (e.g., 50% annual exceedance probability, or 2-year return interval), it could lead to nuisance flooding – which can also be costly (Moftakhari et al., 2017) – or to issues in ecological systems that depend on a certain frequency, duration, and magnitude of these smaller flows.

The occurrence of SEOF and SGWF not only impacts predictions of peak flows, volumes, and timing, but also the pathways of runoff throughout a catchment. These pathways are important for pollutant mobilization and transport. In catchments dominated by SGWF, pollutants from different sources (e.g., from impervious surfaces and from permeable areas) accumulate in the groundwater, and are transported slowly to the receiving water. In catchments dominated by SEOF, areas at high risk of transferring pollutants occur where pollutant areas intersect with areas of high mobilization and propensity for surface runoff generation (Thomas et al., 2016; Walter et al., 2000). In both cases, pervious surfaces such as lawns may be important pollutant sources (Tuomela et al., 2019) although many urban runoff models ignore their contribution (Pitt et al., 2005).

In summary, use of IEOF-based urban hydrologic models to predict runoff from SEOF and SGWF landscapes presents multiple pathways for large errors. These errors stem from a mismatch in processes, spatial, and temporal scales. Namely, because IEOF-based models do not represent SEOF and SGWF processes (e.g., spatial variation in soil moisture dynamics, interaction between subsurface and surface flows, groundwater fluctuation), use of these models in SEOF and SGWF landscapes relies on calibration of IEOF model parameters that may not be representative of these SEOF and SGWF processes. The resulting model does not represent reality, and, while it may accurately replicate the events on which it was calibrated, its application to future scenarios (or design rainfall) presents major risks when its results are used to inform planning and design of infrastructure, such as WSUD.

Ineffective management controls

WSUD management approaches predicated on the assumption of IEOF present multiple challenges in areas that exhibit SEOF or SGWF runoff. At best, the mismatches in processes and spatial and temporal scales that result may lead to ineffective or inefficient management.

At worst, these mismatches may lead to negative outcomes for infrastructure and ecological systems.

The negative outcomes of infiltration based WSUD in shallow groundwater environments can arise either from: (i) the impact of WSUD on shallow groundwater, or (ii) impacts of shallow groundwater on WSUD. Increased infiltration from WSUD in shallow groundwater areas can lead to groundwater mounding, which can slow down or inhibit infiltration to the subsurface, decrease travel time to the groundwater, and subsequently increase the risk of groundwater contamination. At a catchment scale, the spatial distribution of WSUD relative to topographic low points can exacerbate groundwater mounding issues (Bhaskar, Beesley, et al., 2016; Machusick et al., 2011; Endreny & Collins, 2009) and affect groundwater dynamics (K. Zhang & Chui, 2020). These impacts extend beyond the footprint of an individual WSUD facility: infiltrated stormwater has been identified as a potential source of aquifer contamination (Clark & Pitt, 2007), basement and infrastructure flooding, and inflow to wastewater networks leading to waste water treatment plants (Bhaskar, Beesley, et al., 2016). This increases the potential for groundwater flooding, which, compared to fluvial flooding, can leave areas inundated for many months, often results in substantially higher damages (C. Green et al., 2006). For example, in Perth, Western Australia, increased groundwater levels - in part due to increased infiltration from WSUD (C. Ocampo et al., 2017; Barron et al., 2013) - have resulted in groundwater flooding and costly damage to public infrastructure Bhaskar, Hogan, & Archfield (2016); Claydon et al. (2020).

At the same time, high groundwater can compromise the effectiveness of stormwater approaches, e.g., by reducing the unsaturated zone available beneath infiltration-based WSUD (C. Ocampo et al., 2017). This can reduce effectiveness of WSUD in treating surface runoff, or result in increased peak flows and runoff volumes due to groundwater seeping into underdrains during rain events (K. Zhang & Chui, 2019). Worse still, WSUD in high groundwater areas can mobilize nutrients that have accumulated in the subsurface (Gorski & Zimmer, 2020), e.g., build-up of excess applied nitrogen (Fovet et al., 2015; Sebilo et al., 2013) – contributing substantial nitrogen loads to downstream water bodies (Abbott et al., 2018; Dupas et al., 2019). For example, a recent study in Baltimore, Maryland (US) - where SEOF runoff contributes significantly to streamflow (Lim, 2016) - has shown sub-optimal performance of infiltration-based stormwater management approaches in mitigating non-point source pollution (Miles & Band, 2015).

These issues are exacerbated by the current planning approach which emphasizes site-scale implementation and IEOF-based models (Figure 2.9). In accordance with the IEOF assumption, in which the relevant spatial scale corresponds to spatial variation in surface properties, planning and design occurs at the scale of a development site and often disregards scales outside those of a development footprint (e.g., topographic controls or groundwater level controls on saturation). This site-scale focus has led to the preponderance of site-scale performance studies, which similarly do not consider infiltration pathways off-site, and, coincidentally, find that infiltration systems efficiently attenuate peak flows and runoff volume at the site-scale (Davis, 2008; Dietz & Clausen, 2008; Hunt et al., 2006). Catchment scale modeling studies have simulated that infiltration systems are able to reduce peak flows

(Gagrani et al., 2014; Palla & Gnecco, 2015; Damodaram et al., 2010; Burns et al., 2015), and as a consequence reduce the risk of flooding (Burns et al., 2015). However, as described above, most of these models are also based on the assumption of IEOF; their prediction of runoff reduction from infiltration-based WSUD is therefore a product of the model structure and assumptions. These models are not suited for simulating the complex interactions between surface and groundwater that are driven by or impact performance of WSUD, nor their implications for pollutant transport.

Because infiltration-based WSUD are implemented at this scale without full understanding of their limitations under field conditions or their context within the catchment (Urbonas, 2000), their effectiveness at the catchment sale are highly uncertain. Indeed, while there are fewer catchment-scale experimental studies of WSUD, those that exist give mixed results regarding effectiveness of WSUD: some studies have found that infiltration WSUD reduces runoff volumes and peak flows (e.g., Jackisch & Weiler, 2017), while others have found that they have little to no impact at the catchment scale (e.g., Bell et al., 2016; W. Shuster & Rhea, 2013).

2.5 Discussion

Remedying these problems requires modifying the default approach to urban stormwater management so that planning and design frameworks can be cognizant of and apply to a more diverse range runoff generation mechanisms (Figure 2.10). This does not entail abandoning existing stormwater management approaches or retreating from the commitments to Water Sensitive Urban design. Rather it entails broadening these frameworks so that their many advantages and advances, developed over 100 years of urban hydrology, can be brought to bear on a wider range of catchments than at present.

Identify the dominant hydrologic processes

The first fundamental challenge is to ensure that urban runoff management efforts begin by investigating the hydrological processes occurring in urbanized or urbanizing sites. This would be well supported by more research level investigations addressing the diversity and prevalence of different flow pathways in urban areas, through tracer studies (e.g., Jefferson et al., 2015; Christian et al., 2011; Buttle et al., 1995; W. Sidle & Lee, 2006; Pellerin et al., 2008), or through examination of solute concentrations and stream discharge (Gorski & Zimmer, 2020; Thompson et al., 2011; S. E. Godsey et al., 2009). While such investigations are potentially time and resource intensive, they would yield insight into more readily-observable indicators of runoff generation processes, which could be translated into site assessment frameworks suitable for widespread initial evaluations. Identifying areas with uniform or quasi-homogeneous hydrological response to precipitation (i.e., evaporation, infiltration, and runoff processes) could be used to identify the relevant risks, modeling approaches, and management for each unit. For example, in the context of sites likely to be impacted by

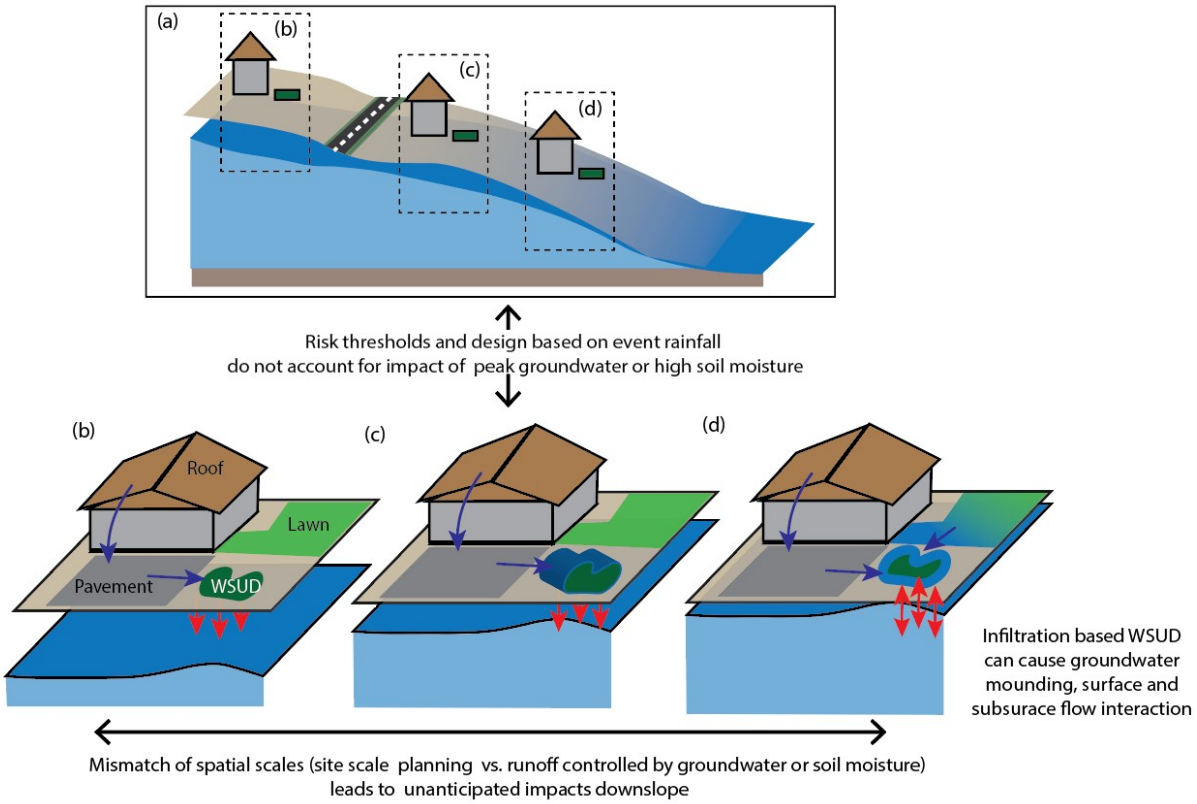

Figure 2.9. Theoretical impacts of infiltration-based WSUD in high groundwater environments. Hillslope-view of shallow groundwater in (a), with site-scale design of infiltration-based WSUD in (b) - (d). In (b), the groundwater is far below the land surface and WSUD would be deemed appropriate in site-scale analysis. Further down the hillslope, however, groundwater levels increase; peak groundwater can be exacerbated by infiltration upslope (c). At the footslope, the groundwater level is nearly at the surface, causing saturation from the subsurface during storm events (d).

shallow groundwater flow, Claydon et al. (2020) developed a risk assessment framework that did not require detailed site investigation or modeling, but which offered guidance as to the appropriate design and investigative approaches suitable to different levels of risk posed by shallow groundwater. Similar risk assessment frameworks addressing hydrological risks related to different runoff mechanisms would be valuable in guiding subsequent analysis, modeling and management.

Adapt management to match dominant processes

The second challenge is then to match these hydrological process(es) to relevant management approaches. Assuming that the broad stormwater management frameworks developed for IEOF - namely assessment of risk of a specific flow level/velocity/volume occurring, and

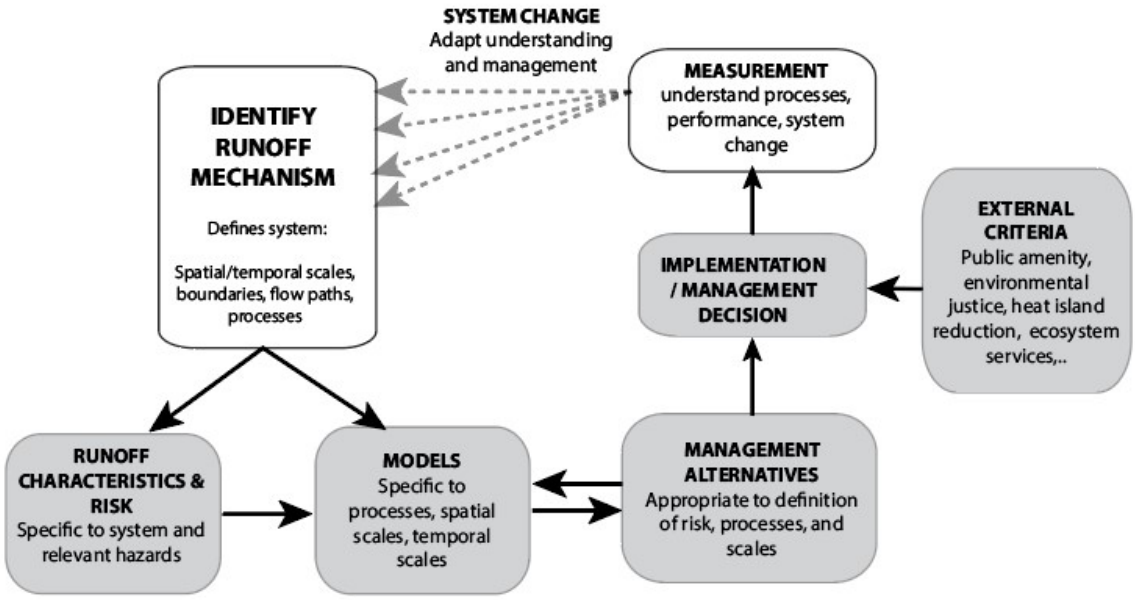

Figure 2.10. Adaptation of runoff management paradigm towards process-based management

designing to manage an acceptable level of risk - would be maintained in catchments with other flow processes, several new management questions arise.

Adopt hazard-specific definitions of risk

First among these is the treatment of risk. Namely, is a flow-based outcome the right hydrological metric to which management 'risks' should be linked? In cases where fluvial flooding is the hazard to be mitigated (e.g., arising from IEOF and SEOF), likely the answer is 'yes'. However, in areas with shallow groundwater, management of the peak height of water table (e.g., the elevation of the phreatic crest) may be more closely tied to flood hazards than is flow in channels or pipes.

Further, as outlined in Section 2.3, the meteorological drivers of runoff generation through mechanisms other than IEOF are generally not solely associated with event-scale rainfall, and spatial drivers are not limited to local or even catchment scales: seasonal variation in rainfall, within-hillslope variation of saturated areas, and regional groundwater gradients can impact – and even drive – runoff generation. Risks may therefore vary depending on conditions outside those of a development footprint, e.g., due to location at intersection of groundwater mounds, or due to topographic controls on saturation risk. The models and methods used to define risk therefore need to align with the processes that drive runoff generation, and account for their variation over appropriate spatial and temporal scales.

Apply process-specific hydrologic models

Secondly is the question of whether current urban hydrologic models can reliably and accurately predict flood risk at the appropriate spatial and temporal scales. The consistency of model integration at different spatio-temporal scales is a major challenge (Wagener, 2003) and is not unique to urban areas. However, the ability to simulate SEOF, SGWF, and IEOF processes together becomes particularly important in urban settings, where extreme spatial variations in land cover (e.g., grass, pavement, trees, gardens, and bare ground) increases the complexity of infiltration and saturation processes (Borgström et al., 2006; Lim, 2016; Miles & Band, 2015; Valeo & Moin, 2000), and pipe networks and infrastructure influence groundwater flows (Lerner, 1990). Such extreme variation in surface and subsurface properties undoubtedly complicate underlying hydrologic mechanisms, affecting the temporal interactions between precipitation time scales and characteristic time scales of catchment response (Robinson & Sivapalan, 1997). This variability presents major challenges for understanding which processes to simulate in urban hydrologic models, and at what scales. At a minimum, models should reflect the conceptual understanding of hydrological processes in the catchment, incorporate driving and response variables across relevant spatial and temporal scales, and inform the design of management infrastructure to mitigate risk. While some attempts have been made to integrate these processes and scales into urban hydrologic models (e.g., urban variable source area modeling censu Valeo & Moin, 2001; Miles & Band, 2015), these approaches are rarely, if ever, applied in practice.

Plan and design process- and scale- appropriate management controls

The final question is whether the current planning and design of management controls (namely, infiltration-based WSUD) are well-suited to mitigate this risk. Where risk is due to impermeable surfaces, enhancing infiltration is desirable. Where risk is due to subsurface saturation, enhancing infiltration is counterproductive, and reducing recharge/enhancing evaporation/retaining or storing water may be preferable (e.g., Burns et al., 2012). Some municipalities have adopted criteria that define where and when infiltration based WSUD is feasible. For example, Western Washington (US) has adopted region-wide criteria that limit infiltration WSUD facilities near drinking water wells, in groundwater protection areas, and in areas of high groundwater or shallow bedrock (Washington State Department of Ecology, 2019). However, such criteria still largely treat a site as independent from its catchment scale context; this can lead to adverse impacts if the factors controlling runoff response occur at larger spatial scales. For example, infiltration WSUD may be feasible a site, but it could exacerbate groundwater flooding in downslope areas if a shallow water table is present (e.g., as in Figure 2.9d).

Regional strategies, environmental justice, and hydrological transitions

The recognition of runoff processes other than IEOF in urban landscapes brings up even broader challenges about how to proactively manage these conditions on regional scales. Desaturation of soils is difficult and may only be achievable via 'hard' engineering approaches such as filling and draining landscapes - processes which are not only costly, but are themselves often problematic. Hydrological regimes should feature in land suitability assessments which inform where new urban land will be released for development. In the same way that 'Room for the river' policies in the Netherlands (see e.g., Samuels et al., 2006) and 'Making space for water' strategy in the United Kingdom (see e.g., Wilby et al., 2008; Samuels et al., 2006) represent a shift in land use planning adaptation to fluvial flood risk, providing 'Room for the groundwater' or 'Room for soggy areas' may be equally important in areas where flooding is driven from the subsurface. Designating hydrologically constrained land to non-urban land uses, e.g., through buyout programs, may be preferable to the alternatives of dramatic and expensive engineering works, or forcing urban residents to live with the problems caused by groundwater or other nuisance flooding.

There are important environmental justice elements to this problem. Low-income and minority communities are disproportionately affected by extreme flood events every year, an inequality that is predicted to grow worse as the frequency and magnitude of floods increase (Walker & Burningham, 2011; D. Bullard et al., 2019). How a 'Room for the groundwater' policy would impact equity in flood prone regions – currently occupied by disadvantaged communities – is unknown. The intersection of exposure to hydrologic risks, privilege, and access to effective migitation of those risks has barely been explored beyond the case of riverine flooding - yet the prevalence of hydrological constraints in the "mortgage belt" of cities like Perth begs the question of environmental justice in this element of regional land use planning.

Mitigation of this problem at site scales with WSUD can also lead to inequities. WSUD are often advertised as 'multi-benefit' or 'multifunctional', providing social, cultural, and health benefits (Lovell & Taylor, 2013; Spahr et al., 2020). For example, in addition to application for urban runoff management, WSUD can also be part of efforts to reduce the urban heat island effect (Norton et al., 2015; Makido et al., 2019; Oke, 1973), or part of smart growth initiatives designed to reduce sprawl by making the central cores of urban regions more attractive. Despite, or perhaps because of, their multiple benefits, such projects can lead to 'environmental gentrification', by increasing property values and displacing residents of low socio-economic status impacted by complex legacies of residential segregation and discriminatory land-use decision-making. Over time, the loss of affordability can result in segregated communities disproportionately burdened by exposure to cumulative health hazards or unable to benefit from the restored environments (Checker, 2011; Bullard, 1994).

All of these challenges are compounded by an uncertain and changing future. On long time scales, climate change and associated changes to rainfall and evapotranspiration patterns can potentially push urban areas into new, novel hydrologic regimes (Zipper et al.,

2018). On shorter timescales, however, urban water management interventions may also shift underlying hydrologic processes. In extreme conditions – e.g., high storage in the subsurface or very low storage in the subsurface – urban water management infrastructure is unlikely to induce a change in hydrologic regime. In less extreme conditions, however, a major challenge is presented by the potential for urban runoff management to lead to a novel hydrologic regime.

Increasingly, researchers have been asking whether such regime shifts could be produced by the widespread use of WSUD. While WSUD often aims to restoring predevelopment hydrology, this rarely occurs. Instead, as proposed by Jefferson et al. (2017), and subsequently supported empirically by multiple studies (e.g., Hopkins et al., 2020; McPhillips et al., 2019), the implementation of WSUD can shift the hydrologic system onto a new trajectory, which may not return it to the initial predevelopment state. For example, the naturally flashy streams in Phoenix, Arizona became less flashy after urbanization due to stormwater control measures that promote infiltration and slow flows (McPhillips et al., 2019). The potential for WSUD to induce hydrologic regime shifts raises important questions. Are WSUD shifting previously well-drained (IEOF) landscapes to 'soggier' conditions? What do these soggy conditions mean for our definitions of risk, our hydrologic models, and our management approaches?

Predicting these regime shifts is the first step towards identifying cities at risk of these shifts, and towards adapting management approaches to achieve a realistic, desired, future state. Such an approach represents a departure from the current urban management paradigm by recognizing that urbanization has shifted the natural hydrologic regime, and that management approaches should aim to shift to a desired future state rather than back to natural conditions.

2.6 Conclusions

The processes involved in urban runoff are not as simple as often assumed under the infiltration excess overland flow (IEOF) paradigm. We have argued that the current paradigms for managing urban stormwater, including the growing acceptance and use of water sensitive urban design approaches is problematic in the many urban areas worldwide where runoff generation mechanisms other than or in addition to IEOF prevail. We have shown that these problems arise due to: (1) the mismatches in the spatial and temporal scales of the most important drivers of IEOF production with the spatial and temporal scales driving the behavior of other runoff generation mechanisms (saturation excess overland flow and shallow groundwater flow); (2) the omission of relevant processes from widely used urban runoff models; and (3) the potential for infiltration-based runoff management approaches to generate or enhance the generation of runoff via subsurface mechanisms.

Developing a process-based management approach therefore requires a better understanding of the range of hydrological processes that prevail in urbanizing areas and

adoption of models that are capable of predicting how these processes will interact and respond to changes in climate, land use, and management approaches. However, the onus for this does not just fall on the stormwater consultant, the stormwater permit manager, or the practicing hydrologist. Rather, this calls for a more deliberate collaboration between researchers, practitioners, and communities to better understand how water flows in urban areas, what this means for risk, and what management of this risk looks like in 'soggy' urban areas under change.

Chapter 3

A geospatial approach for estimating hydrological connectivity of impervious surfaces [1]

Abstract. Recent studies have reported that connected impervious areas – those impervious surfaces that contribute directly to runoff in a storm network or stream – are a better indicator of hydrologic response, stream alteration, and water quality than total impervious area. However, most methods for quantifying connected impervious areas require major assumptions regarding the definition of 'connection', potentially over-simplifying the role of variable climates, slope gradients, soils conditions, and heterogeneous flow paths on impervious surface connectivity. This study presents a new conceptual model and method for estimating hydrologically connected impervious areas (HCIA) that explicitly considers the effect of landscape and storm variability. The model separates impervious surfaces into two categories: directly or physically connected (A_{phys}) and variably connected (A_{var}) (impervious that drains to pervious). Of these categories, we investigated the sensitivity of A_{var} connectivity to varying soil conditions, slope gradients, rainfall properties, and hillslope geometry using PySWMM (a python interface for SWMM5). Simulations spanned a large parameter space with varying soil, slope, rainfall properties and geometries (i.e., relationships between the impervious and downslope pervious areas). PySWMM simulations were used to train and test a regression tree that predicts infiltration and connectivity of runoff from A_{var} surfaces, which provides excellent fidelity with PySWMM outcomes. To enable use of these methods in practice, we developed an ArcGIS tool that (1) delineates subcatchments; (2) extracts the impervious surface categories A_{phys} and A_{var}; (3) applies the regression tree algorithm to predict the fraction of incident rainfall that produces runoff across A_{var}; and (4) summarizes the resulting HCIA by subcatchment. Analysis of the regression feature importance shows

[1] This chapter was published in 2020 with the title "A geospatial approach for estimating hydrological connectivity of impervious surfaces" in the *Journal of Hydrology* with co-authors: Bell, C., Eisenstein, W., Hogue, T., Kondolf, G. M.

that, in general, A_{var} connectivity is highly sensitive to the soil type, rainfall depth, area fraction, and antecedent soil moisture conditions of the downslope pervious area. We find that temporally varying parameters (e.g., rainfall and antecedent soil moisture) control A_{var} connectivity in areas with low permeability soils, while spatial flow path variability (e.g., relative quantity of disconnecting pervious area) controls A_{var} connectivity in areas with highly permeable soils. The methods developed in this study can be used to identify impervious surface connectivity more accurately in urban watersheds, representing an important step forward for incorporating spatial heterogeneity in stormwater modeling and planning.

3.1 Introduction

Increased urbanization involves increased extent of impervious surfaces, such as roads, parking lots, and rooftops. These surfaces prevent infiltration of rainwater and instead shed water by surface runoff into streams, increasing storm runoff for a given rainfall (Leopold, 1968), thereby increasing the erosive force of stormflows, which in turn causes erosion of stream beds and banks (Booth & Jackson, 1997; Gillies et al., 2003; Walsh et al., 2005). By eliminating infiltration and the filtering effect of rainwater flowing through soil, pollutants accumulate on roads, parking lots, and rooftops, and polluted runoff from these impervious surfaces flows directly (untreated) into receiving lakes, bays, and streams as non-point-source pollution (Arnold & Gibbons, 1996a).

By virtue of its easy quantification via mapping from aerial imagery, total impervious area (TIA) – the total area occupied by impervious surfaces – has long been used as an indicator of the degree of urbanization and consequent effects of urbanization on hydrologic conditions. However, TIA does not distinguish between impervious areas that are 'directly connected' to streams (being adjacent or connected via stormwater pipes) from those that are distant and whose runoff flows over pervious surfaces. If runoff from such an impervious surface infiltrates prior to reaching the stream, it is effectively 'disconnected' as it does not contribute directly to storm response in the stream; conversely, if its runoff does not infiltrate, but rather saturates the downslope pervious area and produces runoff that reaches the stream channel, it is termed 'indirectly connected' (Boyd et al., 1993). TIA lumps 'directly connected', 'disconnected', and 'indirectly connected' together and thus is limited in its ability to predict runoff at local scales (McGrane, 2016; Crompton et al., 2019; Fletcher et al., 2013; Lim, 2016; Y. Zhang & Shuster, 2014).

The metric directly connected impervious area (DCIA) was introduced to measure impervious areas that are physically connected to the stormwater network or stream channel, and can be mapped directly, though it may require information beyond that available from aerial imagery, such as maps of storm drainage infrastructure (e.g., Hwang et al., 2017; Lee & Heaney, 2003a; Seo et al., 2013). While the runoff from directly connected surfaces may be straightforward to measure and model, runoff from indirectly connected impervious areas is more complicated because it depends on how much runoff is

infiltrated into pervious areas before reaching a stream, which depends on the flowpath length and slope over pervious soils, and their infiltration rate. Infiltration rate is affected by soil texture, surface roughness, vegetative cover, and soil moisture content (or saturation), which is influenced by antecedent rainfall. Infiltration can also occur in surfaces that we consider to be 'impervious', e.g., through cracks in asphalt or concrete. In an attempt to account for the combined effect of these various factors, the metric effective impervious area (EIA) was introduced by Miller (1978) (S. Epps Ph D. & Hathaway, 2018). While EIA and DCIA are sometimes used interchangeably, their methods of estimation differ. Rather than being mapped directly from surface features EIA is typically back-calculated from streamflow and rainfall (e.g., Boyd et al., 1993; Ebrahimian, Wilson, & Gulliver, 2016; T. H. Epps & Hathaway, 2019; Han & Burian, 2009a; Roy & Shuster, 2009; Walsh et al., 2005), or determined through model calibration (e.g., McNamee, Porter & Seeley, Inc. et al., 1994; Sutherland, 1995). EIA therefore implicitly accounts for catchment characteristics affecting hydrologic response (e.g., soils, slope, surface roughness, spatial patterns, and rainfall). Because EIA relies on stream flow and rainfall inputs, it is limited to the scale and locations at which these data are available, which, despite continuous efforts to accumulate hydrological data, is lacking in most catchments of the world (Blöschl, 2005; Tegegne & Kim, 2018).

DCIA is mapped directly, so its quantification does not depend on stream flow or rainfall data availability. Spatially explicit maps of impervious surface connection inherently assume that 'physical' connectivity is indicative of 'hydrological' connectivity. These two types of connectivity may differ (Bracken & Croke, 2007): physical connectivity refers to the physical connection of points, lines, or polygons, while hydrologic connectivity refers to the connectivity of water pathways across a landscape. Physical connectivity metrics – such as DCIA and TIA – do not implicitly account for hydrologic processes or interactions, so they may or may not correlate with actual hydrologic connectivity (Bracken et al., 2013; Bracken & Croke, 2007; Lexartza-Artza & Wainwright, 2009). For example, impervious areas which are physically and hydrologically disconnected under certain rainfall scenarios may become hydrologically connected under more intense rainfall scenarios as downslope pervious patches become saturated.

The shortcomings of EIA and DCIA, as reflected in the methods used to produce them, present both a challenge and an opportunity to improve our understanding of controls on the hydrologic contribution of impervious surfaces across heterogeneous flow paths. In this study, we define a third metric, hydrologically connected impervious areas (HCIA), to refer to spatially explicit (mapped) estimates of the proportion of impervious surfaces that are hydrologically connected to the storm sewer system or stream network. Here, we use 'impervious' and 'pervious' as contrasting terms, but acknowledge that this is a simplification of the continuum of conditions that exist. HCIA depends on both the physical connectivity of impervious areas, explicitly quantified by DCIA, and the hydro-geomorphic conditions, e.g., soil moisture conditions, soil types, rainfall rate, geology, which are implicitly incorporated in the quantification of EIA.

Current methods for spatially explicit EIA estimation require rainfall and runoff datasets

(e.g., Ebrahimian, Gulliver, & Wilson, 2016; S. Epps Ph D. & Hathaway, 2018), the use of high resolution ecohydrological models (Easton et al., 2007; Miles & Band, 2015), or geostatistical analyses (Ebrahimian, Gulliver, & Wilson, 2016; Lim, 2016). Consequently, these efforts are often site-specific and extrapolation of their results to other watersheds is limited. Thus, a generalizable approach for estimating hydrologically connected impervious areas is needed. The incremental contribution of the present study is to (i) explicitly define controls on impervious surface hydrologic connectivity, and (ii) to present a generalizable model to predict and map hydrologically connected impervious areas, including indirectly connected impervious areas.

In this study, we evaluated the controls on impervious surface runoff contribution by varying spatial arrangements of impervious/ pervious areas, rainfall depth, soil types, and antecedent soil moisture conditions. To facilitate dissemination into practice, we developed a transferable ArcGIS tool that provides estimates of HCIA across urban watersheds, and we present a case study of the ArcGIS tool applied to a residential sewershed.

3.2 Conceptual model of hydrologically connected impervious areas

We define total impervious area within a catchment by two impervious surface categories: rooftops (A_{roof}) and ground-level impervious (A_{ground}), so that TIA = A_{roof} + A_{ground} (Figure 3.1). The portion of roof A_{roof} and A_{ground} that are both physically and hydrologically connected to the storm drainage system are considered 'physically contributing impervious': A_{phys}. Those portions of A_{roof} and A_{ground} that are not physically connected to the storm drainage network but rather produce runoff that flows as 'runon' to pervious areas are considered 'variably contributing impervious': A_{var}. The total hydrologically connected impervious areas HCIA along the flow path shown in Figure 3.1 can thus be described as:

$$HCIA = \phi_{phys} A_{phys} + \phi_{var} A_{var} \tag{3.1}$$

where ϕ_{phys} and ϕ_{var} refer to the fraction of incident rainfall that contributes to runoff response on physically connected surfaces A_{phys} and variably connected surfaces (A_{var}), respectively. A_{phys} and A_{var} are further defined as:

$$A_{phys} = A_{phys,roof} + A_{phys,ground} \tag{3.2}$$

$$A_{var} = A_{var,roof} + A_{var,ground} \tag{3.3}$$

where $A_{phys,roof}$ and $A_{phys,ground}$, refer to the physically connected roof and ground-level impervious areas, and $A_{var,roof}$ and $A_{var,ground}$ refer to the variably connected roof and ground-level impervious areas, respectively.

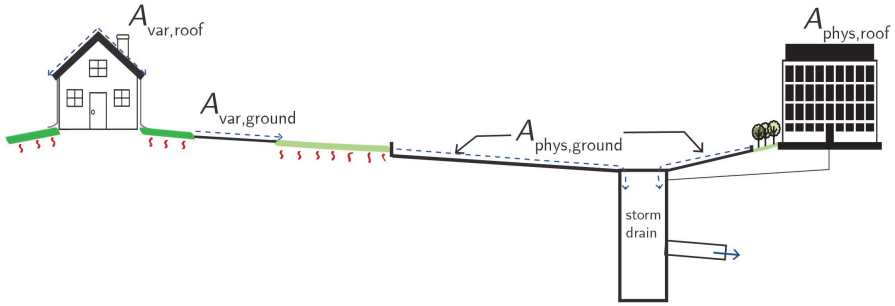

Figure 3.1. Conceptual model of impervious surface categories: directly or physically connected (A_{phys}) and variably connected (A_{var}) (impervious that drains to pervious). A_{phys} is comprised of physically connected rooftop ($A_{phys,roof}$) and ground-level impervious ($A_{phys,ground}$), while A_{var} is comprised of variably connected rooftop ($A_{var,roof}$) and ground-level impervious ($A_{var,ground}$). The hydrological connectivity A_{phys} and A_{var} are given by ϕ_{phys} and ϕ_{var} respectively. In this study, we assume $\phi_{phys} = 1$, so that all physically connected impervious areas are fully connected. ϕ_{var} depends on rainfall, runoff, and infiltration dynamics between A_{var} and the downslope pervious area.

Determining A_{phys} and A_{var}

Remote sensing data can be used to classify types of impervious surfaces into rooftop (A_{roof}) and ground-level impervious areas (A_{ground}). Ground-level impervious areas can be further separated into $A_{phys,ground}$ and $A_{var,ground}$ using a combination of high-resolution digital elevation models (DEM), flow paths, and drainage networks (Han and Burian, 2009). Remote sensing datasets alone cannot directly discern physically or variably connected rooftop areas ($A_{phys,roof}$ or $A_{var,roof}$) (Han & Burian, 2009a; Redfern et al., 2016) because buildings may pipe roof runoff directly to the storm drainage system. Consequently, determining an accurate estimate of $A_{phys,roof}$ and $A_{var,roof}$ may require site-specific and time-intensive surveys and field investigations (Han & Burian, 2009a; Roy & Shuster, 2009). The few studies that have endeavored in such time-intensive surveys often report rooftop connectivity values by land use class (e.g., Alley & Veenhuis, 1983; Lee & Heaney, 2003a). These averages are sometimes applied to other study areas as an estimate of rooftop connection (Han & Burian, 2009a). However, there are a range of local variables – e.g., land use history, development codes, local retrofit programs, and homeowner preference – that influence the connectivity of roof areas. Indeed, there is a

wide range of rooftop connectivity values even within specific land use categories reported in the literature (Ebrahimian, Gulliver, & Wilson, 2016), suggesting that land use is a poor predictor of connectivity across different jurisdictions. Jurisdiction-specific rooftop connectivity surveys, however, may provide a reasonable estimate for $A_{phys,roof}$ or $A_{var,roof}$, particularly if these surveys are paired with review of development codes and development history of the region.

Determining ϕ_{phys} and ϕ_{var}

Estimating the hydrologic contribution of A_{phys} and A_{var} presents a separate challenge. Because A_{phys} does not encounter pervious areas en route to the stormwater network, losses along its flow path are likely to be limited to storage depression and initial abstractions. For simplicity, we assume here that ϕ_{phys}) is some constant value 1. We note, however, that previous research has shown significant variability in the fraction of rainfall that produces runoff (Redfern et al., 2016), with values ranging from 0.09 on brick areas (Mansell & Rollet, 2006), to 0.16 on deteriorated asphalt concrete, to 0.74 on asphalt concrete in good condition (Ramier et al., 2004). There are also cases in which ϕ_{phys} may be greater than 1. For example, if a rain event exceeds the capacity of the downstream drainage system, overflow from A_{phys} may be routed to A_{var}.

In contrast, A_{var} surfaces are routed to pervious areas, therefore their connectivity fractions (ϕ_{var}) are likely to be subject to time varying infiltration loss, and depend on factors like downslope pervious areas, soil conditions, slope, and rainfall intensity (Crompton et al., 2019; Pappas et al., 2008; Y. Zhang & Shuster, 2014; W. D. Shuster et al., 2008). The remainder of this study focuses first on defining the factors that influence ϕ_{var}, and second on developing geospatial methods for extracting areas of these impervious surface connectivity types (A_{phys} and A_{var}), applying respective connectivity fractions (ϕ_{phys}) and ϕ_{var}), and estimating HCIA for ungauged catchments.

3.3 Methods

Overview

Our approach involves three main steps, shown schematically in Figure 3.2 and described below. First, we utilized a Python interface for the Stormwater Management Model (PySWMM) (McDonnell et al., 2020) to model factors that could influence ϕ_{var}. We simulated infiltration and runoff across a range of pervious area fractions, soil textures, antecedent soil moisture conditions, slopes, and rainfall scenarios. Second, we developed a generalized relationship for ϕ_{var} as a function of these factors using a regression tree algorithm. Third, we developed an ArcGIS tool that implements the proposed conceptual framework to estimate HCIA by identifying the impervious surface categories A_{var} and

A_{phys} and applying their respective connectivity fractions ϕ_{var} and ϕ_{phys}). As a case study, we tested this ArcGIS tool in the Berkeley Lake sewershed in Colorado, USA.

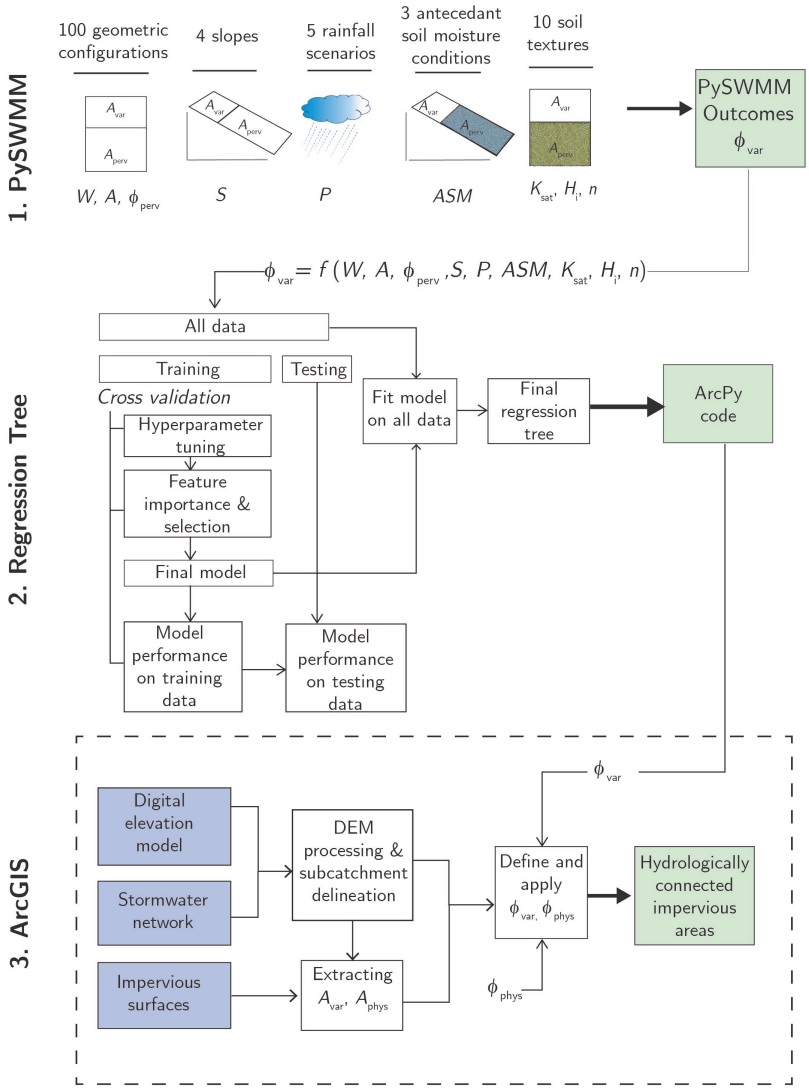

Figure 3.2. Schematic of methods. 60,000 PySWMM simulations of runoff and infiltration across various geometry, soil texture, slope, antecedent soil moisture, and precipitation scenarios are used to compute metrics IF and ϕ_{var} $(1-IF_{runon})$. Regression tree analysis are used to develop generalized relationship between ϕ_{var} and geometry, soil texture, slope, antecedent soil moisture, and precipitation scenarios. The regression tree is translated to ArcPython code, and coupled with an ArcGIS tool that delineates subcatchments, extracts impervious surface categories A_{phys} and A_{var}, applies connectivity fractions ϕ_{phys} (user defined, 1) and ϕ_{var} (from regression tree), and estimates subcatchment HCIA. The dashed line represents the process for which a user of the ArcGIS tool would be subject.

PySWMM modeling to evaluate controls on ϕ_{var}

To determine the sensitivity of A_{var} connectivity to various landscape and storm parameters, we considered only A_{var} surfaces at the ground level, temporarily ignoring effects of A_{roof} and A_{phys}. We used PySWMM to simulate runoff and infiltration at the outlet of an idealized catchment consisting of an impervious area (A_{var}) routed to a downslope pervious area (A_{perv}). We conducted a total of 60,000 model simulations across two parameter sets: (1) 150 plausible rainfall, soil moisture, and soil texture scenarios; and (2) 400 geometric parameter combinations (total area, width, pervious fraction, and slope).

Table 3.1. Summary of parameter ranges used for PySWMM modeling

Parameter	Description	Units	Values
Soil texture	See Table 3.2	–	See Table 2
P	24-hr precipitation depth	cm	0.5, 2.5, 5, 7.6, 10.2
ASM	Antecedent soil moisture	–	SAT, FC, WP
S	Slope	%	1, 2, 3, 4
A	Total subcatchment area	hectare	0 - 1.0
ϕ_{perv}	Pervious fraction	m	0. - 1.0
L	Flowpath length	m	1 - 152
W	Width of overland flowpath	m	A/L
N_{imperv}	Manning's n - impervious	–	0.01 - 0.02
N_{perv}	Manning's n - pervious	–	0.05 - 0.8
D_{imperv}	Storage - impervious	mm	1.27
D_{perv}	Storage - pervious	mm	2.54

The 150 rainfall, soil moisture, and soil texture scenarios (Table 3.1) represent factorial combinations of ten pervious area soil textures, four slopes, five 24-hour rainfall depths, and three antecedent soil moisture conditions (ASM). We used the SWMM Modified Green-Ampt infiltration model to simulate infiltration in pervious areas. Green-Ampt infiltration parameters (saturated hydraulic conductivity k_s, suction head ψ_f, and porosity n) for the ten different soil textures were taken from Rawls et al. (1983). Initial moisture deficit (IMD) – the difference between initial soil moisture ϕ_i and saturated soil moisture ϕ_s – varied according to the three ASM conditions and the soil porosity n: saturated soils ($IMD = 0$), field capacity ($IMD = n$ - $\phi_{i,fc}$) , and wilting point ($IMD = n$ - $\phi_{i,wp}$) (Table 3.2). See Appendix B for additional detail on the SWMM Modified Green-Ampt infiltration model. We used the SCS Type II 24-hr synthetic storm distribution, which typifies high intensity rainstorms and applies to the majority of the US by land area (Usda, 1986). The five rainfall depths (P) ranged from 5 mm to 102 mm (0.6 in. to 4 in.), encompassing 95 percent of daily rainfall values across the US (Shrestha et al., 2013).

The 400 geometric parameter values represented combinations of total area A (equal to $A_{var} + A_{perv}$), pervious fraction ϕ_{perv} (equal to A_{var}/A), catchment width W, and slope S

(%). A, ϕ_{perv}, and W parameter values were generated from 100 random values, with A ranging from 0 to 1 ha (0 to 10,000 square meters), ϕ_{perv} from 1 to 100 percent of the total area, overland flow length L from 0 to 152 m (or 500 feet, the maximum likely overland flow length, James et al. (2010a)) – and thus width W from 0 to A/L. Slope ranged from 1 to 4%. The limited slope range was selected because the majority of urban surfaces (e.g., roads, sidewalks, parking lots) have cross-slopes less than ~ 4 % (e.g., City of Seattle, 2020; Jefferson County, 2019), and because slope has been shown to have a limited effect on runoff volumes (Crompton et al., 2019). Manning's roughness values for impervious and pervious areas, N_{imperv} and N_{perv}, as well as depression storage values, $D_{store-imperv}$ and $D_{store-perv}$, were held constant across simulations.

For each simulation, we calculated ϕ_{var} as $1 - IF_{runon}$, where IF_{runon} was defined as the fraction of total A_{var} runoff that infiltrates in the downslope A_{perv}. It is important to note that because the aim of this model was to simulate connectivity of impervious surfaces, IF_{runon} does not represent the fraction of total inflow that infiltrates, but rather the fraction of impervious runon that infiltrates (see Appendix C). The outcomes of the PySWMM simulations were compiled in Python, and the sensitivity of ϕ_{var} to the different rainfall, soil moisture, soil texture scenarios and subcatchment characteristics were evaluated using boxplots.

Table 3.2. Saturated hydraulic conductivity and initial soil conditions for ten soil texture classes and three initial moisture scenarios. Values from Rawls et al. (1983).

Soil texture class (abbrv.)	k_s **(mm/hr)**	Ψ_f **(mm)**	n	θ_i			IMD		
				SAT	FC	WP	SAT	FC	WP
Sand (S)	120.4	49.0	0.437	0.437	0.062	0.024	0	0.375	0.413
Loamy Sand (LS)	30	61.0	0.437	0.437	0.105	0.047	0	0.332	0.39
Sandy Loam (SL)	10.9	110.0	0.453	0.453	0.19	0.085	0	0.263	0.368
Silt Loam (SiL)	6.6	169.9	0.501	0.501	0.284	0.135	0	0.217	0.366
Loam (L)	3.3	88.9	0.463	0.463	0.232	0.116	0	0.231	0.347
Sandy Clay Loam (SCL)	1.5	220.0	0.398	0.398	0.244	0.136	0	0.154	0.262
Silty Clay Loam (SiCL)	1	270.0	0.471	0.471	0.342	0.21	0	0.129	0.261
Sandy Clay (SC)	0.6	240.0	0.43	0.43	0.321	0.221	0	0.109	0.209
Silty Clay (SiC)	0.5	290.1	0.479	0.479	0.371	0.251	0	0.108	0.228
Clay (C)	0.3	320.0	0.475	0.475	0.378	0.265	0	0.097	0.21

k_s = saturated hydraulic conductivity; Ψ_f = suction head at wetting front; n = porosity; θ_i = initial soil moisture; IMD = initial soil moisture deficit equal to$n$ - θ_i; SAT = saturated, FC = field capacity, WP = wilting point.

Regression Tree to Predict ϕ_{var}

The large simulation space (60,000 simulations) presented an opportunity to relate the predictor variables (P, ASM, soil texture, S, A, ϕ_{perv}, W) to the hydrologic outcome of

interest (ϕ_{var}). However, as is the case with many hydrological variables (Iorgulescu & Beven, 2004), the relationships between these predictor variables and ϕ_{var} is nonlinear and thus not well explained by global linear or polynomial regressions, in which a single formula is expected to hold over the entire dataset. Supervised machine learning algorithms, such as regression trees, are being increasingly applied to hydrological science questions due to their ability to make predictions quickly and to distinguish sensitive variables from non-sensitive variables (Iorgulescu & Beven, 2004; Tyralis et al., 2019). Here, we used a regression tree – one such supervised machine learning algorithm – to predict ϕ_{var} from the predictor variables and to evaluate the relative importance of these variables for predicting ϕ_{var}. Regression trees can be used to estimate a response variable from multiple input variables by building a set of decision rules on the predictor variables (Breiman et al., 1984; Prasad et al., 2006; Tyralis et al., 2019). The decision rules apply recursive partitioning to the variable space (Lawrence & Wright, 2001; Prasad et al., 2006), subdividing the dataset into smaller, more manageable chunks of data over which predictions can be made (Tyralis et al., 2019). The number of tree branches, leaf nodes, and features considered when splitting a node are the tree 'hyperparameters', which are tuned prior to training the regression tree. The following sections describe the process used to develop the ϕ_{var} regression tree.

Cross validation

To avoid overfitting in machine learning algorithms, such as regression trees, a model should be validated using 'new' testing data on which it has not been trained. In cross validation, the data is partitioned into n equal sized subsamples, or folds. For each of the n folds, $n-1$ folds are used to train a model, and the remaining fold is used for model validation. This process is repeated a total of n times, until each fold serves as the validation set. Thus, the overall performance is evaluated on data that was not used to train the model, with each observation contributing exactly once to validation (Reid et al., 2015). After partitioning the PySWMM simulation outcomes into training and testing sets using a 70/30 split, we used a 10-fold cross validation process on the training set to define the model hyperparameters, select model features, and evaluate the performance of the final model. For each of the 10 folds, we computed the mean square error (MSE) between ϕ_{var} as determined by the regression and PySWMM:

$$MSE = \frac{1}{m}\sum(Y_i - Y_i')^2 \tag{3.4}$$

where Y_i is the PySWMM prediction for ϕ_{var} (taken as the 'observed' value), Y_i' is the regression tree prediction for ϕ_{var} (taken as the 'predicted' value), and m is the number of predictions made within the fold. The overall cross-validated error (MSE_{CV}) was computed as the average MSE across the 10 folds.

Hyperparameter tuning

Regression tree hyperparameters control the regressor's flexibility and adaptability to the training data. Careful tuning of hyperparameters can improve generalizability of the model and prevent overfitting of the data. We defined the hyperparameter grid composed of hyperparameter ranges, then used a random search algorithm to sample 100 random values from the hyperparameter grid. We performed 10-fold cross validation for each combination of grid values, resulting in 1000 total fittings. We then selected the set of hyperparameters that minimized MSE_{CV} and used these as the hyperparameters in the final model. Details and results of the hyperparameter tuning process are included in AppendixC.

Feature importance and selection

We computed the regression tree feature importance with the Gini importance index to evaluate the relative significance of model features (i.e., the independent variables) in predicting ϕ_{var}. The Gini importance index represents the mean decrease in node impurity resulting from splitting, weighted by the probability of reaching a node (Tyralis et al., 2019). The higher the feature importance, the more significant that feature is relative to others for predicting response. The feature importance values were then used to choose a parsimonious subset of the predictor variables (model features) that can predict the outcome with accuracy comparable to the performance of the complete input set but with greater computational efficiency.

Model performance

We assessed performance of the regression tree model (defined by tuned hyperparameters and selected features) using 10-fold cross validation on the training dataset. To confirm that the final regression tree performed consistently on data on which it was not trained, we also evaluated the performance of the model on the held-out testing dataset. After estimating model performance, we fit a regression tree with the entire dataset (60,000 simulations), and then exported it into a format readable by ArcPython for implementation in the ArcGIS tool.

Sub-tree feature importance

The feature importance metric described above provided insight into how connectivity varies across different storms (given by rainfall) and landscape geometries (given by geometric parameters) or conditions (given by soil type and antecedent soil moisture). Such an analysis does not provide insight into the relative importance of these features within a given storm or landscape – for example, which parameter(s) control hydrologic connectivity in a landscape with a specific soil type, or for a particular storm. To develop a better understanding of within-storm/landscape hydrologic controls, we additionally trained and tested separate regression trees for specific subsets of the dataset (Table 3.3) – which we refer to as 'sub-trees'

– and evaluated feature importance across these sub-trees. These sub-trees were analyzed to illustrate potential within-storm/landscape controls on connectivity and were not used in any subsequent analysis or within the ArcGIS tool.

Table 3.3. Parameter subsets for evaluating within-storm/landscape sensitivity

Parameter	Parameter subset	# simulations	% of all simulations
P	2.5 cm	12,000	20
	10.2 cm	12,000	20
Soil texture	Sand	6,000	10
	Clay	6,000	10
ϕ_{perv}	< 0.2	12,600	21
	> 0.8	13,200	22
ASM	Saturated	20,000	33
	Field capacity	20,000	33
	Wilting point	20,000	33

ArcGIS Tool

The HCIA ArcGIS tool consists of four main steps: (1) DEM processing and subcatchment delineation; (2) extracting the impervious area connectivity types (A_{phys} and A_{var}); (3) defining connectivity fractions (ϕ_{phys} and ϕ_{var}); and (4) computing HCIA for each subcatchment. Each step is summarized below, and the HCIA ArcGIS tool and its full documentation are available for download on GitHub (https://github.com/anneliesesytsma).

Step 1: DEM processing and delineating subcatchment

Inputs to this step are a high resolution (e.g., 1 m) digital elevation model (DEM) (raster); stormwater inlets that represent the outlet of the subcatchment to be modeled (e.g., catch basin or manhole) (points); and a stormwater network of pipes and ditches (polyline). In this step, the DEM is processed to remove sinks, compute the flow direction and flow accumulation rasters, and extract the stream network. The subcatchments draining to each stormwater inlet are delineated using ArcHydro tools.

Step 2: Classifying impervious areas (A_{phys}, A_{var})

Inputs to this step are the DEM and subcatchments (from Step 1), as well as impervious surfaces separated into ground-level impervious and rooftops (shapefile). In this step, an iterative process is used to classify A_{phys} and A_{var} for ground-surface impervious and rooftop impervious areas. First, an initial guess of physically connected impervious ${A_{phys}}^{o}$

is made: physical connectivity of rooftops is based on user input data from e.g., land use assumptions or field investigations, and physically connected ground-level impervious is based on intersection with the stormwater inlet points. An initial guess of variably connected impervious $A^{o}_{var,roof}$ and $A_{var,ground}{}^{o}$ comprise the remaining A_{roof} and A_{ground} surfaces, respectively. Pervious area flow paths downstream of $A_{var,roof}{}^{o}$ and $A_{var,ground}{}^{o}$ areas are quantified using cost distance allocation and cost path functions; impervious areas with downslope flow paths over pervious areas are designated as A_{var}. This process assumes that the building downspouts are located on the downslope-most edge of $A_{var,roof}{}^{o}$ areas. The remaining $A_{var,roof}{}^{o}$ and $A_{var,ground}{}^{o}$ areas with no downslope pervious flow paths are then added to $A_{phys}{}^{o}$ to give A_{phys}.

Step 3: Defining ϕ_{phys} and ϕ_{var}

The next step in the HCIA ArcGIS tool applies connectivity fractions ϕ_{phys}) and ϕ_{var} to their respective areas within each subcatchment. The user supplies a constant value for ϕ_{phys}, ranging from 0 to 1, and specifies the scenarios on which ϕ_{var} is computed (P, ASM, and soil texture class). ϕ_{phys} is applied to all A_{phys} surfaces, including rooftops and ground-level impervious A_{phys} areas. The regression tree algorithm is used to predict ϕ_{var} for each A_{var} as it depends on the user-selected scenario as well as on the geometric characteristics of the A_{var} and A_{perv} surfaces.

Determining the relevant geometric characteristics for the regression tree algorithm requires developing representative rectangular polygons from irregularly shaped A_{var} and A_{perv} surfaces. The process used to represent A_{var} and A_{perv} as rectangles is shown in Figure 3.3. First, a characteristic width (W) is computed by dividing A_{var} by its maximum overland flow path length, L_{var}. Next, A_{perv} is computed by multiplying W by the distance from the centroid of A_{var} to the nearest downslope A_{phys}, L_{perv}. Finally, ϕ_{perv} is computed by dividing A_{perv} by the total area (A_{var} + A_{perv}).

Step 4: Computing HCIA

The final step in the HCIA ArcGIS tool involves computing the HCIA within each subcatchment. Each A_{phys} are is multiplied by ϕ_{phys}, and each A_{var} area is multiplied by its computed value of ϕ_{var}. The sum of these products within each subcatchment comprises the subcatchment HCIA (see Eqs. (1)–(3)). The percent HCIA within each subcatchment is then calculated as the fraction of total impervious area comprised of HCIA (HCIA/TIA).

Case study

As a test case, we applied the HCIA ArcGIS tool to the Berkeley neighborhood, in northwest Denver, Colorado (Figure 3.4). The study area is a 4.7 square kilometer sewershed in the Berkeley neighborhood (hereon referred to as the 'Berkeley sewershed'), and is primarily comprised of single-family residential land use (54%), parks and recreation areas (18%)

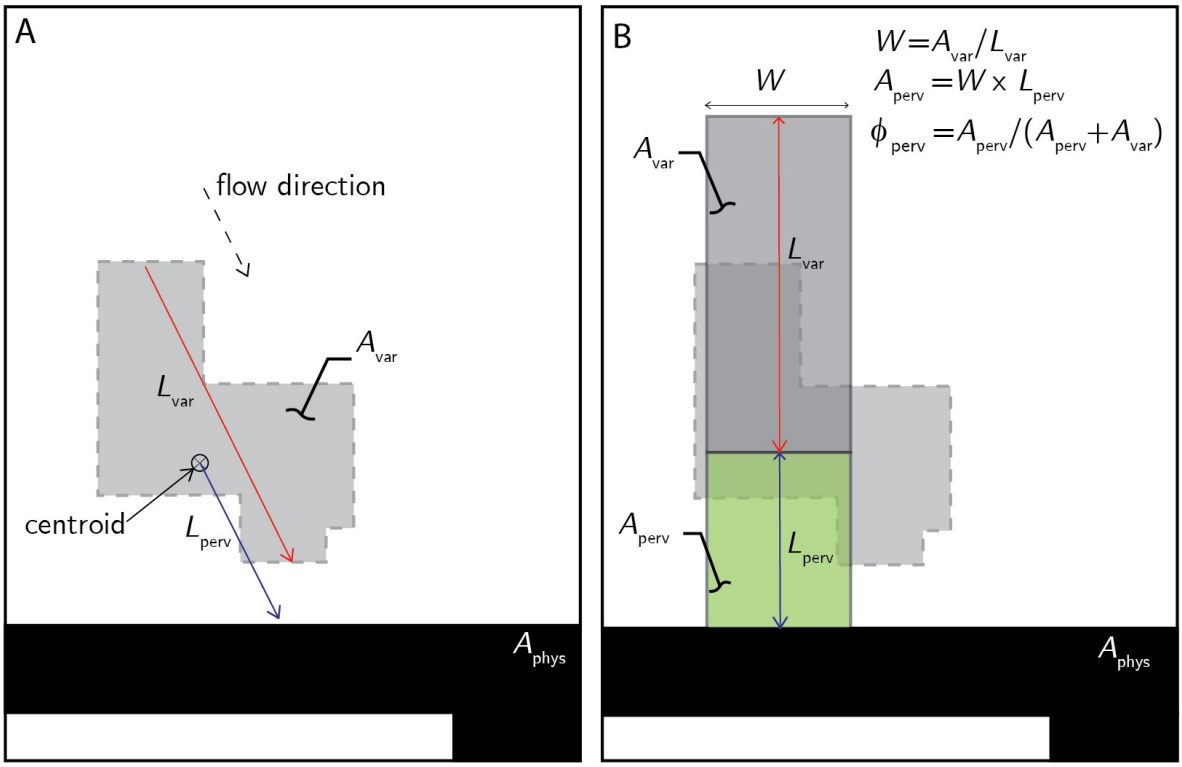

Figure 3.3. Conceptual schematic showing approach to developing representative rectangular polygons for A_{var} and A_{perv} from complex shapes. In Panel A, L_{var} represents the maximum flowpath length across A_{var}, and L_{perv} presents the flowpath length from A_{var} centroid to the nearest downstream A_{phys} surface. In Panel B, A_{var}, L_{var}, and L_{perv} are used to compute W (as A_{var}/L_{var}), A_{perv} (as WxL_{perv}) and ϕ_{perv} (as $A_{perv}/[A_{var} + A_{perv}]$).

and multifamily units (10%) (Panos, Hogue, Gilliom, & McCray, 2018). The majority of buildings in the study area were constructed between the early 1900s and the 1980s (Catalog, 2020), though the neighborhood has been subject to intense infill development in recent years (Cherry et al., 2019; Panos, Hogue, Gilliom, & McCray, 2018). Impervious surfaces comprise 53 percent of the total sewershed area (in 2014). The 2-year, 5-year, and 10-year 24-hour SCS Type II storms for this area correspond to rainfall depths of 4.6, 5.9, and 7.1 cm, respectively (Panos et al., 2020). No soil data are available for the area in the SSURGO NRCS Soil Survey, but near-by area soil textures are classified as C-type clay and loam (Panos, Hogue, Gilliom, & McCray, 2018). Overland flow and stormwater pipes through the sewershed route stormwater runoff from the south (elevation $\sim$ 1670 m) to the north (elevation $\sim$ 1630 m), ultimately discharging into Clear Creek (Figure 3.5).

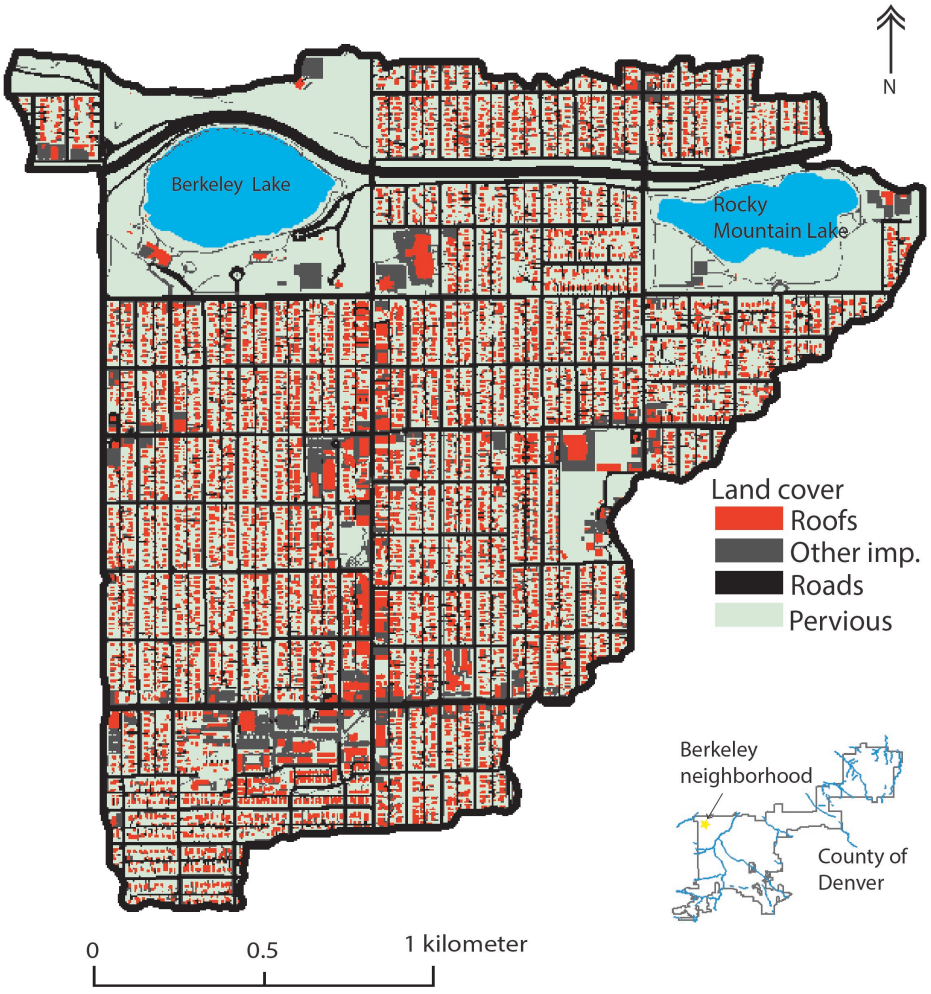

Figure 3.4. Distribution of rooftop and ground-level impervious (roads, other impervious), and locations of two lakes (Berkeley Lake and Rocky Mountain Lake) in the Berkeley neighborhood sewershed, County of Denver.

Input data

Shapefiles of stormwater inlet points (manholes and catch basins), the stormwater network, and impervious surfaces were provided by the City and County of Denver Community Planning and Development Department (CPD) as used in the modeling efforts performed by Panos, Hogue, Gilliom, & McCray (2018). The impervious surface shapefile from CPD distinguishes roofs, roads, and other impervious areas; these were summarized into roofs A_{roof} and ground-level impervious A_{ground}. A 1-m digital elevation model (DEM) of the study area was downloaded from the U.S. Geological Survey (USGS) National Elevation

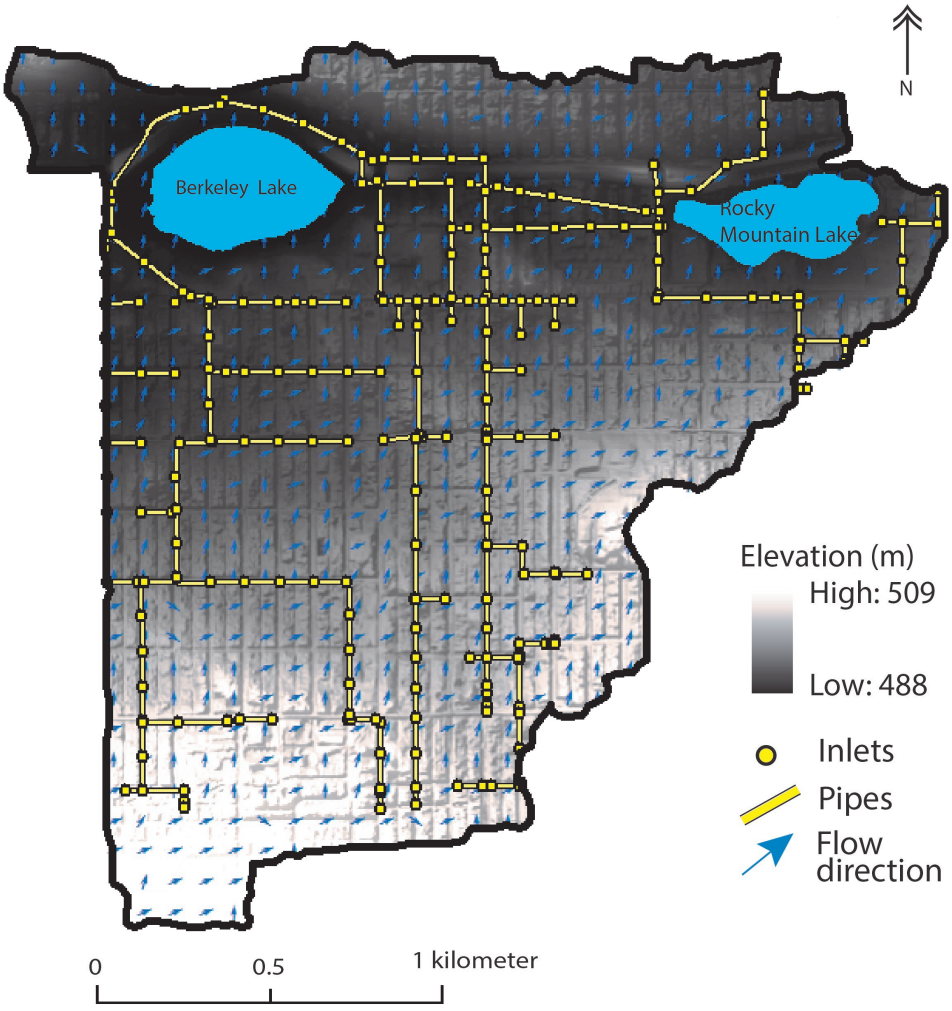

Figure 3.5. Flow direction (blue arrows), stormwater pipes and inlets (in yellow) in the Berkeley neighborhood sewershed.

Dataset (U.S. Geological Survey, 2017). Flow paths and subcatchments draining to inlet points were delineated using the 1-m DEM.

Estimating A_{phys} and A_{var}

To develop an initial estimate of roof connectivity ($A_{phys,roof}{}^{o}$), we evaluated current and historical development codes in the City of Denver for requirements pertaining to roof drainage, gutters, and downspouts. The Denver Building Code (DBC) of 1881 required

that "all buildings... shall be provided with proper metallic leaders to conduct water from the roof [which] shall be connected with the sewer or street gutter" (§21, pp. 11) (Denver Building Code, 1881), which was modified in 1898 to: "No water shall be discharged from conductor pipe upon any sidewalk, but shall be conducted underneath the walk in iron or tile pipes." (§145, pp. 49) (Denver Building Code, 1898). Beginning in 1976, new construction was not permitted to pipe roof discharge directly to the street or storm sewer network, rather, external roof downspouts were to discharge to "concrete blocks at least 12 in. in width by 36 in. in length" except for roofs that drain to the interior of the building (§3211, pp. 32–12) (Denver Building Code, 1976). Interior roof drains are not common in residential development but are used for commercial and industrial development with flat or internally sloped roofs. The 2018 International Plumbing Code, adopted by the City of Denver per the 2019 Denver Building and Fire Code (Denver Building, 2019), requires roof runoff from one- and two-family dwellings to discharge to flat areas, such as lawns, where possible (§1101.2) (International Plumbing Code, 2018). Visual inspection using Google Street Views and Google Maps confirmed that most houses in the neighborhood have visible downspout extensions that route roof runoff to gardens or lawns, while most commercial buildings with flat rooftops appear to use internal roof drainage (visible from satellite imagery), and no downspouts are visible from the outside. Therefore, as an initial estimate of roof connectivity, we assumed that all roof areas within commercial/industrial land use are physically connected (${A_{phys,roof}}^o$), and all roofs within all other land use designations (primarily residential) are variably connected (${A_{var,roof}}^o$). Ground-level impervious surfaces that intersected with the drainage network were initially assumed to be physically connected (${A_{phys,ground}}^o$) all other ground-level impervious were designated as (${A_{var,ground}}^o$). Final estimates of $A_{phys,roof}$, $A_{var,roof}$, $A_{phys,ground}$ and $A_{var,ground}$ were then determined per the ArcGIS tool methods described above.

ϕ_{phys} and ϕ_{var} scenarios

For simplicity, we assumed that all A_{phys} surfaces are 100 percent connected ($\phi_{phys} = 1$) but note that other values for ϕ_{phys} could be applied in the HCIA ArcGIS tool. ϕ_{var} estimation requires user-input for the HCIA scenario (P, ASM, and soil texture class) (Step 3). Lacking soil survey data in the catchment, we used the near-by area soil texture – predominantly C-type clay and loam (Panos, Hogue, Gilliom, & McCray, 2018). To stay within the soil parameters used to develop the regression tree, we assumed soil parameters that represent typical silty-clay-loam soils with k_s of 1 mm/ h (see Table 3.2). Since ASM and P are temporally varying, we computed HCIA across (3) ASM conditions and (5) P scenarios, for a total of 15 estimates of HCIA across the Berkeley sewershed. Total HCIA and percent HCIA within each subcatchment were computed following methods outlined above (Step 4), for each of the 15 ASM and P scenarios.

3.4 Results

Connectivity of impervious surfaces is sensitive to soil texture, soil moisture, rainfall, and pervious area fraction

The sensitivity of ϕ_{var} to soil texture, soil moisture, and rainfall scenarios (soil texture, ASM, and P), and geometric parameters (ϕ_{perv}, A, W, and S) is shown in Figure 3.6. Soil texture, given by k_s, is the most sensitive model parameter, with median ϕ_{var} values ranging from 0 to 0.98 (Figure 3.6A). Though not as sensitive as soil texture, ASM also affects ϕ_{var}, with saturated scenarios resulting in less infiltration (median $\phi_{var} = 0.74$) than soils at field capacity or wilting point (Figure 3.6C). The five rainfall depths also resulted in a range of median ϕ_{var} from 0.34 to 0.84 (Figure 3.6E), with higher ϕ_{var} resulting from higher rainfall depths. Of the geometric parameters tested, ϕ_{var} is highly sensitive to ϕ_{perv} (Figure 3.6B), but insensitive to S, W, and A (Figure 3.6D, F, and G).

These plots also illustrate the complex interactions and non-linearity between these parameters and ϕ_{var}. For example, even for very low ϕ_{perv} values, ϕ_{var} ranges from 0 to ~ 1 (Figure 3.6B), suggesting a different parameter (or combination of parameters) controls ϕ_{var} in these cases. Additionally, while ϕ_{var} generally decreases with increasingly permeable soils, there are some cases in which ϕ_{var} for high permeability soils (e.g., $k_s =$ 120.4 mm/h) exceeds that of lower permeability soils (e.g., $k_s = 0.3$ mm/h) as indicated by the outlier points on Figure 3.6A. This suggests that the effect of low k_s on ϕ_{var} may be moderated or exacerbated by other sensitive parameters. For example, if $k_s = 0.3$ mm/h, $\phi_{perv} = 0.8$, $ASM =$ WP, and $P = 1.5$ cm, ϕ_{var} could be relatively low despite the highly impermeable soils.

Importance of storm/landscape features can vary between and within landscapes

Of the four features selected for the final model (ϕ_{perv}, P, ASM, and soil texture represented by k_s), the most important feature is soil texture, followed by P, ϕ_{perv}, and ASM (Figure 3.7A). This suggests that across storm/landscape scenarios, ϕ_{var} is primarily controlled by soil texture. These results are consistent with the PySWMM sensitivity analysis, which showed that ϕ_{perv}, soil texture, P, and ASM are sensitive parameters, while S, A, and W are relatively insensitive. The final model, which incorporates the four most important features and optimal hyperparameters, resulted in an MSE_{CV} of 0.003, and R^2 of 0.97 (Figure 3.7B).

The importance of each of the final model features varies across the eight sub-trees (Figure 3.8), illustrating the effects of within-storm/landscape variability on the features that control ϕ_{var}. For example, for the sandy soil sub-tree (a regression tree trained only on simulations with sandy soils [$k_s = 120.4$ mm/h]), ϕ_{perv}, and to a lesser extent P, are the most important features (Figure 3.8A) (note that soil texture or k_s is not important in these scenarios as it is no longer varying). However, as k_s decreases (associated here with clay soil texture),

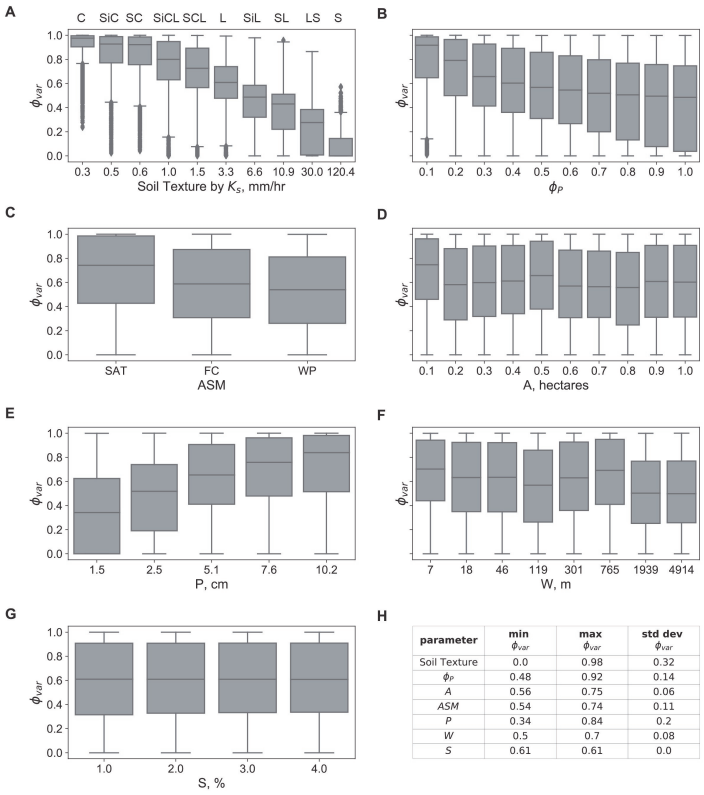

Figure 3.6. Sensitivity of ϕ_{var} to saturated soil texture and saturated hydraulic conductivity k_s (mm/h) (panel A), pervious fraction ϕ_{perv} (panel B), antecedent soil moisture conditions ASM (SAT = saturated, FC = field capacity, WP = wilting point) (panel C), total area A (hectares) (panel D), precipitation depth P (cm) (panel E), width W (m) (panel F), and slope S (%) (panel G). The middle line in each box plot represents the median ϕ_{var}. Soil textures: S = Sand, LS = Loamy Sand, SL = Sandy Loam, SiL = Silt Loam, L = Loam, SCL = Sandy Clay Loam, SiCL = Silty Clay Loam, SC = Sandy Clay, SiC = Silty Clay, C = Clay

the importance of ϕ_{perv} decreases and that of P increases (Figure 3.8A). While k_s is clearly the most important feature across all three antecedent soil moisture conditions, it is more important for the case of saturated soils (ASM = saturated). It decreases in importance for drier soils (ASM = wilting point), while the importance of other parameters (P and ϕ_{perv}) increases (Figure 3.8D).

Application of HCIA ArcGIS tool to the Berkeley sewershed

Across the Berkeley sewershed subcatchments, we found that ground-level impervious (A_{ground}) comprised 63 percent and rooftop impervious (A_{roof}) comprised 37 percent of the

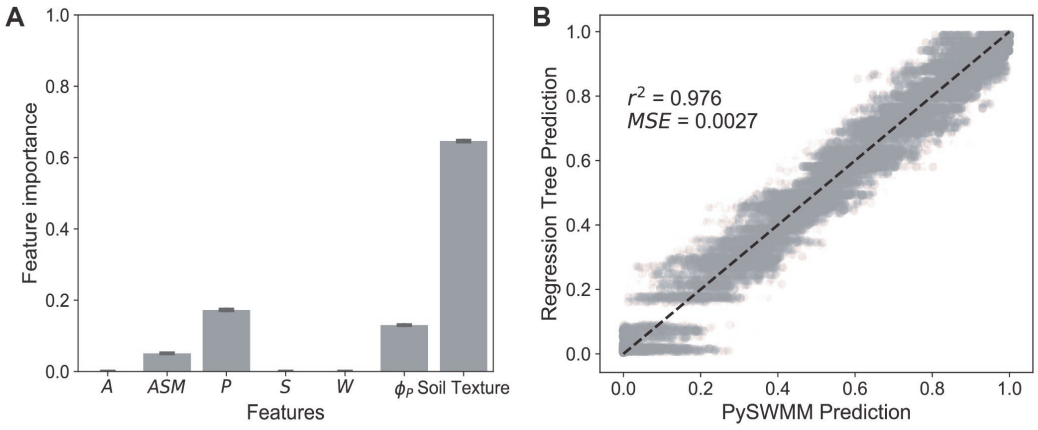

Figure 3.7. Feature importance metrics (panel A) were used to select important features for the final regression: ASM, P, ϕ_{perv}, and soil texture. The final regression tree predictions show excellent agreement with PySWMM predictions of ϕ_{var} (panel B). In panel B, dashed line represents a 1:1 relationship.

total subcatchment impervious areas. A total of 87 percent of A_{ground} and 48 percent of A_{roof} were found to be physically connected; A_{phys} therefore comprised the majority (73 percent) of all impervious surfaces in the study area.

Figure 3.9 shows the spatial variability in contribution of A_{var} to HCIA across the study area subcatchments for the three antecedent soil moisture conditions and five precipitation depths. The contribution of A_{var} to HCIA generally increased with increasing P and increasingly saturated soils. The standard deviation in A_{var} contribution to HCIA across subcatchments also generally increased with P and soil saturation. This illustrates the divergence between subcatchments comprised of A_{var} and those comprised mostly of A_{phys}: while A_{var} contribution changed with P and ASM, A_{phys} contribution remained constant. Interestingly, the A_{var} contribution to HCIA did not vary between field capacity and wilting point soil conditions where $P >= 2.5$ cm, suggesting that for higher storm depths and intensities, the difference between various initially non-saturated soil conditions may be negligible.

3.5 Discussion

Controls on hydrologic connectivity

We found that the factors that exhibit the strongest control on A_{var} connectivity are rainfall depth (P), antecedent soil moisture (ASM), pervious area soil texture (represented by k_s),

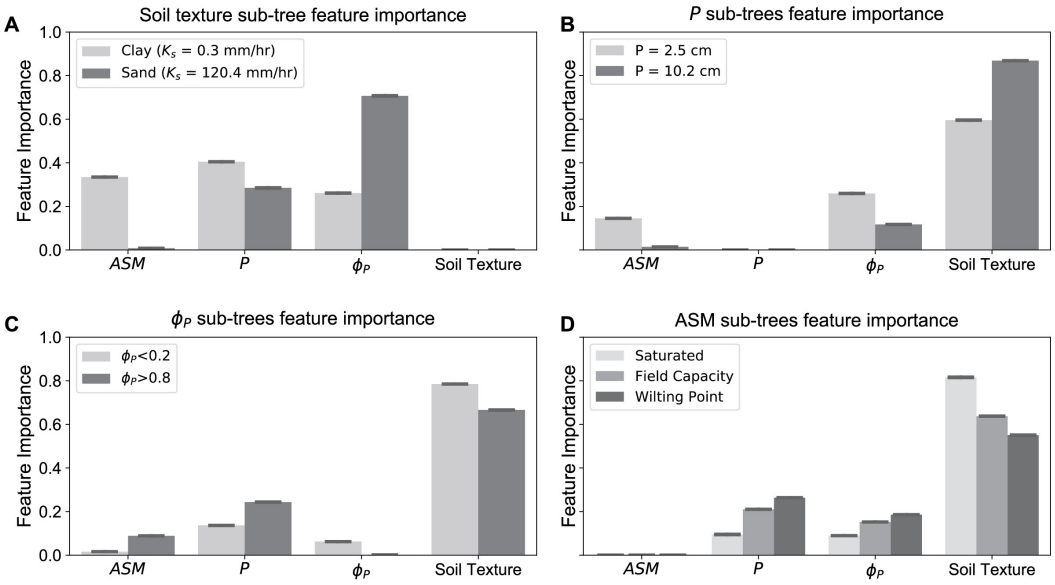

Figure 3.8. Feature importance across four predictor sub-trees. Soil texture sub-trees (clay and sand) illustrate a shift from precipitation (P) to pervious fraction (ϕ_{perv}) dominated connectivity with increasing permeability (panel A). ϕ_{perv} subtrees (< 0.2 and > 0.8) show increasing importance of soil texture at low ϕ_{perv} (panel B). Note that ϕ_{perv} importance in panel B is non-zero because ϕ_{perv} is ranges from 0-0.2 and 0.8-1 in the ϕ_{perv} sub-trees. P sub-trees (P = 2.5 cm, 10.2 cm) (panel C) and antecedent soil moisture ASM sub-trees (saturated and wilting point) show increasing importance of soil texture for high P value or increasing saturation.

and the amount of downslope pervious area relative to total area (given by ϕ_{perv}) (Figure 3.7A). Soil texture was the most important parameter across all simulations, however we observed two key shifts in feature importance when different parameters, such as soil texture, are held constant.

First, for impervious routed to highly permeable soils (i.e., where soil $K_s >$ rainfall intensity), ϕ_{perv} was the most important feature (as shown for sand in Figure 3.8A); however, with increasingly impermeable soils, P became the most important feature. This suggests that in urban areas with predominantly impermeable soils, P controls connectivity of impervious areas more than ϕ_{perv}. These results are consistent with Crompton et al. (2019), who find similar variability in importance of ϕ_{perv}: where k_s is greater than rainfall intensity, ϕ_{perv} closely predicts infiltration because the pervious areas infiltrate most of the runoff that runs onto them. Secondly, the importance of soil texture decreased with increasing ϕ_{perv} (Figure 3.8C) and decreasing soil saturation (Figure 3.8D), while it increased with P (Figure 3.8B). These results make sense given our understanding of infiltration processes. Before soils are saturated, infiltration occurs at a rate equal to the

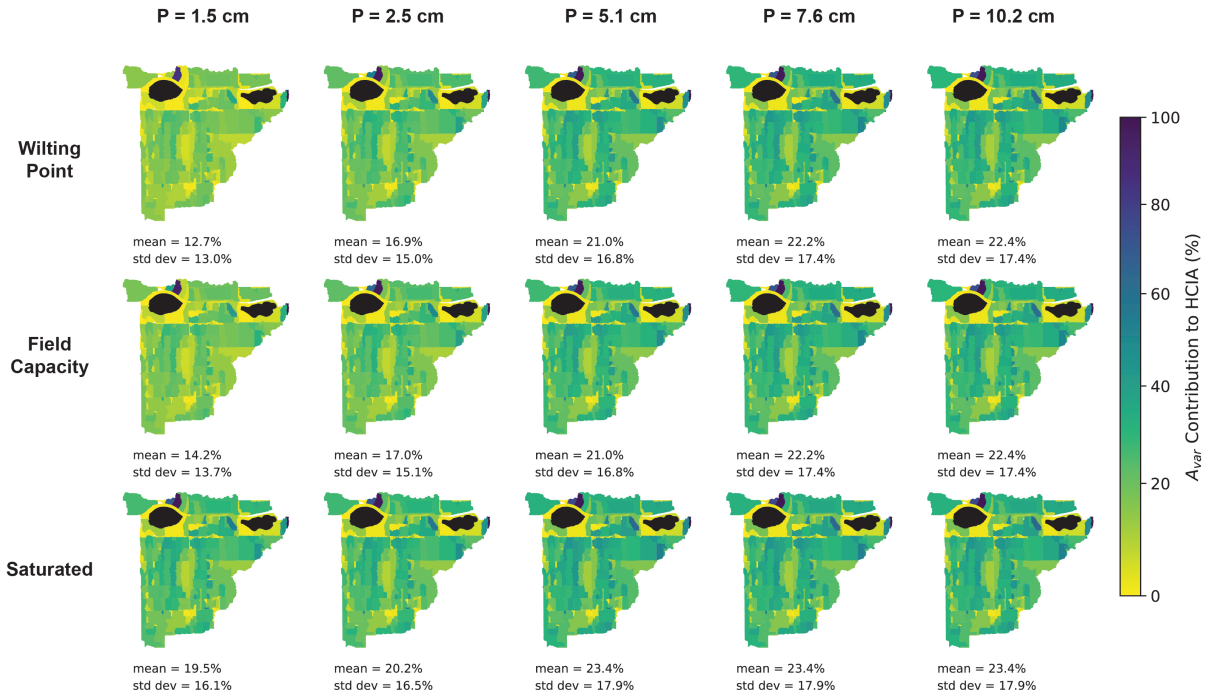

Figure 3.9. Maps showing spatial variability in contribution of A_{var} to HCIA for three antecedent soil moisture conditions (in the rows) and five rainfall scenarios (in the columns) across the Berkeley neighborhood sewershed. Darker hue indicates higher A_{var} contribution, lighter hue indicates lower A_{var} contribution. Lakes are shown in black. Mean contribution of A_{var} to HCIA generally increases with increasing P and increasingly saturated soils, as does its standard deviation across subcatchments.

minimum of rainfall rate and infiltration capacity, where infiltration capacity is defined by the infiltration model. After saturation, infiltration rate decreases to k_s. It follows that ϕ_{var} would depend more strongly on k_s for soils that begin at saturation, whereas ϕ_{var} would depend more strongly on P for soils that begin in unsaturated conditions.

Our results indicate that ϕ_{var} is not sensitive to slope, total area, or width. It is important, however, to consider the modeling framework in which this was determined. First, the outcome of interest in this study, ϕ_{var}, was defined by total runoff and infiltration volumes $(1 - IF_{runon})$; other hydrological outcomes such as peak flow and

runoff timing may be more sensitive to slope and width parameters. Secondly, changes in slope, total area, and width were simulated in tandem with changes to soil types, pervious fractions, and rainfall intensities, all of which proved to be highly sensitive parameters. One can imagine alternative modeling frameworks in which the slope, total area, and width would be sensitive; for example, if the pervious area width, and thus flow path length, were varied independently from the impervious area width.

Role of A_{var} and ϕ_{var} in the Berkeley sewershed

In the Berkeley sewershed, 27 percent of TIA was comprised of A_{var}, but the percent of HCIA comprised of A_{var} varied depending on rainfall and soil saturation conditions. For low rainfall and low soil saturation conditions, A_{var} contributed a small amount to overall HCIA (Figure 3.9, top left). Conversely, A_{var} comprised a larger proportion of HCIA for high rainfall and saturated soil conditions (23 percent on average across the study area and in some cases up to 100 percent of subcatchment HCIA) (Figure 3.9, bottom right). This suggests that even in landscapes with low amounts of A_{var} relative to other impervious areas, and where soil types are assumed to be constant, estimates of connected impervious area based only on A_{phys} can significantly underestimate the impervious area that is hydrologically connected.

A second notable result from the Berkeley sewershed case study is that the A_{var} contribution to HCIA varied across the precipitation and soil moisture conditions, and this variability was not constant across increasing soil moisture conditions or precipitation scenarios. A_{var} contribution to HCIA was low at low precipitation depths and increased rapidly with increasing precipitation and initial soil moisture conditions. However, as evidenced by the standard deviations in Figure 3.9, the variability in A_{var} contribution became more constant above moderate rainfall depths (above $\sim$ 5 cm) and initial soil saturation (field capacity); i.e., contribution of A_{var} reaches a maximum as HCIA approaches TIA.

Implications for hydrologic modeling

The importance of A_{var} for HCIA depends not only on the specific parameters tested in this study, but also on the goal of the study or planning effort. In areas with relatively low soil permeability, such as the Berkeley sewershed, temporally variable parameters drive connectivity. Here, the contribution of A_{var} to HCIA is significant for a wide range of rainfall and antecedent soil moisture conditions, therefore, both modeling and planning efforts should consider the effect of A_{var} on HCIA. However, in areas with higher soil permeability, these temporally varying parameters are less influential relative to spatially varying parameters (e.g., pervious areas downstream). In these cases, the contribution of A_{var} to HCIA across the watershed as a whole is likely to be minimal (as ϕ_{var} decreases with increasing permeability), but the spatial variability in the contribution of A_{var} to HCIA across subcatchments may be significant. Therefore, consideration of A_{var} in these cases depends on the scale of the analysis. A_{var} may be less important for analyses concerned with watershed-scale runoff

(in which the variation in A_{var} contribution might 'average out' across the watershed) but could be important for those related to spatial variability in runoff or spatial distribution of stormwater controls.

This study demonstrates the potential to use hydrologic modeling and machine learning to quantify impervious surface connectivity for single-event models. However, additional simulations are needed to cover the range of potential storm distributions and durations. The HCIA ArcGIS tool is currently limited to the 24-hr SCS Type II rainfall distribution and five rainfall depths, and preliminary comparisons indicate that different storm distributions and durations have the potential to significantly alter the resulting connectivity of impervious surfaces (see Appendix C). The approach applied in this study could be replicated to test the sensitivity of ϕ_{var} to different design storms and durations, and the resulting regression tree could be applied in the HCIA ArcGIS tool. Such an approach would essentially downscale single-event SWMM overland flow simulation to a quasi-distributed hydrologic model in the form of an ArcGIS tool. This would have clear benefits for planners and practitioners hoping to evaluate spatial distribution of overland flow at small subcatchment scales, for e.g., siting distributed stormwater controls, a common goal of current hydrological modeling efforts in urban settings.

While the concept of HCIA presented in this study could be potentially useful to planners and practitioners interested in single-event storm behavior, it may not necessarily be appropriate for use in continuous simulation models. By definition, HCIA is a time-varying metric that, like EIA, is storm- and landscape- specific — dependent on storm depth, duration, land cover patterns, soil texture, and antecedent soil moisture. A single, static HCIA value will not necessarily represent the impervious source area in a continuous simulation model. Therefore, rather than claiming that the HCIA metric presented in this study provides a 'better' estimate of HCIA that can (or should) be incorporated into continuous hydrologic models, we offer an approach and complementary geospatial tool for practitioners to apply for event-based hydrologic analysis.

Limitations and applications of the HCIA ArcGIS tool

This research focused on the hydrologic connectivity of impervious surfaces routed to downslope pervious areas and made several simplifying assumptions. Conceptually, the HCIA framework and modeling performed in this study presumes that runoff is generated as infiltration excess overland flow. While this is a common assumption in urban areas (Dunne & Leopold, 1978; Horton, 1933), there is ample evidence that other runoff mechanisms (e.g., shallow groundwater flow, saturation excess overland flow) can dominate in some urban areas (Bhaskar & Welty, 2015; Easton et al., 2007; Miles & Band, 2015). Practitioners and users of the HCIA ArcGIS Tool must be confident that the runoff in the study catchment is generated via infiltration excess, rather than saturation excess or groundwater flow. Further, the HCIA ArcGIS tool does not account for effects of spatially-varying rainfall, which can have a significant effect on runoff (Chaubey et al.,

1999; Singh, 1997). Thus, the methods presented here may be are more suitable for small watersheds, over which spatial variations in storm patterns are minimal.

Secondly, as a consequence of the presumed runoff generation mechanism and rainfall patterns, this approach assumes that any variation in connectivity is due solely to heterogeneous flow paths and pervious area infiltration. It does not consider the impact of depression storage or other non-infiltration losses. While this assumption may hold true where impervious areas have been recently constructed and have minimal depression storage, the accuracy of HCIA presented in this study could be further improved by incorporating variability in infiltration across impervious surfaces due to weathering (e.g., potholes, cracks) and pavement type. This variability can be modeled indirectly in the HCIA ArcGIS tool through user-specification of ϕ_{phys}, or the PySWMM modeling could be revised to include variable depression storage. Unfortunately, high resolution datasets of pavement condition and type are rare. A potentially more fruitful path forward for determining the variability in HCIA resulting from non-infiltration losses would be to utilize the proposed HCIA methods to constrain infiltration losses, allowing for calibration of non-infiltration losses. The HCIA framework and results presented here could conceivably be combined with prior research efforts to improve spatially explicit estimates of HCIA by further constraining non-infiltration losses through recursive validation (S. Epps Ph D. & Hathaway, 2018) with observed streamflow and runoff data (Ebrahimian, Wilson, & Gulliver, 2016).

Thirdly, the HCIA ArcGIS tool requires a user to designate roofs as physically connected or variably connected, thus limiting its application in areas where such data is not readily available. We present one method for estimating the rooftop physical connectivity, via development code review and Google maps analysis, but acknowledge that lacking detailed site surveys, such an analysis presents only an estimate. While out of scope of the current study, increased resolution of LiDAR and aerial imagery may give rise to datasets that could be used for the purposes of improving estimates of roof surface connectivity and pavement conditions.

Lastly, this study relies on theoretical modeling scenarios, rather than empirical or observed data. Consequently, the results of this study are limited to the specific storm and landscape conditions considered in the theoretical modeling scenarios. Further, because these theoretical modeling scenarios are based on SWMM overland flow routing (non-linear reservoir) and infiltration (Green-Ampt) models (see Appendix B), the results and implications of this HCIA ArcGIS tool are valid provided the assumptions of these runoff and infiltration schemes are met. For example, because non-linear reservoir routing does not simulate surcharging or backflow, results of the HCIA ArcGIS tool may be invalid for cases where storm drainage networks are undersized relative to their inflow, and surcharging results in backflow onto A_{phys} and A_{var} areas. Such cases require dynamic runoff routing and hydraulic considerations that are not included in this study. While the runoff and infiltration schemes used here are clearly idealized, previous studies have validated the non-linear flow routing methods for overland flow (Akram et al., 2014; Xiong & Melching, 2005) and Green-Ampt infiltration approach (Bouwer, 1969-12, 1976; Childs &

Bybordi, 1969; Chu, 1978) under a range of conditions.

Despite these limitations, the HCIA ArcGIS tool has potential to improve siting and performance of distributed stormwater controls by providing spatially explicit estimates of hydrologically connected impervious area. The effectiveness of such distributed stormwater controls depends on location within a watershed, and in particular, the location relative to heterogeneous flow paths (Fry & Maxwell, 2017; Jarden et al., 2016b; Di Vittorio & Ahiablame, 2015). For example, T. H. Epps & Hathaway (2019) show greater efficiency in runoff reduction from distributed stormwater controls when placed strategically to target HCIA compared to more random placement strategies.

3.6 Conclusion

Previous work has defined urban runoff heterogeneity with the metrics 'DCIA' and 'EIA', however neither metric provides spatially explicit estimates of hydrologically connected impervious areas. An inherent limitation of DCIA is that it represents connectivity as binary and static (i.e., connected or not connected), an assumption which is at odds with the dynamic nature of hydrologic process and connectivity. Changes in hydrologic pathways and connectivity can occur over time (e.g., with changes to rainfall intensity), and space (e.g., with changes in soil infiltration rate). EIA inherently accounts for these changes to hydrologic pathways but requires hydrologic data which are not always available for urban catchments.

We used a combination of hydrologic modeling in PySWMM, machine learning, and geospatial analysis to develop spatially-explicit estimates of hydrologically connected impervious areas (HCIA) in ungauged urban catchments that accounts for variability in hydrologic pathways that result from variability in soil types, pervious and impervious areas, rainfall events and soil moisture conditions. Study results shed light on variably connected impervious surfaces (A_{var}), showing that for the storms and soils evaluated, soil texture defined by saturated hydraulic conductivity (k_s) is the most important feature determining the degree of impervious surface hydrological connectivity. Temporal forcing (represented by rainfall and antecedent soil moisture) control connectivity within watersheds with low permeability soils, while spatial flow path variability (represented by relative quantity of disconnecting pervious area) controls connectivity within watersheds with highly permeable soils. These results suggest that, for catchments consisting of highly impermeable soils, A_{var} contributes to HCIA such that HCIA approaches TIA, but for catchments with highly permeable soils, A_{var} does not contribute significantly to HCIA, and thus DCIA could be used as a suitable surrogate for HCIA. In between these two extremes, however, lies a wide range of conditions that call for detailed and spatially explicit estimates of A_{var} connectivity.

Chapter 4

Assessment of SWMM parameter transferability across novel changes in climate and land cover conditions

Abstract. Urban runoff modeling is heavily reliant on semi-distributed models, where the smallest spatial scales resolved are urban subcatchments. These models must confront the representation of heterogeneity – e.g., in land cover and permeable area characteristics – within the modeled subcatchments. One approach to address this problem is to use 'effective' model parameters that average across the small-scale heterogeneity. This approach, although widespread in hydrology, generates known difficulties with model calibration and parameter identifiability. These challenges are particularly pronounced when the value of effective parameters is unstable across variations in model forcing. Here, we demonstrate that calibrated effective parameters such as 'width' and 'connected impervious area' in the widely used urban hydrological model SWMM, exhibit such instability. Instead of representing the landform and morphology of a subcatchment independently of soil, storm and land cover patterns, calibrated effective parameters co-vary with these forcing parameters. This covariation can result in significant prediction error when a calibrated SWMM model is applied to predict runoff following climate and landcover changes – common applications for the SWMM model. These errors are large, ranging between over-estimation of infiltrated runoff volumes up to $> 60\%$ and under-estimation of as much as $< -60\%$. These results point to a need for additional research and investment to determine how to use urban hydrologic models capable of robust predictions under variable future scenarios.

4.1 Introduction

Background

Urban hydrological models are used to plan, design and manage the urban water cycle. A wide array of urban hydrological models are available, from highly resolved and distributed models such as InfoWorks ICM (Innovyze, 2014) and MIKE FLOOD, DHI (DHI, 2010), to simple spreadsheet based approaches. Some of the most widely used tools in both urban hydrology research and practice are semi-distributed hydrological models (Petrucci & Bonhomme, 2014; Elliott & Trowsdale, 2007; Petrucci & Bonhomme, 2014; Elliott & Trowsdale, 2007), including the SWMM (James et al., 2010a), CANOE (Boutaghane & Ouerdachi, 2012), and MOUSE (Dhi, 2017) models, among others. Semi-distributed models disaggregate urban basins into subcatchments and represent routing between these subcatchments explicitly (Carpenter & Georgakakos, 2006a; Golden & Hoghooghi, 2018; Petrucci & Bonhomme, 2014). In these models, processes occurring at scales smaller than the subcatchment are not explicitly simulated; instead, the hydrological response of the subcatchment is modeled and parameterized as a unit. The emergence of simplified, self-organized hydrologic behavior at subcatchment scales (Sivapalan, 2003; Wood et al., 1988; Klemeš, 1983) allows for simplifications to model structure and parameterization compared to fully-distributed models (Brink & TenBroek, 1995); and such simplifications are often required due to computational limitations.

Model simplification, however, also distances the subcatchment model structure and its parameters from physically measurable quantities or processes (Petrucci & Bonhomme, 2014; Jakeman & Hornberger, 1993). Instead of explicitly representing conservation of mass, momentum, and energy, the models represent 'emergent' phenomena that result from parameterizing these processes. While some parameters in such models are directly-measurable physical entities - e.g., total subcatchment area, impervious fraction, or average slope - many parameters of such models are not; these 'effective' parameters are estimated through calibration (Niel et al., 2003; Reed et al., 2004; Gupta et al., 1996). Calibrating effective parameters generates a number of well known problems, including those related to obtaining accurate calibration and validation data (Sorooshian & Gupta, 1995), selecting which parameters to calibrate, and defining functions that measure model performance (Khatami et al., 2019). A pernicious problem arises when such performance measures fail to meaningfully distinguish between multiple parameterization choices (i.e., the problem of equifinality; K. Beven, 2006b; H. H. G. Savenije, 2001; H. H. Savenije, 2009; Khatami et al., 2019). A broad range of approaches can be used to address these problems, including sensitivity analysis (e.g., Saltelli et al., 2019) and uncertainty analysis (e.g., Shin et al., 2013; Saltelli et al., 2019), with the Generalized Likelihood Uncertainty Estimation methodology (GLUE, K. Beven & Binley, 1992, 2014) widely used for the latter in hydrological modeling (e.g., Bell et al., 2017; C. A. Shields & Tague, 2012; Sun et al., 2014; Vezzaro et al., 2012).

Calibrating models for rapidly changing urban environments brings up an even more basic

issue: the optimal effective calibration parameter values may vary with forcing conditions (e.g., rainfall, land cover). As the growing literature on catchment-scale hydrological regime shifts highlights (e.g., Penny et al., 2020b; Foufoula-Georgiou et al., 1969b; Niel et al., 2003; Schaefli, 2016), dominant hydrological processes can change in response to non-stationary land cover or background climate conditions. Likewise, model sensitivity to different sources of uncertainty can vary in response to changing land cover or climate conditions (C. Shields & Tague, 2015; C. Z. Li et al., 2012). Increasingly, urban hydrological model predictions need to be made under novel future conditions characterized by concurrent changes in urbanization patterns, urban development practices, and climate conditions (Martin et al., 2017; Penny et al., 2020b; Milly et al., 2008). If optimal calibration parameters are sensitive to changing conditions, this may undermine the predictive power of urban hydrological models. While calibration should ideally be performed using data that is representative of a wide range of forcing conditions (Sorooshian & Gupta, 1995; Sorooshian et al., 1983), in practice it is often not possible to fully span future states and dynamics of models with available calibration data.

While there is a wide literature dealing with non-stationarity in hydrologic predictions (e.g., Clarke, 2007; Klemeš, 1983; Koutsoyiannis, 2006; C. Z. Li et al., 2012), the ability of existing models to cope with this non-stationarity remains questionable (Wagener et al., 2010) and is largely unaddressed for urban hydrological modeling (Fry & Maxwell, 2018). In this study we identify the transferability of urban semi-distributed hydrologic models across distinct environmental and climatic conditions. We use the EPA Storm Water Management Model (SWMM) – one of the most widely used urban stormwater models since its development in the 1970's (Niazi et al., 2017) – as a case study urban hydrological model, and focus on its subcatchment runoff component.

Effective model parameters in SWMM

In SWMM, subcatchment geometry and topography are simplified and represented as planar rectangles with area A, width W, and mean slope S (see Figure 4.1a and b). Surface properties arising from differences in infiltration capacities among impervious roofs, road and paved surfaces, and pervious soils, are also simplified. SWMM lumps all pervious surface areas in the subcatchment together (A_{perv}), and treats the remainder of the subcatchment area as impervious (A_{imp}). Users specify this partitioning of surface properties with a 'percent impervious' parameter, here referred to in its fractional form as $\phi_{imp} = A_{imp}/A$. Other surface parameters, including Manning's roughness n and the depression storage d, are also specified separately for impervious and pervious areas. Users select one of three routing options between these lumped surface area types: (i) runoff from impervious and pervious areas is routed independently to the outlet (outlet routing); (ii) runoff from a fraction of the pervious area is routed to the impervious area (impervious routing); or (iii) runoff from some fraction of the impervious area is routed to the pervious area (pervious routing) (Huber, 2001). In the latter case, the fraction of impervious area that is directly routed to the outlet is defined as $\phi_{idc} = A_{idc}/A_{imp}$, where A_{idc} is the directly connected impervious area (Figure

4.1c). Previous modeling studies have found that hydrologic response is highly sensitive to ϕ_{idc} (Janke et al., 2011; Lee & Heaney, 2003b; Guo, 2008).

Of course, real urban subcatchments contain interleaved patterns of pervious and impervious areas, such that individual flowpaths may traverse multiple pervious/impervious surfaces en route to a storm drain or outlet. In SWMM, the effects of this spatial complexity must be accounted for in the selection of the routing scheme and choice of ϕ_{idc}. This implies that – although geospatial models (e.g., Sytsma et al., 2020; S. Epps Ph D. & Hathaway, 2018; Han & Burian, 2009b) or rainfall-runoff relationships (e.g., Ebrahimian, Gulliver, & Wilson, 2016; Boyd et al., 1993) can be used to infer ϕ_{idc} – this parameter may in practice not be physically interpretable and must be estimated through calibration.

Similar arguments apply to the geometric approximations employed in SWMM: given the planar rectangular assumptions made in the runoff model, the subcatchment 'width' parameter is best understood to control the mean non-channelized flowpath length $\bar{L}$, as $A = \bar{L}W$ (Rossman & Huber, 2016). Numerous studies demonstrate that travel time, runoff attenuation, and hydrograph properties are sensitive to the subcatchment width parameter (Brink & TenBroek, 1995; C. Li et al., 2014; James et al., 2010a). While SWMM offers users the option of calibrating W directly, it can be difficult to interpret whether calibrated W values are 'reasonable'. To facilitate interpretation of whether calibrated W values are reasonable, the width parameter can be expressed as $W = k_{width}A$ (James et al., 2010a; Guo & Urbonas, 2009), where $k_{width} = \frac{1}{\bar{L}}$. Because the maximum overland flowpath length (i.e., the length prior to channel formation) is finite and often in the range 0–150 m (James et al., 2010a; Rossman & Huber, 2016), meaningful physical bounds can be placed on k_{width}. Here, we constrain k_{width} to the range 0.01–0.1 m, corresponding to $\bar{L}$ ranging from 10–100 m. Furthermore, since the flowpath length is often geormophically controlled by local soils and landforms, it is potentially transferable across subcatchments of different areas (unlike calibrated W values). Thus, throughout, we calibrate k_{width} rather than W directly. Like W, however, k_{width} remains a generally unobservable parameter (Guo & Urbonas, 2009), requiring calibration.

Consequently, at the subcatchment level, SWMM confronts practitioners with two highly sensitive, effective parameters requiring calibration: ϕ_{idc} and k_{width}. For a subcatchment with a given area and slope, these parameters are expected to vary in response to the extent and spatial distribution of pervious and impervious surfaces. They may also, however, vary with storm and soil hydraulic properties (Fry & Maxwell, 2018). For example, where storm intensity greatly exceeds the infiltration capacity of pervious soils, the subcatchment will approximate the behavior of a uniformly impervious area. Furthermore, calibration of a typical SWMM subcatchment model immediately raises the potential for equifinality and compensating behavior between the effective parameters.

One way to investigate these calibration and parameterization problems is through the use of virtual experiments (Weiler & McDonnell, 2004). Virtual experiments have been used to identify hillslope controls on connectivity (Hopp & McDonnell, 2009), to simulate overland runoff across heterogeneous surfaces (Crompton et al., 2019), and to determine climatic and

landscape controls on runoff partitioning (C. Li et al., 2014). The advantage of designing virtual experiments is that everything about the model is known and controllable (Weiler & McDonnell, 2004). For example, the hillslope geometry can remain constant while soil properties are changed, and vice versa. Virtual experiments are distinct from sensitivity and uncertainty analysis because the goal of the experiments is not to assess the global sensitivity of a model, nor identify optimal parameter values, but rather to evaluate controls on hydrologic outcomes through systematic variation of inputs.

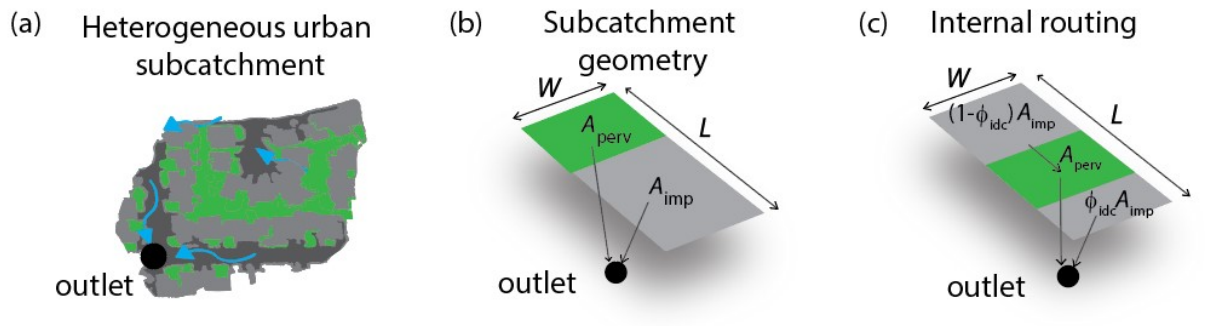

Figure 4.1. Conceptual schematic of a heterogeneous urban subcatchment (a), represented in SWMM by a rectangular hillslope of width W and length L (b), and with overland flow routing between impervious and pervious sub-areas (c). By default, SWMM routes impervious and pervious area runoff directly to the outlet (as shown in panel b). Users can specify alternative routing, as shown in panel (c), where some portion of impervious area (ϕ_{idc}) is routed directly to the outlet, while the remaining impervious area (1-ϕ_{idc}) is routed to the pervious area, then to the outlet.

Study aims and approach

The goal of this work is to explore the implications of calibration parameter sensitivity to changes in model forcing for urban hydrological prediction. This exploration is organized around three research questions:

1. How sensitive are the calibrated parameters ϕ_{idc} and k_{width} to varying environmental conditions (given by storm intensity, impervious fractions, and saturated hydraulic conductivity of pervious areas)?

2. Do parameters calibrated under one set of environmental conditions perform well in predicting the same subcatchment's hydrological responses to different environmental conditions?

3. If not, what magnitude of errors can be expected when a calibrated SWMM model is applied to different environmental conditions?

We used virtual experiments to explore the dynamics of constant-intensity rainfall on planar, bi-phasic (impervious and pervious) hillslopes with initially saturated soils and no initial losses, i.e., no depression storage. Spatial patterns of impervious and pervious areas were obtained by binarizing aerial imagery of urban areas. The binarization thresholds were varied to produce a range of hillslope-scale impervious fractions, creating a set of realistic and geometrically related land cover patterns. For each pattern, a number of storm and soil conditions were simulated using the Saint Venant Equations (SVE). These simulations were taken to represent 'true' runoff behavior. SWMM k_{width} and ϕ_{idc} were then calibrated to the SVE predictions resulting in 'behavioral parameter sets' for each pattern, storm, and soil condition. We examined the stability of the behavioral parameter sets across pattern, storm, and soil conditions by: (i) quantifying the overlap in behavioral parameter sets across these conditions; and (ii) quantifying the error that can arise when behavioral parameter sets are applied across these conditions. These methods are described in detail below.

4.2 Methods

Governing equations

'True' runoff behavior in the virtual experiments was obtained from the output of the two-dimensional Saint-Venant Equations (SVE) for shallow sheet flow. The SVE combine the fluid continuity and momentum equations, and are written (in one-dimension for brevity) as:

$$\frac{\partial h}{\partial t} = (p - f) - \frac{\partial (Uh)}{\partial x} \tag{4.1}$$

$$\frac{\partial U}{\partial t} + U\frac{\partial U}{\partial x} + g\frac{\partial h}{\partial x} + g(S_f - S) + \frac{U(p-f)}{h} = 0 \tag{4.2}$$

where h represents the depth of flow [L], U is the depth-averaged flow velocity [L/T], x is the horizontal coordinate [L], t is the time [T], p the effective rainfall intensity (rainfall minus interception) [L/T], f is the infiltration rate [L/T], S is the ground surface slope and S_f is the friction slope (energy gradient) (both in [L/L]). To relate S_f to U, Manning's Equation for surface roughness was employed:

$$U = \frac{1}{n} h^{2/3} S_f^{1/2}, \tag{4.3}$$

where n is Manning's roughness coefficient $[T/L^{1/3}]$. The SVE model used in this study is based on the finite volume approach presented in Bradford & Sanders (2002), and described in detail in Crompton et al. (2019).

Solving the SVE requires specification of rainfall and infiltration boundary conditions (p and f in Eqn. 4.1). Infiltration typically varies in time as initially dry soils saturate. Modeling infiltration as time-varying (for example, using the Green Ampt equation

H. W. Green & Ampt (1911)), however, introduces several extra degrees of freedom to any model. To avoid adding these complexities to the study, we considered only the situation where soils are initially saturated in both SWMM and SVE models. Under these conditions, the infiltration capacity is a constant $f_c = k_s$. At each timestep, infiltration f is thus given by the minimum of k_s and the rainfall rate p.

In SWMM, runoff is computed using the 'nonlinear reservoir routing' model (Rossman & Huber, 2016):

$$\frac{\partial h}{\partial t} = (p - f) - \frac{1}{Ln}(h - d)^{5/3} S^{1/2} \tag{4.4}$$

where d is the maximum depression storage depth (a threshold depth required for runoff to occur), and L is the length of the plane (and equal to A/W). Eqn. 4.4 is based on the lumped kinematic wave approximation to the SVE (Brutsaert, 2005). This approximation assumes that the flow is uniform and the friction slope S_f is approximately equal to the ground surface slope S (i.e., frictional resistance balances gravitational acceleration). For planar, uniform flow with U described by Manning's Equation, the continuity and lumped kinematic wave equation combine into Eqn. 4.4 (Brutsaert, 2005).

The nonlinear reservoir routing equation is used to convert rainfall to runoff in SWMM. The equation is applied separately to the lumped impervious or pervious areas of a subcatchment (i.e, the three areas shown in Figure 4.1c). Runoff routed from the lumped up-gradient areas is distributed uniformly over the down-gradient area, as if it were rainfall (Huber, 2001; James et al., 2010a; Rossman & Huber, 2016). For example, in Figure 4.1c, runoff from the upslope impervious area would be distributed uniformly across the downslope pervious area.

Model set up

Our virtual experiment modeling approach for the SWMM and SVE is shown schematically in Figure 4.2 and described below. All SWMM simulations were performed using PySWMM (the python API for SWMM) (McDonnell et al., 2020), and all SVE simulations were also performed in Python.

Urban image processing

We drew on real images of urban areas to generate realistic urban land cover patterns. We extracted 18 urban land cover images from a LiDAR-derived, 1-m resolution impervious/ pervious surface raster for the Petaluma River watershed (California, US) (Mapping & LiDAR Program, 2016). Each image covered a 100 m $\times$ 50 m area that was manually chosen to be representative of residential block-scale development.

The 4-band raster was collapsed to a single band image using the Normalized Difference Vegetation Index (NDVI) (Jensen, 2000). NDVI is widely used to classify urban areas as vegetation (high NDVI), or impervious surface (low NDVI) at or around a specified NDVI

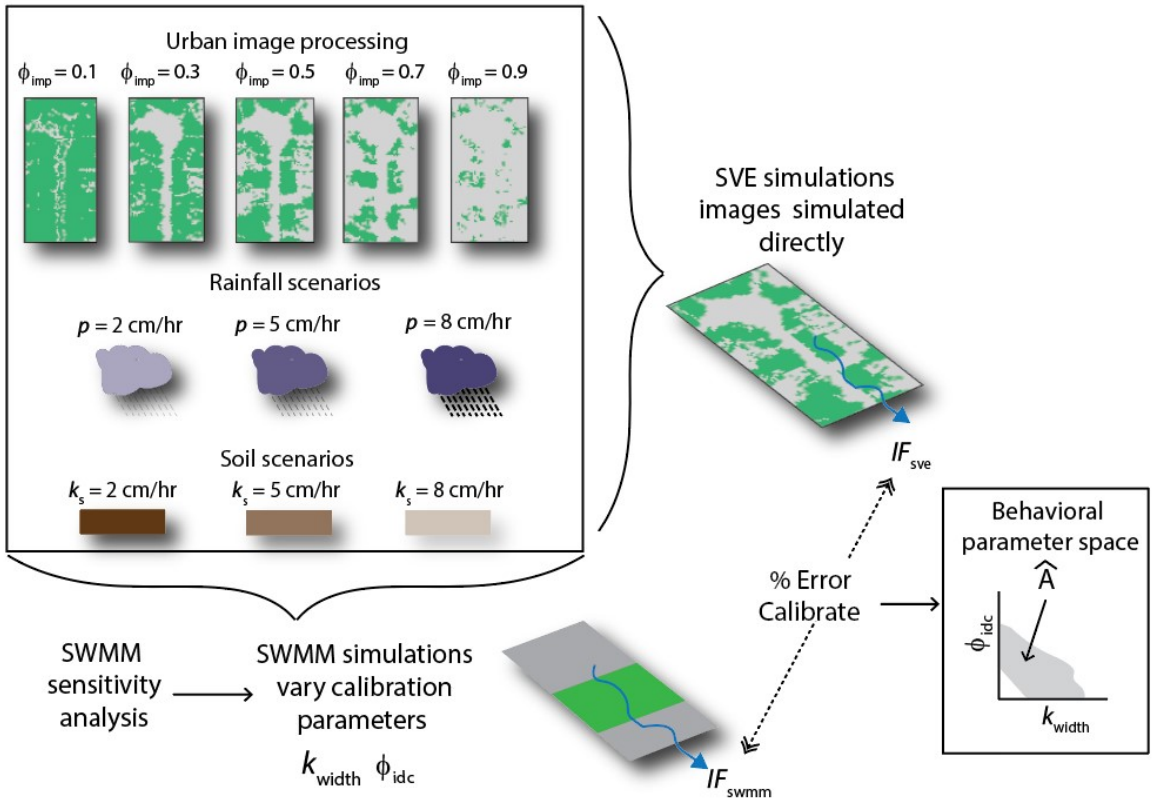

Figure 4.2. Conceptual schematic of SWMM and SVE simulations and calibration. SVE simulations were conducted across all 9 rainfall (p) and soil (k_s) conditions, for all urban land cover patterns (for a total of 162 simulations). For the same land cover patterns and p and k_s conditions, analogous simulations in SWMM were performed by extracting ϕ_{imp} and varying sensitive SWMM parameters (ϕ_{idc} and k_{width}). Calibrated sets of ϕ_{idc} and k_{width} were determined by comparing the % Error in infiltration fraction, IF. Calibrated parameter sets were then used to define the behavioral parameter space, $\hat{A}$.

threshold (Knight & Voth, 2010; Kaspersen et al., 2015; Zha et al., 2003; Jensen, 2000). For each image, we tuned the NDVI threshold to produce five impervious and pervious area binarizations that correspond to five ϕ_{imp} values ($\phi_{imp} = 0.1$, 0.3, 0.5, 0.7, and 0.9). This resulted in a set of 90 unique urban land cover patterns, comprised of 18 images and five ϕ_{imp} values.

SVE simulations

We adopted an idealized view of runoff generation, whereby overland flow is generated in SWMM and SVE by constant-intensity rainfall on a planar, bi-phasic (impervious and pervious) hillslope with initially saturated soils and no initial losses, i.e., no depression storage.

We assumed that the impervious areas (as delineated in the binarized images) were completely impervious ($k_s = 0$), and that pervious areas were uniform with the same k_s everywhere. Simulations were run for the 9 combinations of three k_s values (2, 5, and 8 cm/hr) and three p values. For each of the nine p and k_s combinations, runoff and infiltration were simulated for each of the 90 urban land cover patterns using the SVE. Table 4.1 outlines the parameterization for all simulations.

The first-order control on runoff production on pervious soils is whether the rainfall rate exceeds the infiltration capacity. This can be measured using the ratio p/k_s, where runoff production is associated with $p/k_s > 1$. The higher p/k_s, the greater the excess precipitation and rate of runoff production. The range of p/k_s values in the experiment was 0.25 to 4, spanning a wide profile of different runoff production behaviors.

Table 4.1. Summary of parameters used for SVE and SWMM modeling

Parameter	Description	Values
	Constants	
n_{imp}	Manning's n on impervious	0.01
n_{perv}	Manning's n on pervious	0.1
d_{imp}	Depression storage on impervious (mm)	0.0
d_{perv}	Depression storage on pervious (mm)	0.0
S_o	Surface slope (%)	1
A	Area (m^2)	5,000
	Soil and storm conditions	
p	30-min rainfall intensity (cm/hr)	2, 5, 8
k_s	Saturated hydraulic conductivity (cm/hr)	2, 5, 8
p/k_s	Rainfall excess ratio	0.25, 0.4, 0.62, 1.0, 1.6, 2.5, 4
	Urban land cover patterns	
Image	Urban images	18 images
ϕ_{imp}	Impervious fraction	0.1, 0.3, 0.5, 0.7, 0.9

SWMM sensitivity analysis

Before calibrating SWMM, we used Sobol' sensitivity analysis to verify that SWMM runoff and infiltration are sensitive to k_{width} and ϕ_{idc} parameters (Sobol', 1990). Sobol' analysis is a variance-based global sensitivity analysis that can be used to determine how much each parameter contributes to the overall variance of the model output (the total-order index) (Nossent et al., 2011). The higher a parameter's contribution to overall variance, the more sensitive it is.

We imposed some limitations on the sensitivity analysis. Specifically, we considered only SWMM parameters that have direct impacts on overland flow (see Eqn. 4.4). Secondly, we recognized the large literature that demonstrates SWMM's high sensitivity to the physically observable ϕ_{imp} parameter. While this sensitivity is helpful to modelers, it can mask the model's sensitivity to the calibrated parameters targeted in this study. Therefore, we limited the sensitivity analysis to six *e*ffective SWMM subcatchment parameters, i.e., those parameters that cannot be readily observed or estimated using geospatial methods. These parameters are: the hillslope width factor k_{width}, connected impervious fraction ϕ_{idc}, roughness on pervious areas n_{perv} and impervious areas n_{imp}, and depression storage on pervious areas d_{perv} and impervious areas d_{imp}.

We used the SALib Sobol python package (Herman & Usher, 2017) to generate random parameters and conduct the Sobol' analysis. We specified parameter ranges for the six overland flow parameters in accordance with previously reported values (see Appendix D.1 for full documentation), with k_{width} ranging from 0.01 to 0.1. These k_{width} values correspond to overland flowpath lengths of 10 to 100 m in a 5000 m^2 subcatchment, equivalent in size to the urban images described above). These parameter values were cross-sampled using the Saltelli method, which generates $N * (2D + 2)$ samples (Saltelli, 2002; Saltelli et al., 2010), where N is the number of samples to generate (here, 100) and D is the number of parameters (here, 6). This resulted in 1,400 unique parameter sets. For each parameter set, we systematically varied the rainfall intensity p, saturated hydraulic conductivity of pervious areas k_s, impervious fraction ϕ_{imp}, and slope (S), for a total of 189,000 SWMM runs (simulated in Python). This approach allowed us to determine if the sensitive parameters were consistent across these forcing criteria.

The sensitivity of each overland flow parameter was measured in terms of it's contribution to overall variance in the storm-scale infiltration fraction IF. IF is a time and space integrated measure of model predictions, defined as the fraction of incident rainfall that infiltrates in the subcatchment:

$$IF = \frac{F}{P} \tag{4.5}$$

where F is the cumulative infiltration depth, and P is the rainfall depth.

Although we leave further discussion of the sensitivity analysis results to the Results (Section 4.3), we note here that, as anticipated, k_{width} and ϕ_{idc} emerged as the most sensitive

of the effective model parameters, supporting our choice to focus calibration efforts on these parameters.

SWMM parameter calibration and objective function

We calibrated SWMM to the SVE using a global random search calibration algorithm (Sorooshian & Gupta, 1995). For each SVE simulation, 100 simulations were run in SWMM with k_{width} and ϕ_{idc} sampled from uniform distributions (Table 4.2), holding all other parameters constant between the two models (p, k_s, ϕ_{imp}, n_{imperv}, n_{perv}, S_o, and A). This produced 81,000 SWMM simulations across the p, k_s, and ϕ_{imp} conditions. While global random search algorithms are rarely used in hydrologic modeling due to their inefficiency (Sorooshian & Gupta, 1995), in this case they offer the advantage of simulating a consistent suite of parameter sets for comparison across the p, k_s, and ϕ_{imp} conditions.

Table 4.2. SWMM Calibration Parameters

Parameter	Description (units)	Values[a]
k_{width}	Hillslope width factor (m)	U [0.01,0.1]
ϕ_{idc}	Connected impervious fraction (–)	U [0.01,0.1]

[a]U = Uniform distribution.

We used the infiltration fraction IF to compare the SWMM and SVE model predictions, denoted as IF_{swmm} and IF_{sve} respectively. For each IF_{sve} prediction, there were 100 IF_{swmm} predictions corresponding to the 100 unique parameter sets (k_{width}, ϕ_{idc}). SWMM performance was quantified using the percent error between IF_{swmm} and IF_{sve}, PE_{IF} (%):

$$PE_{IF} = \frac{IF_{sve} - IF_{swmm}}{IF_{sve}} \times 100, \tag{4.6}$$

which provides a simple measure of agreement between the models. PE_{IF} is positive when $IF_{swmm} < IF_{sve}$, indicating that SWMM underestimates infiltration depth while overestimating runoff. SWMM was calibrated to minimize the absolute value of PE_{IF}. This allowed for the definition of a single threshold under which parameter sets (k_{width}, ϕ_{idc}) are 'behavioral', in the sense that they result in a model that adequately reproduces the observed watershed behavior (e.g., sensu Worqlul et al., 2018; Yen et al., 2015).

Defining behavioral parameter space

We explored how the model performed for different calibration parameter sets as the ratio p/k_s and the impervious fraction ϕ_{imp} were varied. Based on this performance we mapped the behavioral parameter space (i.e., the space defined by the behavioral parameter sets) as these climatic/soil and land use conditions changed. This process had three steps:

1. For each p/k_s and ϕ_{imp} combination, we binned the parameters into 10 k_{width} bins x 10 ϕ_{idc} bins, and computed the mean $|PE_{IF}|$ for each bin (e.g., Figure 4.3a and b).

2. For each p/k_s and ϕ_{imp} combination, we then calculated the 5^{th}, 15^{th}, and 25^{th} percentile $|PE_{IF}|$ values. The 25^{th} percentile corresponds to an average $|PE_{IF}| < 10\%$ when averaged across p/k_s and ϕ_{imp} conditions (see Table S2 in Supporting Information).

3. Finally, for each p/k_s and ϕ_{imp} combination, we interpolated $|PE_{IF}|$ contours (Figure 4.3c) from (1), using average $|PE_{IF}|$ values for each percentile defined in (2).

We defined the 'behavioral parameter space' ($\hat{A}$) as the parameter combinations contained by the 15^{th} percentile $|PE_{IF}|$ contour (Figure 4.3d). This contour is associated with good model performance ($|PE_{IF}| \leq 7\%$) and was also the lowest threshold contour (of the three tested) for which a behavioral parameter space existed for all p/k_s and ϕ_{imp} combinations (see Supporting Information Table S2). $\hat{A}$ contains the behavioral parameter sets ($\hat{k}_{width}$, $\hat{\phi}_{idc}$), which vary for different combinations of p/k_s and ϕ_{imp}.

We checked the sensitivity of the parameter space to the independent values of p and k_s (in contrast to their ratio p/k_s). For three cases where $p = k_s$ but individual values of p and k_s varied: 2, 5, and 8 cm/hr, we found the resulting $\hat{A}$s were effectively identical (see Supporting Information Figure S5) supporting the use of the ratio p/k_s to define $\hat{A}$.

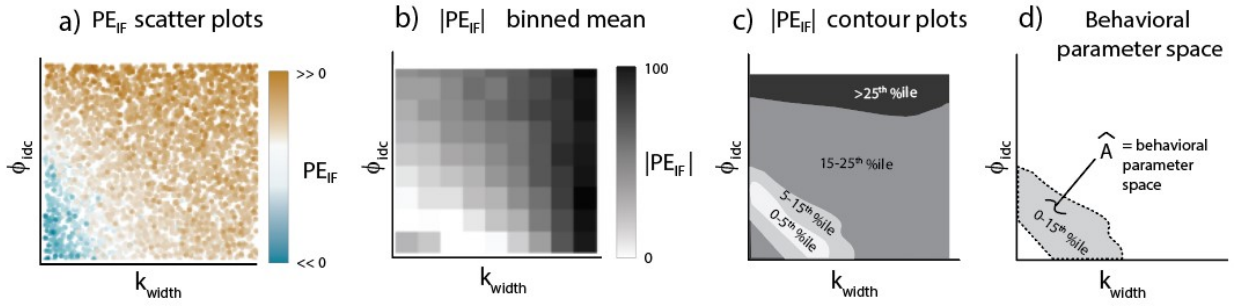

Figure 4.3. Conceptual schematic showing process for defining behavioral parameter space $\hat{A}$ for each p/k_s and ϕ_{imp} scenario. Parameter sets (k_{width}, ϕ_{idc}) are plotted in (a), with color corresponding to PE_{IF}. The parameter sets ranges were binned (10 bins each), and the mean $|PE_{IF}|$ for the parameter sets within each of the resulting grid cells are plotted in (b). Contour plots in (c) were obtained by interpolating the gridded $|PE_{IF}|$ plots, with thresholds corresponding to the average 5^{th}, 15^{th}, and 25^{th} percentiles of $|PE_{IF}|$ across p/k_s and ϕ_{imp} combinations. The behavioral parameter space $\hat{A}$ in (d) was defined by the 15^{th} percentile contour.

Quantifying transferabilty of behavioral parameter spaces

A model has 'transferable' parameters if it performs adequately under non-stationary conditions: i.e., under both the 'initial' conditions when the model is calibrated, as well as the future conditions to which the model will be applied. Transferable parameters means that the behavioral parameter spaces (and the behavioral parameter sets within them) should be the same under initial and future conditions (KlemeŠ, 1986; Hartmann & Bárdossy, 2005). This transferability (T) can therefore be measured as the fractional overlap of $\hat{A}$ under initial (i) and future (f) conditions. That is, $T = \frac{\hat{A}^i \cap \hat{A}^f}{\hat{A}^i}$, where $\hat{A}^i$ and $\hat{A}^f$ are the initial and future condition parameter spaces, respectively, and $\hat{A}^i \cap \hat{A}^f$ is their overlapping area (see Figure 4.4). As defined, $T = 0$ when no overlap exists between initial and future behavioral parameter spaces, and $T = 1$ when the initial and future behavioral parameter spaces are identical.

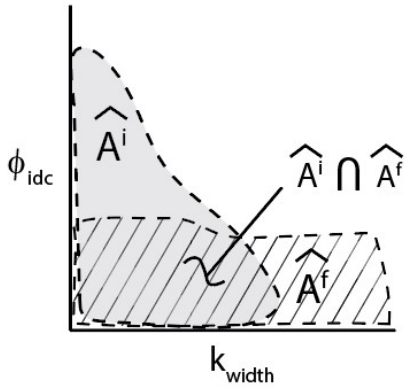

Figure 4.4. Conceptual schematic showing behavioral parameter spaces for initial conditions $\hat{A}^i$ and future conditions $\hat{A}^f$. The transferability of the behavioral parameter spaces T is defined as $T = \frac{\hat{A}^i \cap \hat{A}^f}{\hat{A}^i}$. It represents the agreement between calibrated 'initial' and 'future' behavioral parameter spaces.

We computed T for each combination of p/k_s and ϕ_{imp}, assuming that one combination would representing 'initial' and another 'future' conditions. We plotted T against the difference in each parameter between initial and future cases: $\Delta p/k_s$ and $\Delta\phi_{imp}$:

$$\Delta p/k_s = (p/k_s)^f - (p/k_s)^i \tag{4.7}$$

$$\Delta\phi_{imp} = {\phi_{imp}}^f - {\phi_{imp}}^i \tag{4.8}$$

Implications for model error

Given the definition of behavioral parameter space (which correspond roughly to calibration sets that result in less than 7% error in IF), extreme values of T (i.e., 0 or 1) implies that the magnitude of error that could arise from transferring behavioral parameter sets between conditions is likely to be greater than 7% (for $T = 0$) or less than 7% (for $T = 1$). In between these two extreme cases, however, T as defined does not quantify the magnitude of error occurring if a behavioral initial parameter set is applied under future conditions. We therefore calculated the error (in PE_{IF}) occurring for each potential p/k_s and ϕ_{imp} initial-to-future transition. Transitions were given by $\Delta p/k_s$ and $\Delta\phi_{imp}$. We plotted the resulting errors against the transition, i.e., $\Delta p/k_s$ and $\Delta\phi_{imp}$.

While many different initial-to-future transitions are possible in theory, SWMM is often used to predict changes to infiltration and runoff resulting from future development (increased imperviousness) and/or climate change (increased rainfall intensity) (e.g., Panos et al., 2021; Panos, Hogue, Gilliom, & McCray, 2018). To explore the implications of non-transferability for these typical applications of SWMM, we show the distributions of errors that can arise when calibrated parameter sets from initial conditions ${\phi_{imp}}^i = 0.1$ and ${p/k_s}^i = 0.25$ were subsequently used to make predictions under three different future conditions (Figure 4.5): (1) land cover change, ${\phi_{imp}}^f = 0.9$ ($\Delta\phi_{imp} = 0.8$); (2) climate change, ${p/k_s}^f = 4$ ($\Delta p/k_s = 3.25$); and (3) both land cover + climate change, ${\phi_{imp}}^f = 0.9$ ($\Delta\phi_{imp} = 0.8$) and ${p/k_s}^f = 4$ ($\Delta p/k_s = 3.25$).

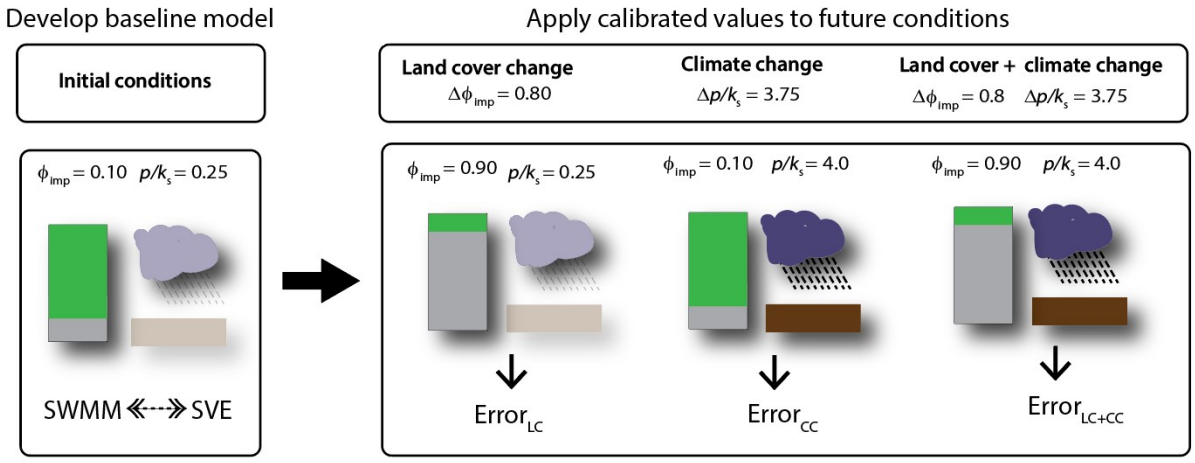

Figure 4.5. Potential development and climate change conditions to illustrate the impacts of calibration parameter instability on model error.

4.3 Results

SWMM sensitivity analysis

Figure 4.6 shows the mean contribution of each effective parameter to output variance in IF. The Sobol' total-order indices for each effective parameter across S, p/k_s and ϕ_{imp} conditions are shown in Supporting Information S1. In general, the pervious area parameters (n_{perv}, d_{perv}) are more sensitive than their impervious area counterparts (n_{perv}, d_{perv}). This is likely due to two factors. Firstly, there is wider variability in these parameters – and therefore a wider range of their typical values – across pervious areas than across impervious areas (see Table D.1 in Appendix D.1). Secondly, variation in these parameters impact the rate of flow across a surface, and the longer water spends on pervious areas the more infiltration happens (thus directly impacting IF). Detaining or slowing down runoff across a pervious area, however, does not necessarily lead to less infiltration, because the impervious area may or may not lead to a downslope pervious area over which the detained runoff could infiltrate. This could explain, in part, the high sensitivity of ϕ_{idc} – a measure of how connected these impervious areas are to downslope pervious areas.

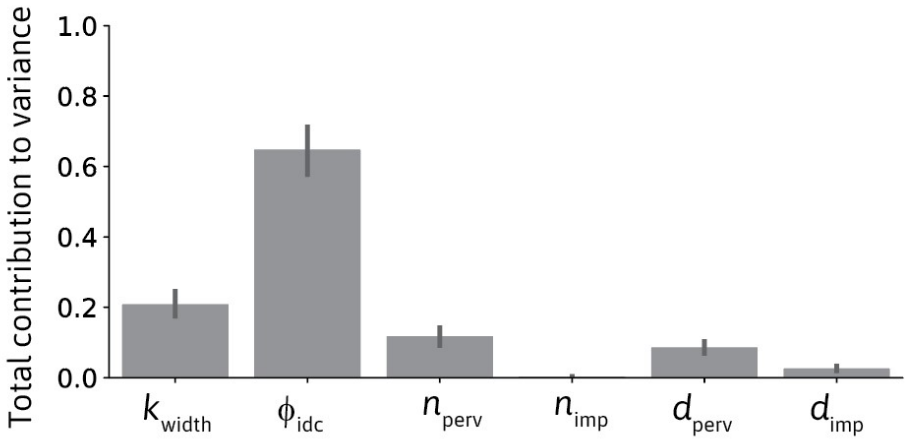

Figure 4.6. Summary of Sobol' sensitivity analysis results. Bar charts show SWMM parameter (x-axis) mean contribution to output variance in IF (y-axis). Standard deviation bars for each parameter indicate variability in contribution to variance across ϕ_{imp}, p/k_s, and S combinations.

SWMM calibration and behavioral parameter space

Figure 4.7 shows the percent difference between SWMM and SVE predictions of IF as a function of k_{width} (x-axis) and ϕ_{idc} (y-axis), across ϕ_{imp} (columns) and p/k_s (rows). Behavioral parameter spaces, shown in grey and enclosed by dashed lines, vary as p/k_s and

ϕ_{imp} change (i.e., between subplots). In general, for low ϕ_{imp} and p/k_s (lower left corner), many parameter combinations produce behavioral results. This means parameters are not highly identifiable (likely because most rainfall infiltrates under these conditions, largely independently of the calibrated parameters). Conversely, for high ϕ_{imp} and p/k_s (upper right corner), the area of the behavioral parameter set is much smaller, leading to highly identifiable of parameters.

Variation in the shapes of the behavioral parameter spaces are indicative of which parameter exerts more control on SWMM outcomes for any given p/k_s and ϕ_{imp} combination. For example, the range of behavioral k_{width} values is smaller (more constrained) than the range of behavioral ϕ_{idc} values for low ϕ_{imp} and high p/k_s (upper left corner), while the opposite is true for low ϕ_{imp} and p/k_s (lower left corner).

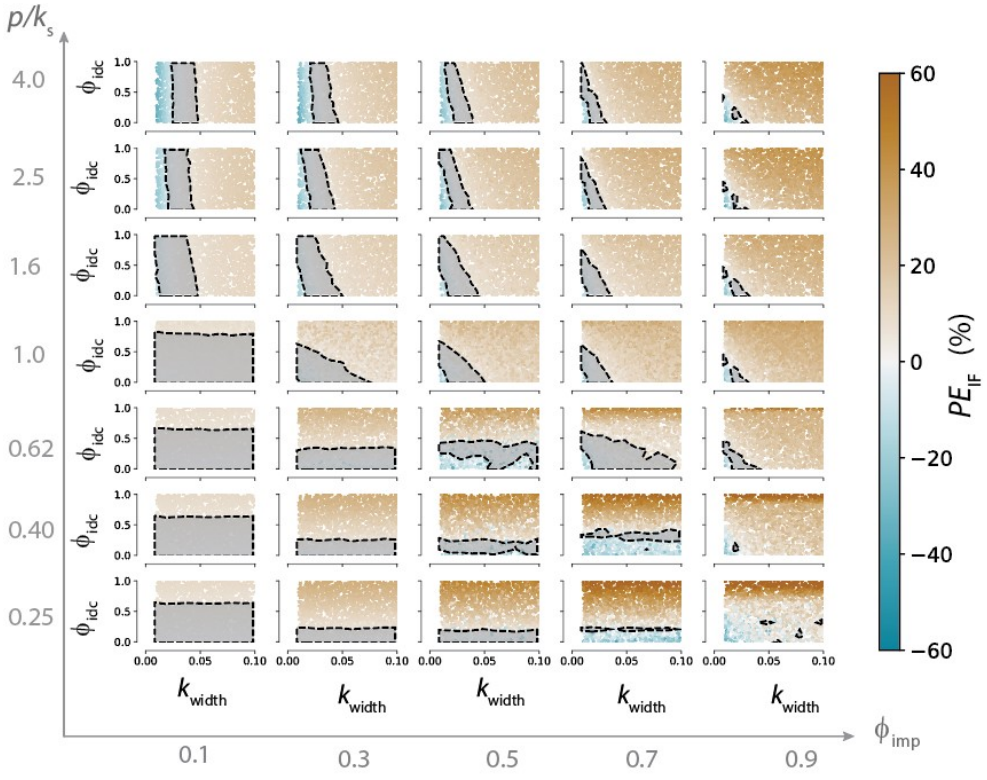

Figure 4.7. SWMM calibration results. PE_{IF} errors are plotted as a function of k_{width} (x-axis) and ϕ_{idc} (y-axis) values, across varying ϕ_{imp} (columns) and p/k_s (rows). Behavioral parameter spaces $\hat{A}$ are the areas enclosed by the dashed line.

Transferability of behavioral parameter space

Figure 4.8 is a heatmap showing the fraction of overlap between behavioral parameter spaces for all potential combinations of p/k_s and ϕ_{imp}. Darker colors indicate greater overlap (higher T).

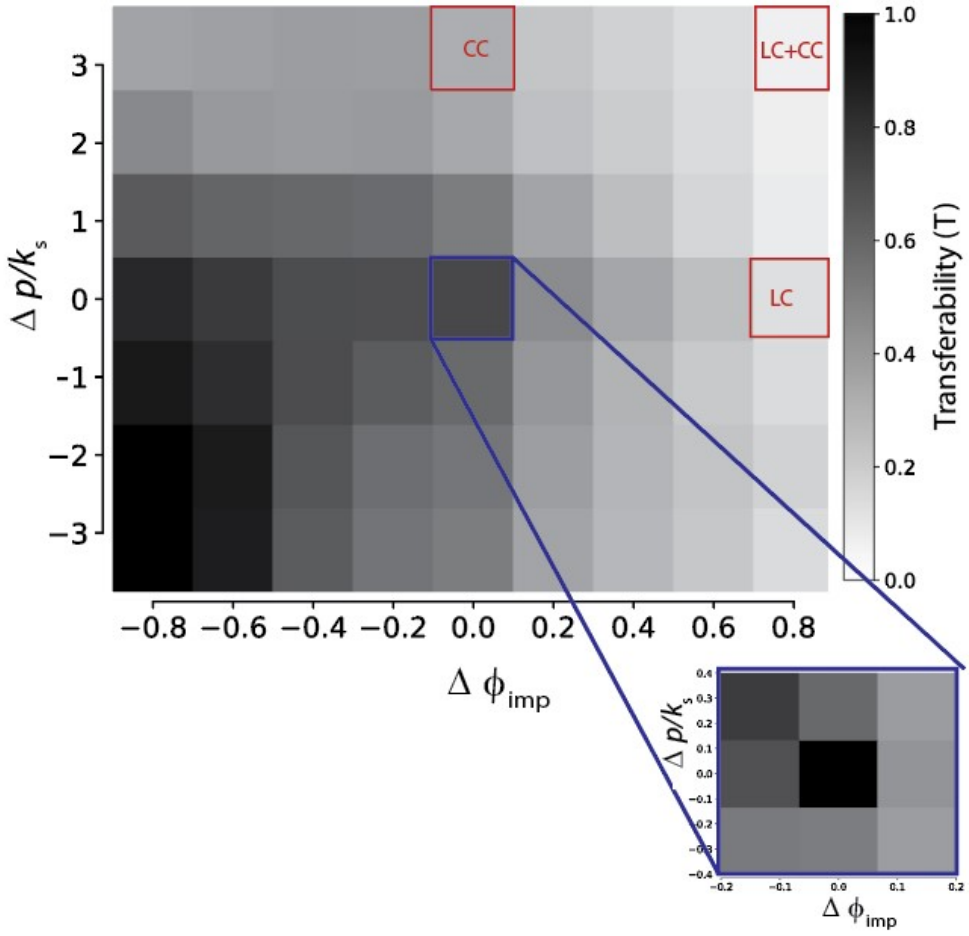

Figure 4.8. Transferability T between behavioral parameter space for initial and final conditions, plotted as a function of $\Delta\phi_{imp}$ (x-axis) and $\Delta p/k_s$ (y-axis). T values are averaged within each $\Delta\phi_{imp}$ and $\Delta p/k_s$ bin. The inset shows smaller $\Delta\phi_{imp}$ and $\Delta p/k_s$ bins around $\Delta\phi_{imp} = 0$ and $\Delta p/k_s = 0$. Darker hues correspond to higher overlap between behavioral parameter spaces, and thus more transferable initial behavioral parameter sets. Illustrative scenarios for which errors are quantified are outlined in red (land cover change (LC), climate change (CC), land cover and climate change (LC + CC)).

As defined, T must equal 1 if initial conditions are the same as the final conditions (i.e.,

when $\Delta\phi_{imp}$ and $\Delta p/k_s$ equal 0). This cannot be seen directly in Figure 4.8 due to the relatively coarse $\Delta\phi_{imp}$ and $\Delta p/k_s$ bins used. An inset is provided using a finer resolution for this binning, which reveals the $T = 1$ for $\Delta\phi_{imp} = \Delta p/k_s = 0$ situation.

Under non-stationary conditions, T is greatest for negative $\Delta\phi_{imp}$ and negative $\Delta p/k_s$ (see lower left corner of Figure 4.8). These results are consistent with Figure 4.7, as this indicates a shift towards conditions with the largest $\hat{A}$ areas. Similarly, shifts towards smaller behavioral parameter spaces (e.g., towards high ϕ_{imp} and high p/k_s in Figure 4.8) result in low values of T.

Implications for model error

Figure 4.9 illustrates the range of errors that arise when behavioral parameter spaces are transferred across environmental conditions. The panels of Figure 4.9 correspond to the lower 95% CI error (a), mean error (b), and upper 95% CI error (c) as a function of $\Delta p/k_s$ (x-axis) and $\Delta\phi_{imp}$ (y-axis). This figure shows that high magnitude of errors in IF can result from initial-to-future transitions characterized by positive $\Delta\phi_{imp}$ (i.e., where future impervious is higher than initial impervious). This error can lead to over-estimation in IF up to 60% (panel c) or under-estimation as low as -60% (panel c). However, initial-to-future transitions characterized by negative $\Delta\phi_{imp}$ and negative $\Delta p/k_s$ lead to relatively low error (as shown by the light grid cells in panels (a) and (c)).

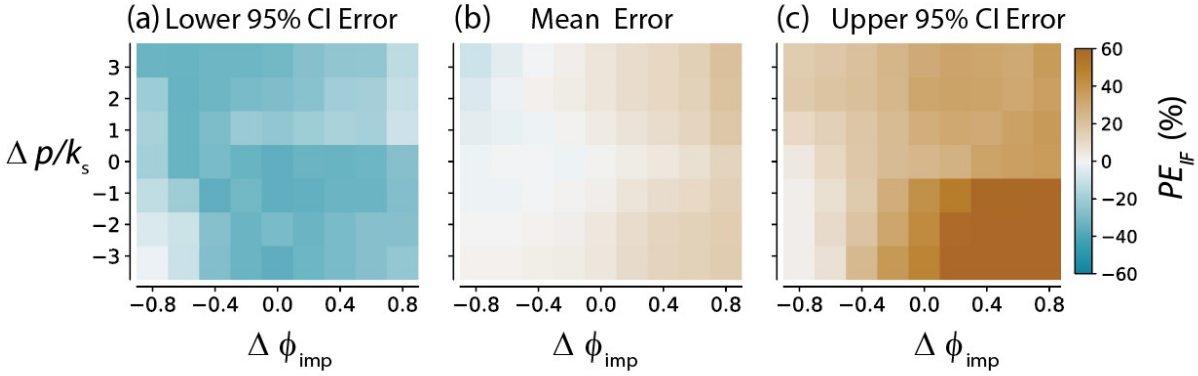

Figure 4.9. Potential over-estimation (brown) and under-estimation (blue) in IF as a function of transitions in p/k_s and ϕ_{imp}. $\Delta p/k_s$ and $\Delta\phi_{imp}$ can be computed for any initial and future condition, and can be applied to (a), (b) and (c) to determine the 95% CI range in PE_{IF}.

Figure 4.10 illustrates the errors that could arise due to poorly transferable model parameters for the three 'typical' SWMM transitions shown in Figure 4.8. Figure 4.10a shows PE_{IF} as a function of k_{width} and ϕ_{idc} for the initial conditions. Figure 4.10b-d shows the same PE_{IF} plots but for future conditions. The initial (pale grey shapes) and future

(striped shapes) behavioral parameter spaces are superimposed on each panel. Figure 4.10e-h shows corresponding distributions of PE_{IF} associated with choosing a behavioral parameter set based on the initial conditions in Figure 4.10a. When the behavioral parameter space obtained for the initial conditions is reapplied to those initial conditions, the PE_{IF} values range from 0 to 6% - as expected given the definition of 'behavioral' used. When the initial behavioral parameter space is applied to future conditions, however, PE_{IF} ranges from -60 % to 40%, with 95% PE_{IF} CIs ranging from -28% to 36% (Figure 4.10f-h). The distribution of error varies across the future scenarios, with the lowest mean error being associated with the land cover change condition (2.1%) (Figure 4.10f) and highest mean error associated with joint land cover and climate change (21%) (Figure 4.10h).

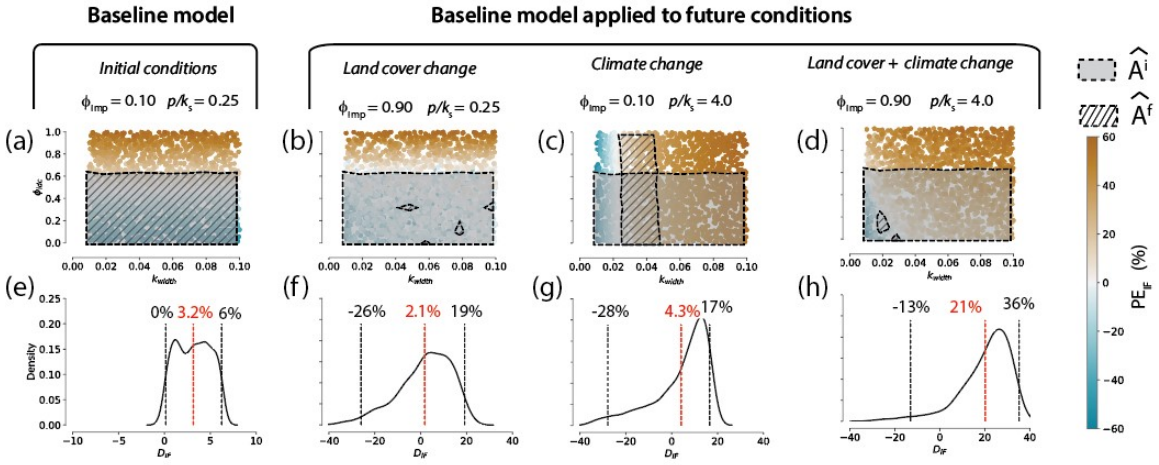

Figure 4.10. PE_{IF} as a function of k_{width} and ϕ_{idc} across initial and future conditions, overlayed by the behavioral parameter spaces (a - d) (reproduced from Figure 4.7). Initial condition behavioral parameter space $\hat{A}^i$ is shown in grey, while behavioral parameter space each future condition $\hat{A}_f$ is shown with hatching. Distributions of PE_{IF} errors associated with choosing a parameter set within the $\hat{A}^i$ are shown for each future condition in (e - h), with 95% CIs on PE_{IF} shown in black, and mean PE_{IF} shown in red.

4.4 Discussion

Variability in behavioral parameter space across conditions

The study results clearly indicate that the performance of calibrated SWMM parameters ϕ_{idc} and k_{width} are sensitive to environmental conditions (defined by ϕ_{imp} and p/k_s). This emphasizes the 'effective' nature of the calibration parameters, demonstrating that they are not physically-based properties of subcatchments, that would be invariant as climate, soil, or land cover changed.

Effective model parameters often display sensitivity to climate drivers. For example, calibrated hydrological model parameters are often sensitive to 'wet' vs. 'dry' conditions (C. Z. Li et al., 2012; Gan et al., 1997; Gharari et al., 2013). However, the extent of this sensitivity within the SWMM model has not been robustly assessed to date. Some of the most common applications of SWMM aim to predict urban runoff production across changing climates (e.g., Panos et al., 2021; Bai et al., 2018; Waters et al., 2003) or changing land cover characteristics (e.g., Panos, Hogue, Gilliom, & McCray, 2018; Jang et al., 2007). The validity of the model calibration as these conditions change is almost never assessed in these studies (but see studies of transferability on: SWMM green roof parameters Johannessen et al. (2019); distributed model parameters in urban areas Mittman et al. (2012); and lumped model parameters in non-urban catchments C. Z. Li et al. (2012)). This is problematic, because the error in IF demonstrated here due solely to non-transferability of parameters across climate and land cover conditions are as large as ±60%.

These errors arise from the non-transferability of the calibrated parameters, which itself reflects that the main controls on runoff change along with climate, soil, and land cover properties. Under low p/k_s conditions, the behavioral parameter space was more constrained by ϕ_{idc} than k_{width} (see Figure 4.7). Under these conditions, pervious areas do not produce runoff, and runoff routed across pervious areas will infiltrate. Almost all subcatchment-level runoff is thus generated on the directly connected impervious areas. Crompton et al. (2019) also found that directly connected impervious area was an important predictor of runoff under low rainfall intensities (i.e., low p/k_s).

At high p/k_s ratios, however, k_{width} provides a stronger constraint on the behavioral parameter space than ϕ_{idc}. This is consistent with previous findings that runoff is sensitive to flowpath length under moderate to high rainfall intensities (Mayor et al., 2008). Additionally, the behavioral parameter space areas are larger for low ϕ_{imp} than they are for high ϕ_{imp} – likely reflecting that in subcatchments with large pervious areas, most rainfall infiltrates regardless of how routing parameters k_{width} and ϕ_{idc} are specified. Models parameters obtained by calibration under low p/k_s and low ϕ_{imp} conditions are thus unlikely to be transferable to high p/k_s and high ϕ_{imp} conditions, as illustrated in Figure 4.8, while transferability is more probable for change in the opposite direction (from high to low p/k_s and high to low ϕ_{imp} values).

The transferability of behavioral parameter space, however, does not always predict the magnitude of resulting errors. Errors in IF are high under positive $\Delta\phi_{imp}$, but low for

positive $\Delta p/k_s$ (Figure 4.9) – even through transferability is low in both cases (Figure 4.8). And even though positive $\Delta p/k_s$ changes have less transferability of parameters than negative $\Delta p/k_s$, the resulting errors are smaller than for negative $\Delta p/k_s$ (see Figure 4.9a, c).

For high ϕ_{imp} and low p/k_s, the behavioral parameter space spans multiple, non-contiguous regions of ϕ_{idc} and k_{width}. The fractured nature of these behavioral parameter spaces suggests that, for these conditions, spatial patterns other than ϕ_{idc} and ϕ_{imp} have non-trival impacts on IF_{sve}. In other words, under certain conditions, runoff and infiltration from the SVE may be related to spatial patterns – other than those captured by ϕ_{idc} and ϕ_{imp} – that are not accounted for in SWMM. Under other ϕ_{imp} and p/k_s conditions, however, the behavioral parameter spaces are continuous, implying that the spatial metrics in SWMM (ϕ_{imp} and ϕ_{idc}) are likely also the most important spatial patterns for IF_{sve}.

Implications for planning and design

Urban hydrologic models must often predict the effects of development, for example the expansion of impervious surfaces; of climate change, which could impact p/k_s positively or negatively; or of the installation of stormwater management controls (e.g., green infrastructure) on runoff. For many such transitions, parameter transferability is low (Figure 4.8) and the potential for over- and under-estimation is high (Figure 4.9). This means that when models calibrated to existing conditions are applied to simulate runoff under future conditions, the predictions may be subject to large uncertainty. For example, as shown in the 'land cover change' panels of Figure 4.5, a model calibrated to 'undeveloped' ($\phi_{imp} = 0.1$) and low p/k_s (0.25) conditions can produce errors of -60 to +40 % when applied to developed conditions ($\phi_{imp} = 0.9$). Furthermore, the errors due to non-transferability of parameters generally increase with increasing changes to forcing parameters (Figure 4.9). The reliability of predictions using historical model calibration will therefore diminish over time in changing catchments (Thompson et al., 2013).

This is particularly problematic when designing infrastructure and regulating future development to mitigate the impacts of climate or land cover change. Under-sized stormwater infrastructure (resulting from under-estimates of runoff) can increase flood risk and decrease water quality treatment performance (Brown & Hunt, 2011). Oversized infrastructure can intrude on public open space, perform poorly and increase maintenance burdens (Lapides et al., 2021; Blecken et al., 2008; Tu et al., 2020; Brown et al., 2015). Where stormwater management policies and regulations are based on predictions from runoff models (e.g., Panos, Hogue, Gilliom, & McCray, 2018), this uncertainty risks ineffective or sub-optimal policies.

On a more positive note, we found relative stability and low errors associated with decreasing impervious surface area (negative $\Delta\phi_{imp}$ in Figure 4.8 and 4.9). This suggests confidence can be attached to SWMM studies that address the effectiveness of *reducing* ϕ_{imp} for mitigating storm runoff and water quality issues arising from existing development (e.g., Avellaneda et al., 2017; Jarden et al., 2016a).

Limitations of study approach

The applicability of this study to "real world" conditions depends on how well the SVE model described in Section 4.2 represents runoff production in the modeled landscapes. The SVE model omits real-world heterogeneity in depression storage, roughness, and topography, as well as any urban drainage infrastructure. The SVE also neglects temporal variations in rainfall and infiltration capacity or the effects of saturating a soil of finite depth (Grayson & Blöschl, 2001; Minet et al., 2011). Omitting these processes from the SVE (and also from SWMM), however, greatly simplifies the interpretation of the results. The virtual experiments presented here are also limited to small hillslopes (100 m $\times$ 50 m) and time scales (30 minute events). Thus, the results are most reliably applied to similarly small spatial and temporal scales, and should not be applied to larger hillslopes and longer time scales. It is likely that the spatial features which control hydrologic responses are scale dependent – for example, larger scales may 'average out' some of the variability arising from spatial pattern, and thus reduce variation in calibration values (K. J. Beven, 1989; Wood et al., 1988).

Urban hydrologic predictions under change

Despite the uncertainty associated with non-transferability of model parameters, water resource managers need hydrologic predictions to assist with future decision-making (Thompson et al., 2013). Historical observations (e.g., of rainfall, runoff, and land cover) are crucial for process representation in models, but different approaches are needed to cope with changing behavior in hydrologic systems (Wagener et al., 2010).

Currently, non-stationarity in climate is primarily addressed by either: (i) calibrating and validating models across a range of historical conditions that are analogous to expected future hydroclimatic regimes (e.g., Vaze et al., 2010); or (ii) Calibrating models for discrete and distinct time periods (e.g., 'wet' and 'dry' conditions) within which the hydrologic regime is considered to be stationary (e.g., Gharari et al., 2013; C. Z. Li et al., 2012). Both approaches have drawbacks - historical datasets may not contain periods that provide adequate analogues for future states (Wagener et al., 2010; Westra et al., 2014), while re-calibration of models across multiple time periods my simply be impossible for long-term forecasting.

No analogues to these methods are formalized for non-stationarity in land cover: the literature contains minimal discussion of whether current approaches to calibration adequately samples different land cover conditions, or whether calibration should be adapted to address different land cover configurations separately (i.e., as disparate 'land cover regimes'). Indeed, unlike climatic drivers which are resolved on fine timescales in hydrologic models, land cover is often not treated as a time varying model forcing at all. Incorporating time series of impervious area into urban modeling - particularly when calibrating and validating models - would be a useful first step to avoid confounding non-stationarity in land cover with non-transferability of effective model parameters.

An alternative to relying on historical calibration is to adopt data-assimilation modeling approaches which can update model parameters in response to observations (Beck, 1987; Hoke & Anthes, 1976; Merz et al., 2011). Data assimilation is valuable for improving short-term predictions in response to non-stationarity or simply in response to more observational data availability (e.g., model 'learning') (Milly et al., 2008; Fries & Kerkez, 2018; Hutton et al., 2014) - an approach with strong synergies to 'adaptive management' philosophies (Dietze et al., 2018). There are, however, some significant limitations to data assimilation. Firstly, it is necessarily data-hungry, limiting its application to well observed systems. Secondly, while data assimilation can respond to 'near-term' non-stationarity (i.e., occurring between initial calibration and application of the model), it does not resolve the issues that 'long-term' non-stationarity poses for making predictions in a future state for which no observations are available.

Where now for SWMM?

Should models like SWMM – i.e., those that depend on calibrating effective model parameters – continue to be used? The fact that these parameters are not observable or transferable suggests that the problem cannot be fixed simply by adding more observations to model calibration and parameterization. Instead, the situation suggests there is a trade-off between: (i) retaining the use of familiar tools like SWMM, and accepting the error and limitation on model transferability associated with reliance on effective parameters; and (ii) requiring that more physically-driven models should be used for urban stormwater predictions, potentially reducing error at the expense of a more data-hungry and challenging modeling process.

At present, this trade-off is difficult to navigate in part because it is not clear to what extent changes in calibration practice such as those outlined above could mitigate errors associated with non-transferable parameters. Evaluating error due to non-transferable parameters will require long-term datasets for urban runoff and flows, which continue to be limited in their availability. Thus, evaluating the suitability of continuing to use tools like SWMM will either be constrained to insights available from synthetic experiments like those presented here, or will become contingent on the broader problem of monitoring urban hydrology, developing suitable real-time monitoring and modeling techniques within urban environments (Wong & Kerkez, 2016; Hutton et al., 2014; Wong & Kerkez, 2018; Bartos et al., 2019), and the willingness of practitioners and regulators to move to more adaptive management systems (Dietze et al., 2018).

4.5 Conclusion

Virtual experiments demonstrated that non-stationarity in climate and land use undermines the performance of calibrated SWMM models. Parameters calibrated in one set of climate and land use conditions were generally not the optimal calibrated parameters under different conditions. Predicting across distinct conditions with calibrated models thus introduced

variable ranges of model error. Urban hydrologic modeling and planning often requires that modeling inform decisions about managing development, climate change, or installation of green infrastructure. The virtual experiments suggest that such modeling scenarios risk significant prediction error of ±60%.

With many urban prediction studies relying on semi-distributed models such as SWMM to predict novel conditions in urban catchments, non-transferability of parameters is likely to be a widespread problem. Resolving this problem is unlikely to be straightforward given the nearly ubiquitous use of semi-distributed models for urban runoff predictions and the barriers posed by data needs, training needs, and access to software (all of which currently limit the adoption of fully distributed models). In the short term, useful measures could include ensuring that practitioners and researchers are aware of the non-transferability problem, developing improved benchmarks of the likely errors that result from non-transference of parameters, and designing modeling studies to account for the problem using different calibration, data assimilation, or study design techniques.

Chapter 5

Conclusions

This dissertation aimed to improve understanding of urban runoff processes by exploring how spatial patterns of impervious and pervious surfaces influence urban runoff when subject to varied rainfall and soil conditions, and to create frameworks which make such relationships relevant to policy and planning. The major contributions of this research are presented in response to the guiding questions posed in Chapter 1.

What are the implications of different hydrologic processes for the production of urban stormwater and its management?

> The current approach to urban runoff management approaches hinges on the assumption that runoff is generated via infiltration excess overland flow (IEOF). In line with this assumption, the current paradigm for urban runoff management is based on risk defined by event-scale rainfall, models that presume IEOF, and management controls that prioritize infiltration. However, two other runoff mechanisms – saturation excess overland flow (SEOF) and shallow groundwater flow (SGWF) – can also arise in urban areas. Unlike IEOF, both SEOF and SGWF runoff mechanisms depend on subsurface processes. Controls on these subsurface processes generally act over larger spatial scales and longer temporal scales than do the controls on surface processes relevant for IEOF: consequently, SGWF processes can occur over large spatial scales and fluctuate on seasonal time scales, and SEOF scales correspond to scales of soil saturation. We argue that (1) management approaches based on IEOF may be ineffective in areas that are dominated by SEOF, SGWF, or combinations of these runoff mechanisms; and (2) this inapplicability stems from a mismatch in the characteristic spatial and temporal scales between SEOF/ SGWF and the management approach defined by IEOF. This mismatch in spatial and temporal scales risks poorly defined or inapplicable management standards, hydrologic modeling approaches, and stormwater management controls.

How do local landscape patterns, land cover characteristics, and climate variability impact the spatial production of urban runoff?

> Within IEOF landscapes, impervious areas are a major control on hydrologic response, but this control is moderated by presence and variability of interspersed pervious areas. Impervious surfaces can be separated into two categories: directly or physically connected (A_{phys}) and variably connected (A_{var}) (impervious that drains to pervious). A_{var} contribution to runoff (or, its 'hydrologic connectivity', defined as ϕ_{var}), is controlled by spatial variability of pervious area characteristics and temporal variability in pervious area conditions and rainfall. Temporally varying parameters (e.g., rainfall and antecedent soil moisture) control A_{var} connectivity in areas with low permeability soils, while spatial flow path variability (e.g., relative quantity of disconnecting pervious area) controls A_{var} connectivity in areas with highly permeable soils.

How do land cover characteristics and climate variability impact calibration and predictive accuracy of semi-distributed runoff models?

> The shape of the two-dimensional behavioral parameter space (defined by two calibrated model parameters) varies with land cover and climate conditions. Inter-dependencies between calibration parameters and environmental conditions can result in significant errors when the calibration parameters are used to predict hydrologic impacts of changes to these environmental conditions (e.g., novel changes in land cover and climate). These errors generally increase with increasing changes to environmental conditions, suggesting that uncertainty and error arising from predictions made by such models will grow over time as catchments change and the model assumptions diverge from reality. These results point to a need for additional research and investment in urban hydrologic models capable of robust predictions under uncertain futures.

This dissertation presents a new direction for research on urban hydrology and planning: one that seeks to (1) relate landscape heterogeneity within urban environments to hydrologic response across physiographic and climatic contexts; and (2) account for inter-dependencies between landscape heterogeneity, environmental conditions, and hydrologic processes in urban hydrologic models; and (3) develop a range of tools and approaches for adaptive urban runoff management in these contexts. Given the rate of invention and technological advancements, these future research initiatives will have the benefit of increased access to and existence of data resources. As we enter the 'digital age', sensors, satellites, and real-time controls will produce unprecedented amounts of data at finer scales than ever before. Machine learning algorithms may be used to relate catchment response at every scale to high-resolution and distributed catchment characteristics. The

methods and frameworks presented in this dissertation serve as a starting point for this future research by providing a structure for analyzing increasingly data-rich methods (e.g., machine learning, distributed hydrologic modeling) with practical implementation (e.g., Arc GIS tools, semi-distributed models, management frameworks).

Appendix A

Notation

Table A.1. Table of notation and abbreviation used in this manuscript

A	Subcatchment Area [L^2]
$\hat{A}^i$	Initial conditions parameter space area [L^2]
$\hat{A}^f$	Final conditions parameter space area [L^2]
A_{imp}	Impervious area [L^2]
A_{perv}	Pervious area [L^2]
A_{idc}	Connected impervious area [L^2]
α	average storm depth [mm]
CC	Climate cover change scenario
d	Storage depth in reservoir [L]
d_{imperv}	Storage depth on impervious area [L]
d_{perv}	Storage depth on pervious area [L]
ET_{max}	Maximum evapotranspiration rate [mm/d]
η	Frequency with which a 1D soil column is dried by evapotranspiration occurring at potential (maximum) rates, w_o/ET_{max} [day$^-$1]
F	Cumulative infiltration depth [L]
f	Infiltration rate [L/T]
f_c	Infiltration capacity [L/T]
γ	ratio of w_o/α
h	Flow depth [L]
$IEOF$	Infiltration excess overland flow
IF_{sve}	Fraction of incident rainfall that infiltrates from SVE simulations [L^3/L^3]
IF_{swmm}	Fraction of incident rainfall that infiltrates from SWMM simulations [L^3/L^3]
k_s	Saturated hydraulic conductivity [L/T]
k_{width}	Subcatchment width factor [1/L]
L	Subcatchment overland flowpath length [L]

LC	Land cover change scenario
λ	storm frequency [day$^-$1]
n	Manning's n [T/L$^{1/3}$]
n_{imperv}	Manning's n on impervious area [T/L$^{1/3}$]
n_{perv}	Manning's n on pervious area [T/L$^{1/3}$]
p	Rainfall intensity [L/T]
P	Rainfall depth [L]
PE_{IF}	Percent error in infiltration fraction between the SVE and SWMM.
p/k_s	Ratio of rainfall to soil saturated hydraulic conductivity $[L/T/L/T]$
$p/k_s{}^i$	Initial conditions p/k_s value $[L/T/L/T]$
$p/k_s{}^f$	Final conditions p/k_s value $[L/T/L/T]$
$SEOF$	Saturation excess overland flow
$SGWF$	Shallow groundwater flow
S_o	Ground surface slope [L/L]
S_f	Friction slope [L/L]
T	Transferability of behavioral parameter space across environmental conditoins
t	Time coordinate [T]
U	Depth-averaged overland flow velocity [L/T]
W	Subcatchment overland flowpath width [L]
$WSUD$	Water Sensitive Urban Design
w_o	maximum available soil water storage in a 1D soil column [mm]
x	Coordinate pointing downslope [L]
θ_s	Saturated soil moisture content
θ_i	Initial soil moisture content
ψ_f	Matric pressure potential at wetting front [L]
ϕ_{perv}	Pervious fraction $[L^2/L^2]$
ϕ_{idc}	Connected impervious fraction $[L^2/L^2]$
ϕ_{imp}	Impervious fraction $[L^2/L^2]$
$\phi_{imp}{}^i$	Initial conditions ϕ_{imp} value $[L^2/L^2]$
$\phi_{imp}{}^f$	Final conditions ϕ_{imp} value $[L^2/L^2]$

Appendix B

SWMM Background

SWMM is a continuous or event-based rainfall-runoff simulation model developed by the EPA that has been widely used for planning, design, and analysis related to urban drainage systems and urban development (Panos, Hogue, Gilliom, & McCray, 2018; James et al., 2010b; Rosa et al., 2015). The SWMM model components that are relevant to this application include runoff generation mechanisms, overland flow routing, and infiltration, which are described below.

B.1 Non-linear reservoir routing

Subcatchments in SWMM are represented as idealized rectangular storage reservoirs of area A, width W, land surface slope S, pervious fraction ϕ_{perv}, and storage depth d. Runoff occurs once the depth of water in the area h [L] exceeds the maximum depression storage depth d [L]. The depth of water over the subcatchment, h, is computed continuously at each time step by solving the continuity equation over the entire subcatchment:

$$\frac{\partial h}{\partial t} = (p - f) - \frac{\partial (Uh)}{\partial x} \tag{B.1}$$

where U is the depth averaged flow velocity [L/T] assuming the kinematic wave approximation (Brutsaert, 2005), x is the distance from the head of the plane [L], t is the time [T], p the effective rainfall intensity (rainfall minus abstractions) [L/T], f the infiltration rate [L/T].

Manning's Equation for surface roughness relates U to friction slope S_f. Assuming kinematic flow in which flow is uniform and the friction slope S_f is approximately equal to the ground surface slope S (i.e. frictional resistance balances gravitational acceleration), Manning's equation is written as:

$$U = \frac{1}{n} h^{2/3} S^{1/2}, \tag{B.2}$$

where n is Manning's roughness coefficient $[T/L^{1/3}]$.

In SWMM, runoff is computed using the 'nonlinear reservoir routing' model (Rossman & Huber, 2016), which combines the continuity equation (B.1) and Manning's equation for kinematic flow (B.2):

$$\frac{\partial h}{\partial t} = (p - f) - \frac{1}{Ln}(h - d)^{5/3} S^{1/2} \tag{B.3}$$

where d is the maximum depression storage depth, i.e., a threshold depth required for runoff to occur, and L is the length of the plane (given by A/W).

B.2 Subcatchment routing

Runoff generated on upslope impervious or pervious sub-areas of a catchment are routed to the downslope area by modifying precipitation on the downslope sub-area. In other words, the runon from upslope areas is distributed uniformly on the downslope sub-area (Huber, 2001). One could achieve the same results by routing runoff between impervious and pervious subcatchments: when outflow from one subcatchment is routed to another subcatchment, SWMM distributes it uniformly over the downstream subcatchment (Rossman, 2015; United States Environmental Protection Agency, 2018). In this study, we modeled sub-areas as separate subcatchments for ease of computation in PySWMM.

B.3 Infiltration

Infiltration losses in SWMM are described by one of three models: Green-Ampt (H. W. Green & Ampt, 1911), Horton (Horton, 1933), or the SCS-Curve Number. While Horton and SCS-CN are empirical approaches to infiltration, Green-Ampt is physically based solution to infiltration, which assumes a ponded surface, uniform and deep soils, and a sharp wetting front which separates initial moisture content θ_i in the subsurface from saturated surface soils θ_s, taking the form:

$$f = k_s(1 + \psi_f \frac{\theta_s - \theta_i}{F}) \tag{B.4}$$

Where f is infiltration rate; k_s is saturated hydraulic conductivity; ψ_f is the average matric pressure at the wetting front; and F is cumulative infiltration volume. This model is often preferred over other infiltration models because the parameters on which it depends can be obtained from physically measured quantities (Rawls et al., 1983; Viessman & Lewis, 2011). Because Green-Ampt assumes a ponded surface, however, its application is limited to cases in which the precipitation intensity exceeds k_s. To cope with this restriction and simulate infiltration when precipitation intensity is less than k_s, SWMM adopts the Mein-Larson formulation of the Green-Ampt model (Mein & Larson, 1973). The Mein-Larson formation is an empirical soil moisture accounting scheme that considered two cases or stages infiltration.

- Stage 1: $F < F_s$. The first stage considers infiltration prior to saturation of the surface. If $i < k_s$, all rainfall infiltrates ($f = i$ and $F = I$). If $i > k_s$, SWMM predicts the volume of rainfall that will infiltrate before the surface becomes saturated (F_s). At each timestep for which $i > k_s$, the value of F_s is calculated and compared with the volume of rainfall that has already infiltrated for the event (F).

- Stage 2: $F > F_s$: The second stage considers infiltration after saturation of the surface. After this point infiltration follows the original Green-Ampt equation. Once the underlying soils are saturated $\theta_s - \theta_i = IMD = 0$, rainfall infiltrates at a rate equal to k_s.

SWMM includes two versions of the Mein-Larson formulation, which differ only slightly. In the original Mein-Larson SWMM formulation, the difference in soil moisture ($\theta_s - \theta_i$, or IMD) is updated at each timestep for which $i < k_s$, and this updated value is used in the subsequent steps. However, updating the moisture deficit between the surface and subsurface soil layers prior to surficial soil saturation (Stage 1) lacks physical justification as the subsurface soils will not saturate until the surface is saturated (under the assumed infiltration mechanism). Thus, the modified Mein-Larson SWMM formulation (incorporated in SWMM3 and subsequent versions of SWMM) does not update the difference in soil moisture in Stage 1 while $i < k_s$ (United States Environmental Protection Agency, 2018; Rossman, 2015).

Appendix C

HCIA Methods

C.1 PySWMM Model

We used PySWMM to simulate runoff and infiltration at the outlet of a catchment consisting of impervious area (A_{var}) routed to a downslope pervious area (A_{perv}) (Figure A1).

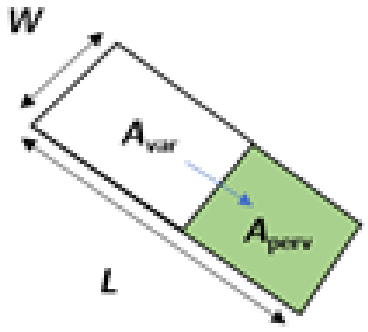

Figure C.1. Impervious area (A_{var}) routed to pervious area (A_{perv}). The total catchment area, A, is the sum of A_{var} and A_{perv}. The width, W, of the catchment is constant across A_{var} and A_{perv}.

In the case of impervious surface connectivity, we are mainly interested in the fraction of impervious runon that infiltrates downslope, rather than the fraction of total inflow to the previous area that infiltrates. We define this fraction of impervious runon that infiltrates as the "runon infiltration fraction", or IF_{runon}. The default configuration of SWMM does not provide estimates of the volume of runon that infiltrates, only of total infiltration. However, we can estimate the volume of runon that infiltrates through simple mass balance. The total infiltration volume F_{total} can be split into two separate volumes: the volume of infiltration due to impervious runon F_{runon} and the volume of infiltration due to rainfall on pervious $F_{rainfall}$ (Equation C.1).

$$F_{total} = F_{runon} + F_{rainfall} \tag{C.1}$$

Rearranging Equation C.1 gives the volume of infiltration from runon F_{runon} (Equation C.2).

$$F_{runon} = F_{total} - F_{rainfall} \tag{C.2}$$

To get the value F_{runon} for each simulation run, we simulated two catchments for each simulation (Figure C.2): (1) impervious routed to pervious, giving a value of F_{total} (Figure C.2A); and (2) pervious only, giving a value of $F_{rainfall}$ (Figure C.2B). F_{runon} is then equal to the difference in infiltration volumes (Equation C.2).

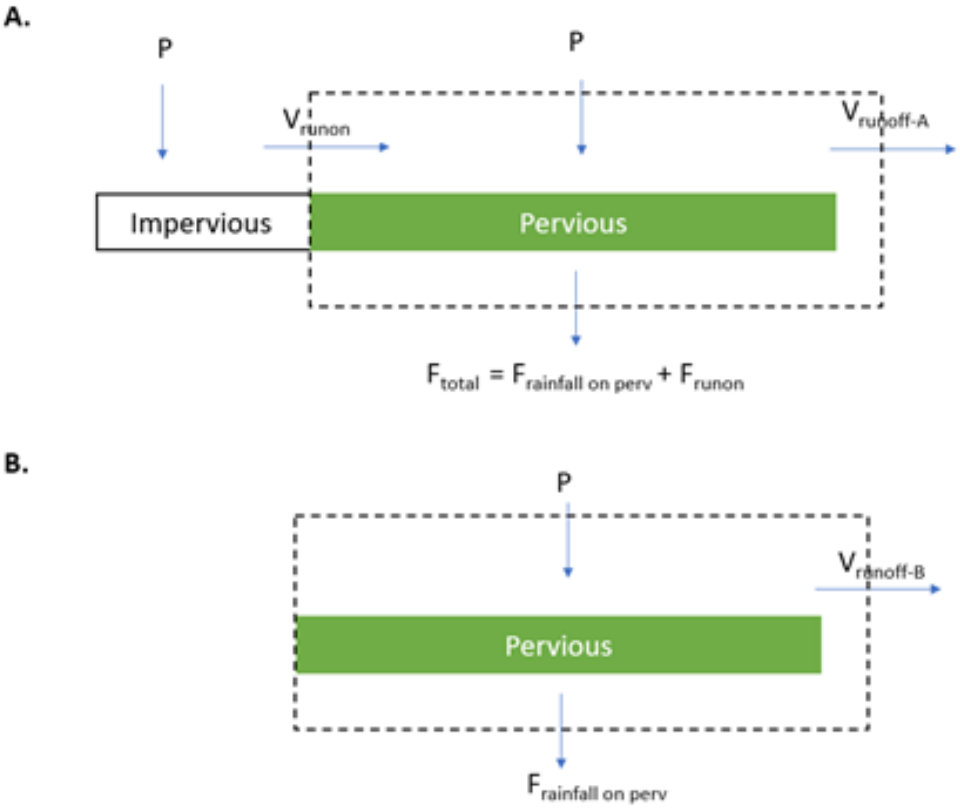

Figure C.2. Mass balance diagrams showing the catchments simulated to estimate F_{runon}. Infiltration resulting from pervious only (panel B) was subtracted from infiltration resulting from impervious routed to pervious (panel A).

Finally, we computed the IF_{runon} for each simulation as:

$$IF_{runon} = \frac{F_{runon}}{V_{runon}} \tag{C.3}$$

where V_{runon} is the volume of impervious runon to the pervious area.

C.2 Regression tree hyperparameters

Regression tree hyperparameter ranges are summarized in Table C.1 and sensitivity to these ranges are shown graphically in Figure C.3. The results of the hyperparameter tuning and sensitivity analysis shows that the model's MSE is insensitive to splitter method (Figure C.3A), number of features to consider for each split (Figure C.3C), the minimum samples split (Figure C.3E), the minimum samples at each leaf (Figure C.3F), and presort option (Figure C.3H). In contrast, the MSE appears to be sensitive to maximum depth of the tree, minimum impurity decrease, and maximum number of leaf nodes. The MSE decreases significantly as the maximum depth of the tree increases, but at a depth $\sim$ 10, the MSE maintains a value of around 0 (Figure C.3B). The MSE increases sharply at a minimum impurity decrease of $\sim$ 2, suggesting that lower minimum impurity threshold is needed for accurate predictions (Figure C.3D). The MSE decreases with increased leaf nodes. Thus, a high value for maximum number of leaf nodes has potential overfit a model (Figure C.3G).

C.3 Alternate design storms

This study applied the SCS Type II storm distribution, with a 24-hr storm duration, across five rainfall depths. However, both the storm distribution and duration have the potential to effect impervious surface connectivity. SCS Type I and IA storms characteristic of Pacific Coast Mediterranean climates have lower intensity rainfall than the SCS Type II storm distribution used in this study. Shorter duration and higher intensity storms could result in significant changes to infiltration.

To test sensitivity of ϕ_{var} to different storm distributions and durations, we ran the PySWMM simulations with two different design storms: (1) SCS Type 1, 24-hr storm distribution and (2) SCS Type 2, 6-hr storm distribution. Figure C.4 shows the sensitivity of ϕ_{var} to these storm distributions and durations.

Of the distributions and durations tested, the SCS Type 2, 6-hr duration storm results the highest median values for ϕ_{var}, suggesting that in regions with shorter, more intense rainfall, ϕ_{var} may be greater than that predicted by the regression tree and HCIA ArcGIS tool. In contrast, the SCS Type 1, 24-hr storm had consistently the lowest values for ϕ_{var}, which suggests that for the same landscape and soil conditions, regions with lower intensity rainfall (e.g., Type 1, 1a) may have lower HCIA than regions with higher intensity rainfall distributions (e.g., Type 2).

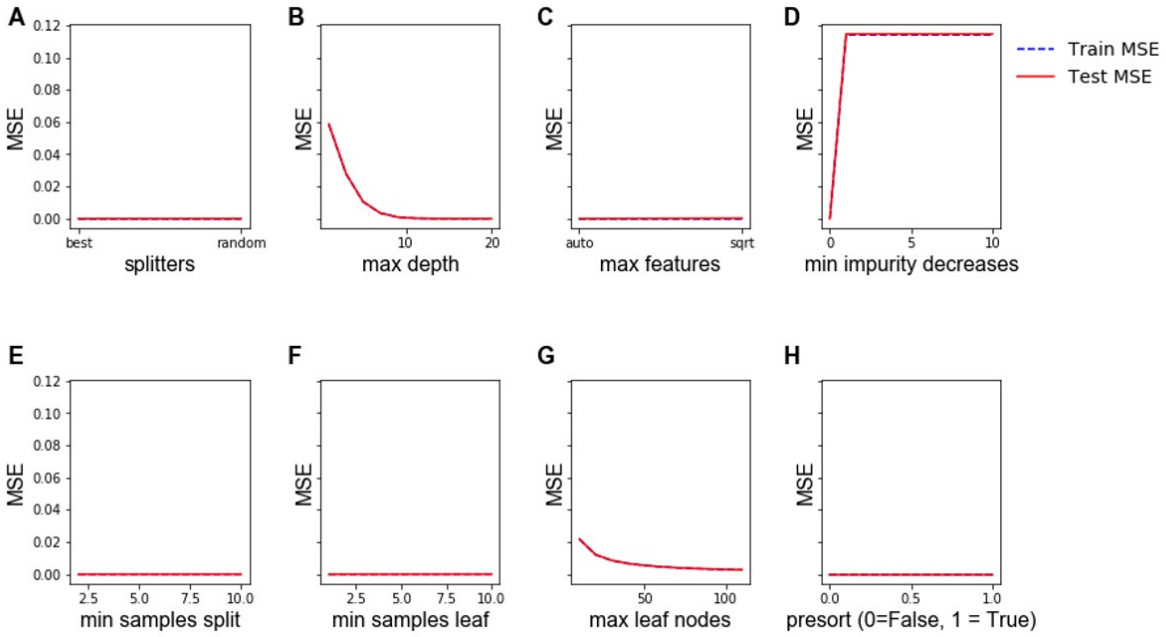

Figure C.3. Sensitivity of regression tree hyperparameters across hyperparameter ranges. The blue dashed line represents the MSE across the training data, and the red line represents the MSE across the testing data.

Hyper-parameter	**Description**	**Default value**	**Tested range**	**Final value**
Splitter	Strategy used to choose the split at each node	Best	Best, Random	Best
Max depth	Maximum depth of tree	None	1 to 20	13
Max features	The number of features to consider when looking for the best split.	None	auto, square root	auto
Min impurity decrease	Threshold for node impurity before branch is split; tells the algorithm when to stop splitting a branch. A higher minimum impurity threshold leads to lower information gain.	0	0 to 10	0
Min samples split	Minimum number of samples required to split an internal node: Increasing the values of min samples split risks under-fitting the data. When we require 100% of the data samples for a split, the MSE increases because the model cannot learn enough about the data.	2	2 to 10	5
Min samples leaf	Minimum number of samples required to be at a leaf node. As min samples leaf increases, more of the variability is included at each leaf node. Allowing for more samples at each leaf risks under-fitting the data.	1	1 to 10	1
Max leaf nodes	Maximum number of levels in tree.	None	10 to 110	110
Presort	Whether to presort the data to speed up the finding of best splits in fitting.	False	True, False	True

Table C.1. Regression tree hyper-parameters and range of random search ranges

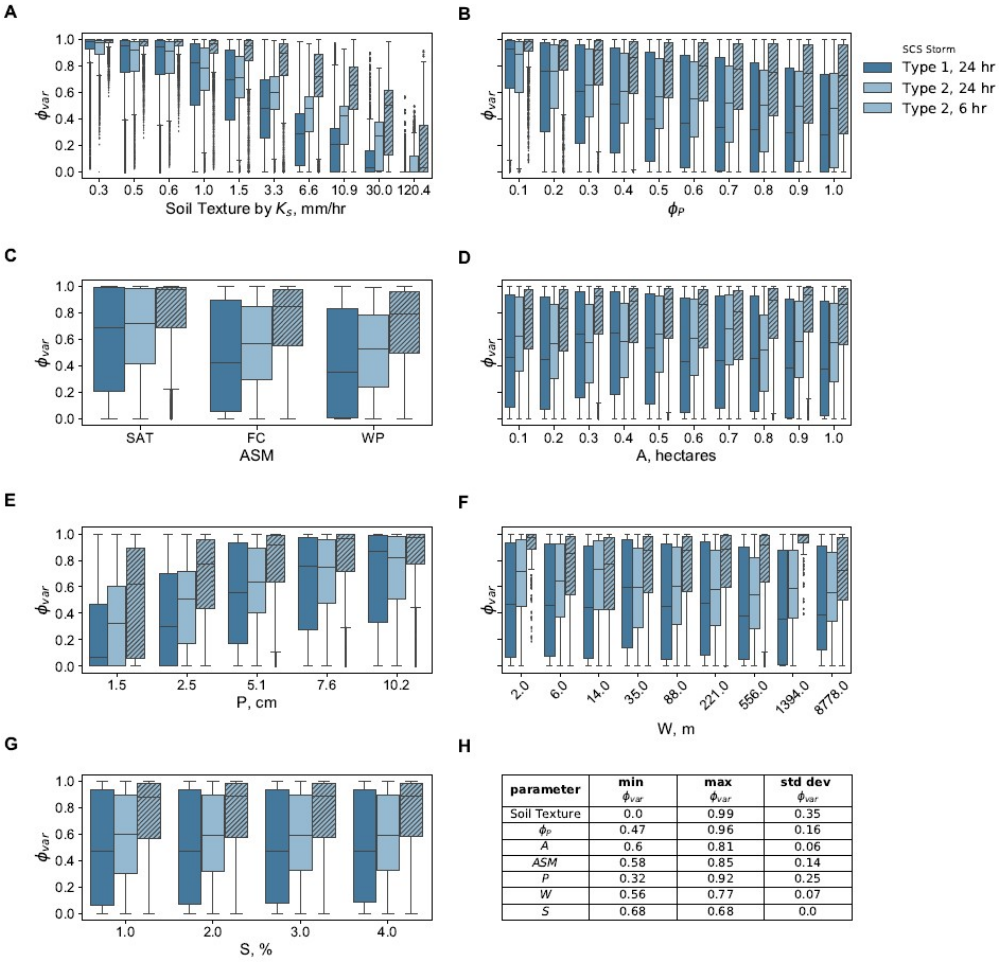

parameter	min ϕ_{var}	max ϕ_{var}	std dev ϕ_{var}
Soil Texture	0.0	0.99	0.35
ϕ_P	0.47	0.96	0.16
A	0.6	0.81	0.06
ASM	0.58	0.85	0.14
P	0.32	0.92	0.25
W	0.56	0.77	0.07
S	0.68	0.68	0.0

Figure C.4. Box plots showing sensitivity of ϕ_{var} to different storm distributions and durations.

Appendix D

SVE – SWMM Calibration: Additional Results

D.1 SWMM sensitivity analysis

To explore the sensitivity of SWMM outcomes to changes in overland flow inputs, we undertook a Sobol' sensitivity analysis across a range of soil/storm scenarios. Sobol' sensitivity analysis The higher a parameter's contribution to overall variance, the more sensitive it is. The sum of the total-order indices can be indicative of parameter interactions: for linear models, the parameters do not interact and the sum of the total order indices is equal to 1, and for non-linear models, the sum of all of the total order indices is greater than 1 due to interactions between variables.

Using saltelli sampling methods, we generated 1,400 unique parameter sets defined by total area A, width factor k_{width}, connected impervious fraction ϕ_{idc}, manning's roughness values n_{imperv} and n_{perv}, as well as depression storage d_{imperv} and d_{perv} values. We set a lower bound on k_{width} of 0.01, and upper bound at 0.1. For a subcatchment area of $5{,}000m^2$, this range in k_{width} corresponds to a width of 50 to 500 m and overland flowpath length of 100 to 10 m, respectively. These effective parameters were simulated across three soil saturated hydraulic conductivities k_s, three rainfall intensities p, three surface slopes S, and five impervious fractions ϕ_{imp}, resulting in a total of 189,000 model runs. Value ranges for these parameters are summarized in Table D.1.

Full results of the Sobol' sensitivity analysis across all ϕ_{imp}, p/k_s, and S scenarios are shown in Figure D.1. As expected given the non-linear reservoir model on which SWMM is based, the sum of total-order indices is greater than 1, indicating that parameter interactions exist. Overall, the most sensitive parameters are k_{width} (dark blue) and ϕ_{idc} (orange), but this varies across the p/k_s and ϕ_{imp} scenarios. For $p/k_s < 1$, ϕ_{idc} is the most sensitive across all ϕ_{imp} scenarios. For $p/k_s > 1$, k_{width} is the most sensitive parameter by a narrower margin, as other parameters (such as n_{perv}) also contribute substantially to variance. These results motivate further inquiry into the two most sensitive effective parameters – ϕ_{idc} and k_{width} –

across varying p/k_s and ϕ_{imp} scenarios.

Table D.1. Summary of sensitivity parameter ranges used for sensitivity analysis

Parameter	Description	Value Range
n_{imperv}	Manning's n for impervious	0.01 - 0.015 [a]
n_{perv}	Manning's n for pervious	0.0 - 0.8 [b]
d_{imperv}	Depression storage on impervious (mm)	0 - 3 [c]
d_{perv}	Depression storage on pervious (mm)	2 - 6 [d]
k_{width}	Width factor ($1/L$) (m)	0.01 - 0.1
ϕ_{idc}	Connected impervious fraction	0 - 1
A	Area (m^2)	5,000
ϕ_{imp}	Impervious fraction	0.1, 0.3, 0.5, 0.7, 0.9
k_s	Saturated hydraulic conductivity (cm/hr)	2, 5, 8
p	30-min precipitation intensity (cm/hr)	2, 5, 8
S	Surface slope (%)	1, 5, 10

[a] 0.01-0.015 James et al. (2010b)
[b] 0.02-0.8 James et al. (2010b)
[c] 0.3 - 2.54 mm James et al. (2010b)
[d] 2.54 - 5.1 mm James et al. (2010b)

D.2 Behavioral parameter threshold sensitivity

To enable comparison between ϕ_{imp} and p/k_s scenarios, it is important to choose a single behavioral parameter threshold that can be applied to each scenario. We defined the behavioral parameter threshold that was applied to each scenario in three steps.

1. We binned k_{width} and ϕ_{idc} into a 10 x 10 grid and computed the mean $|PE_{IF}|$ within each bin. The resulting plots are shown in Figure D.2, with color corresponding to $|PE_{IF}|$.

2. We computed the 5^{th}, 15^{th}, and 25^{th} percentile $|PE_{IF}|$ for each scenario. These values are tabulated in Table D.2. Average $|PE_{IF}|$ values for each percentile are all less than 10%.

3. We created contour plots from (1), using average $|PE_{IF}|$ values for each percentile defined in (2). The results of this are shown in Figure D.4.

The mean 15^{th} percentile threshold was the lowest threshold for which the behavioral parameter space area was greater than 0 for each ϕ_{imp}, p/k_s scenario. Therefore, we chose a behavioral parameter threshold that corresponds to the mean 15^{th} percentile gridded error ($|PE_{IF}|$) across the ϕ_{imp} and p/k_s scenarios, corresponding to a mean $|PE_{IF}| = 6.5\%$.

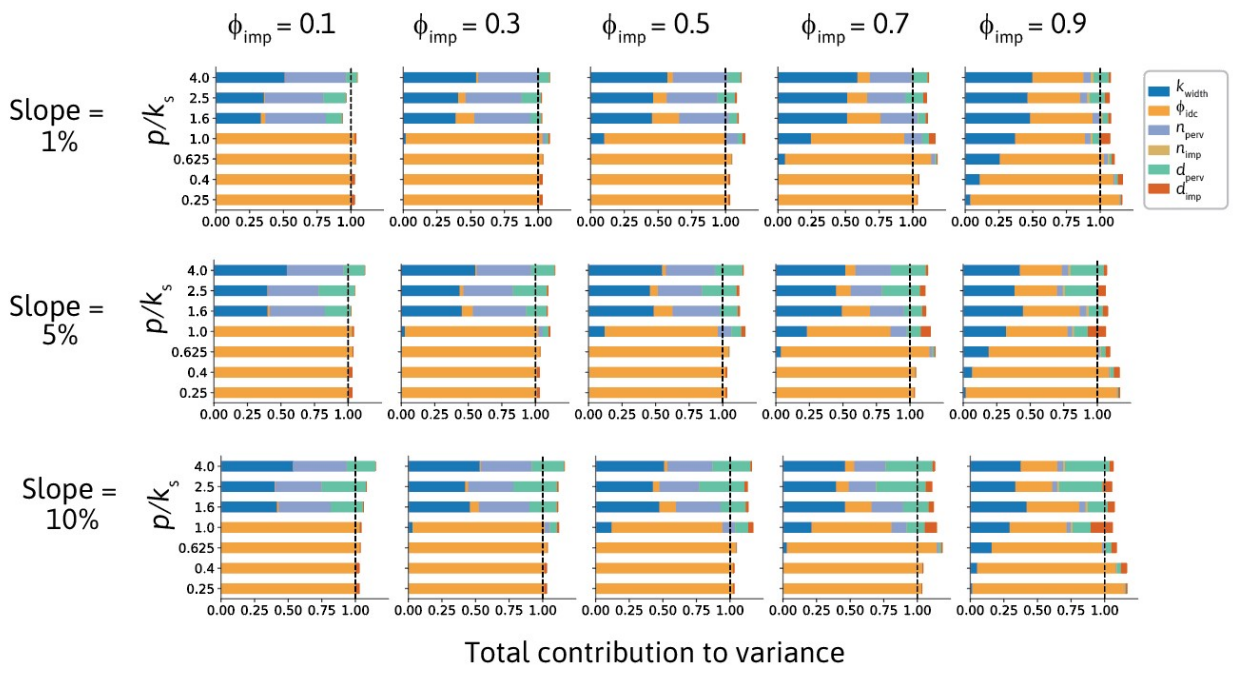

Figure D.1. Results of Sobol' sensitivity analysis. Horizontal bar charts show SWMM parameter contribution to the output variance (total-order index) (x-axis) across ϕ_{imp}, p/k_s, and S scenarios, with color corresponding to the six effective parameters. The dashed line at a total variance of 1 is the Sobol' threshold for linear and non-linear models.

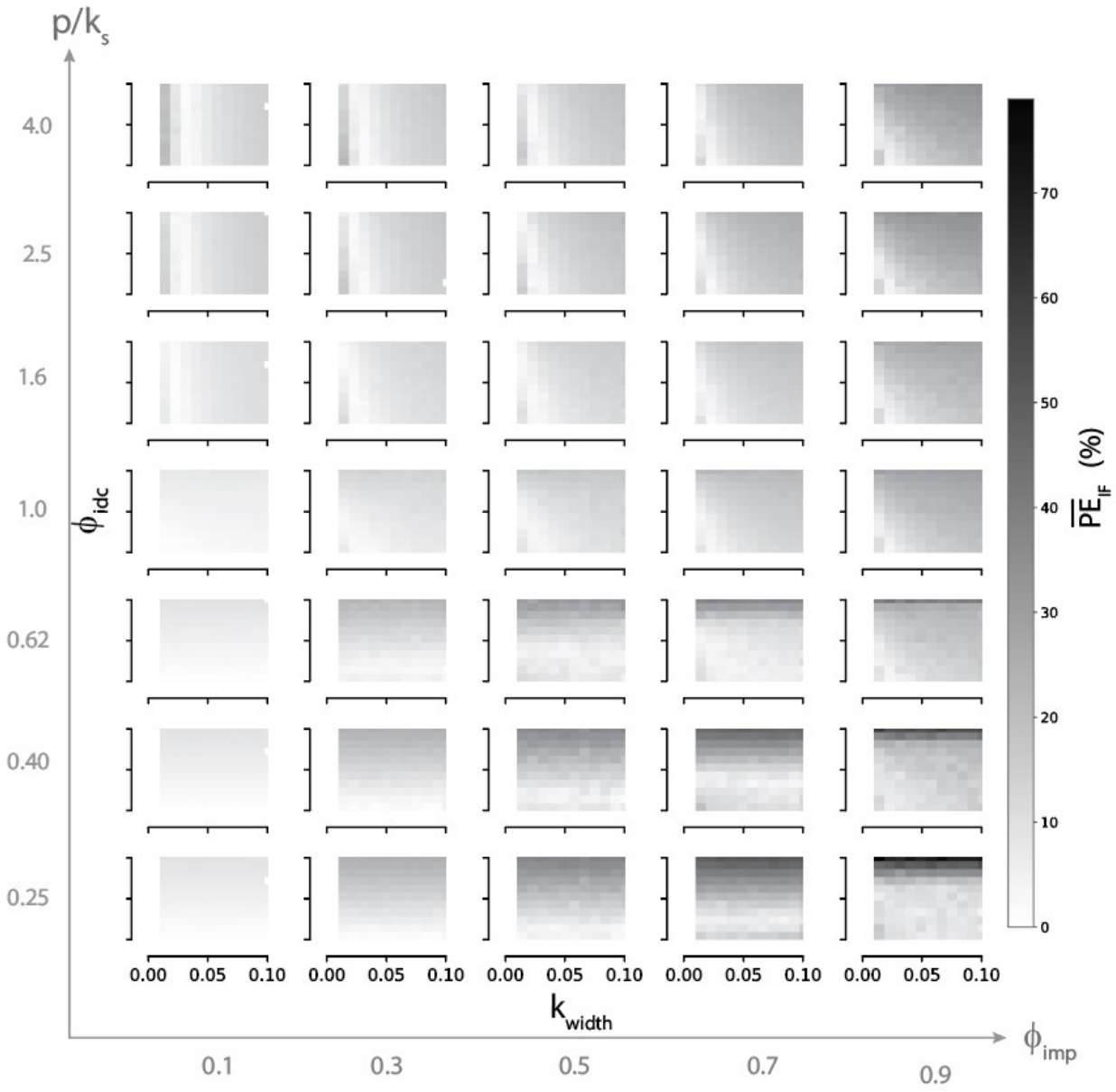

Figure D.2. Gridded mean errors $|PE_{IF}|$ across ϕ_{imp} (columns) and p/k_s (rows)

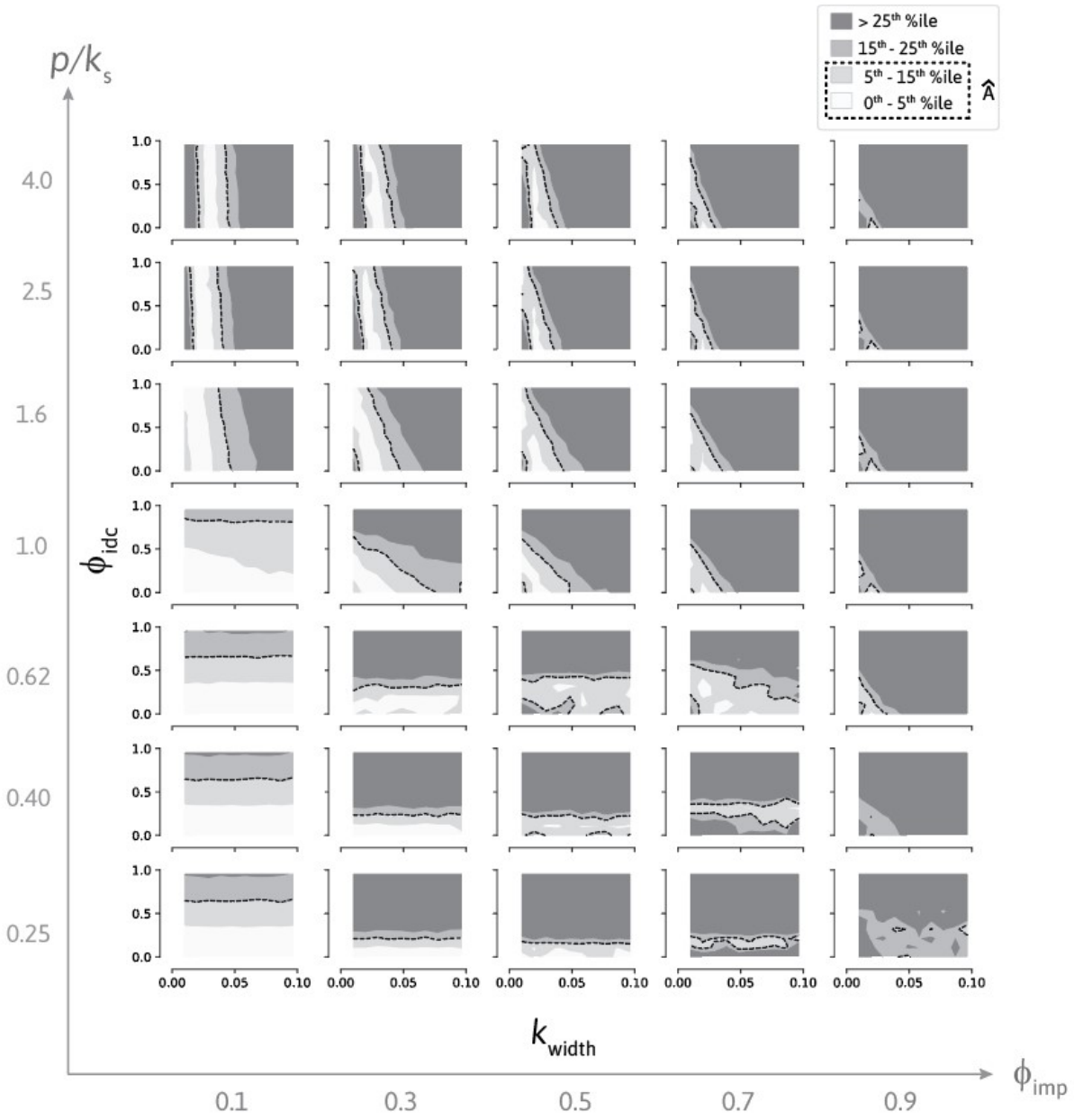

Figure D.3. Contours corresponding to $0-5^{th}$ percentile ($|PE_{IF}| < 3.5$), $5-15^{th}$ percentile ($3.5 < |PE_{IF}| < 6.5$), $15-25^{th}$ percentile ($6.5 < |PE_{IF}| < 9$), and $> 15^{th}$ percentile ($|PE_{IF}| > 9$).

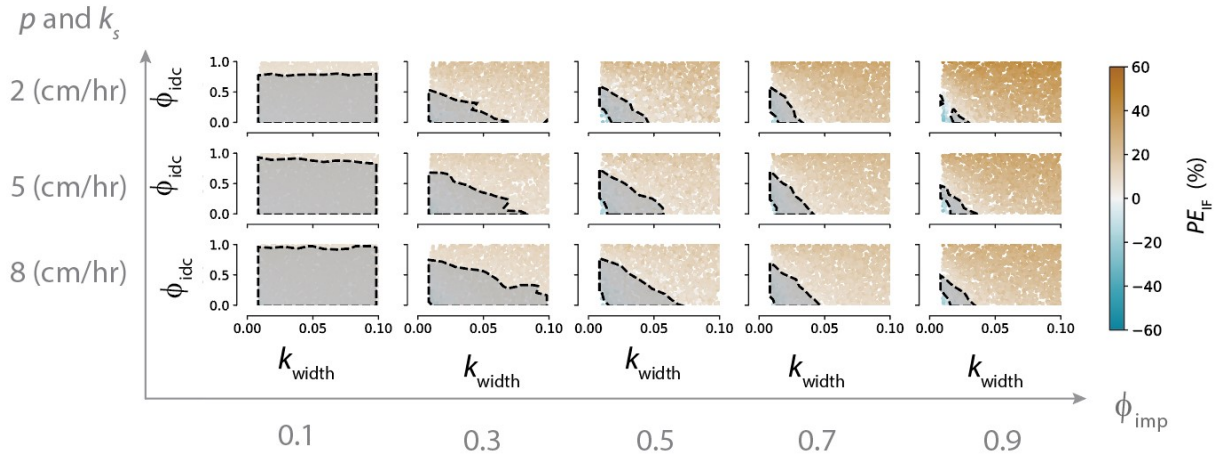

Figure D.4. Behavioral parameter spaces for $p/k_s = 1$ scenarios: $p = k_s = 2$ cm/hr (top row), $p = k_s = 5$ cm/hr (middle row), $p = k_s = 8$ cm/hr (bottom row). The variability in behavioral parameter space is minimal across the $p/k_s = 1$ scenarios for a given ϕ_{imp}.

Table D.2. 5^{th}, 15^{th}, and 25^{th} percentile $|PE_{IF}|$ for each scenario. $|PE_{IF}|$ averaged across scenarios is shown in the last column.

Percentile	p/k_s	ϕ_{imp}					Average
		0.1	0.3	0.5	0.7	0.9	
5th	0.25	0.4	1.2	2.8	5.8	7.1	
	0.40	0.4	1.6	3.7	5.1	7.9	
	0.62	0.3	2.6	3.4	3.8	5.2	
	1.00	1.3	2.8	3.3	3.5	5.5	3.5
	1.60	1.9	2.0	2.9	3.1	6.8	
	2.50	1.8	2.7	3.3	3.3	6.6	
	4.00	2.5	2.3	3.1	3.6	8.4	
15th	0.25	1.2	2.9	4.8	9.3	8.3	
	0.40	1.2	2.6	5.7	7.4	11.0	
	0.62	1.0	3.7	5.2	4.4	10.7	
	1.00	2.5	4.6	6.0	8.2	13.9	6.5
	1.60	3.1	3.7	5.1	7.7	13.4	
	2.50	5.6	5.2	6.3	8.2	15.2	
	4.00	3.6	6.4	6.3	8.3	15.9	
25th	0.25	2.3	6.0	7.6	10.5	9.2	
	0.40	2.3	5.4	8.4	8.7	12.8	
	0.62	2.2	4.7	5.9	5.7	13.7	
	1.00	3.1	6.3	8.4	11.5	17.3	9.0
	1.60	5.2	6.1	7.3	10.7	16.2	
	2.50	6.9	8.0	9.8	14.0	20.8	
	4.00	7.4	8.6	9.6	12.9	20.9	

Bibliography

Abbott, B. W., Gruau, G., Zarnetske, J. P., Moatar, F., Barbe, L., Thomas, Z., ... Pinay, G. (2018). Unexpected spatial stability of water chemistry in headwater stream networks. *Ecology Letters*, *21*(2), 296–308. doi: 10.1111/ele.12897

Addor, N., & Melsen, L. A. (2019, January). Legacy, rather than adequacy, drives the selection of hydrological models. *Water Resources Research*, *55*(1), 378–390. Retrieved from https://onlinelibrary.wiley.com/doi/abs/10.1029/2018WR022958 doi: 10.1029/2018wr022958

Akram, F., Rasul, M. G., Masud, M., Khan, K., Imam, S., & Amir, I. (2014). Comparison of Different Hydrograph Routing Techniques in XPSTORM Modelling Software : A Case Study. *International Journal of Environmental, Ecological, Geological and Mining Engineering*, *8*(3), 213–223.

Alley, W. M., & Veenhuis, J. E. (1983). Effective impervious area in urban runoff modeling. *Journal of Hydraulic Engineering*, *109*(2), 313–319.

Arnold, C. L., & Gibbons, C. J. (1996a). Impervious surface coverage: The emergence of a key environmental indicator. *Journal of the American Planning Association*, *62*(2), 243–258. Retrieved 2019-01-21, from http://www.tandfonline.com/doi/abs/10.1080/01944369608975688 doi: 10.1080/01944369608975688

Arnold, C. L., & Gibbons, C. J. (1996b, June). Impervious surface coverage: The emergence of a key environmental indicator. *Journal of the American Planning Association*, *62*(2), 243–258. Retrieved from http://www.tandfonline.com/doi/abs/10.1080/01944369608975688 doi: 10.1080/01944369608975688

Assouline, S. (2004). Rainfall-induced soil surface sealing: A critical review of observations, conceptual models, and solutions. *Vadose Zone Journal*, *3*(2), 570–591. doi: 10.2136/vzj2004.0570

Avellaneda, P. M., Jefferson, A. J., Grieser, J. M., & Bush, S. A. (2017, April). Simulation of the cumulative hydrological response to green infrastructure. *Water Resources Research*, *53*(4), 3087–3101. doi: 10.1002/2016wr019836

Bai, Y., Zhao, N., Zhang, R., & Zeng, X. (2018). Storm water management of low impact development in urban areas based on SWMM. *Water (Switzerland)*, *11*(1). doi: 10.3390/w11010033

Baiamonte, G. (2020). A rational runoff coefficient for a revisited rational formula. *Hydrological Sciences Journal*, *65*(1), 112–126. Retrieved from https://doi.org/10.1080/02626667.2019.1682150 doi: 10.1080/02626667.2019.1682150

Barron, O. V., Barr, A. D., & Donn, M. J. (2013). Effect of urbanisation on the water balance of a catchment with shallow groundwater. *Journal of Hydrology*, *485*, 162–176. Retrieved from http://dx.doi.org/10.1016/j.jhydrol.2012.04.027 doi: 10.1016/j.jhydrol.2012.04.027

Bartlett, M. S., Parolari, A. J., McDonnell, J. J., & Porporato, A. (2016). Beyond the scs-cn method: A theoretical framework for spatially lumped rainfall-runoff response. *Water Resources Research*, *52*(6), 4608–4627. doi: 10.1002/2015wr018439

Bartos, M., Park, H., Zhou, T., Kerkez, B., & Vasudevan, R. (2019). Windshield wipers on connected vehicles produce high-accuracy rainfall maps. *Scientific Reports*, *9*(1), 1–9. Retrieved from http://dx.doi.org/10.1038/s41598-018-36282-7 doi: 10.1038/s41598-018-36282-7

Beck, M. B. (1987). Water quality modeling: A review of the analysis of uncertainty. *Water Resources Research*, *23*(8), 1393–1442. doi: 10.1029/WR023i008p01393

Bell, C. D., McMillan, S. K., Clinton, S. M., & Jefferson, A. J. (2016, October). Hydrologic response to stormwater control measures in urban watersheds. *Journal of Hydrology*, *541*, 1488–1500. Retrieved from https://linkinghub.elsevier.com/retrieve/pii/S002216941630539X doi: 10.1016/j.jhydrol.2016.08.049

Bell, C. D., Tague, C. L., & McMillan, S. K. (2017). A model of hydrology and water quality for stormwater control measures. *Environmental Modelling and Software*, *95*, 29–47. Retrieved from http://dx.doi.org/10.1016/j.envsoft.2017.05.007 doi: 10.1016/j.envsoft.2017.05.007

Berghuijs, W. R., Woods, R. A., Hutton, C. J., & Sivapalan, M. (2016). Dominant flood generating mechanisms across the united states. *Geophysical Research Letters*, *43*(9), 4382–4390. doi: 10.1002/2016gl068070

Betson, R. P. (1964, April). What is watershed runoff? *Journal of Geophysical Research*, *69*(8), 1541–1552. Retrieved from http://doi.wiley.com/10.1029/JZ069i008p01541 doi: 10.1029/JZ069i008p01541

Beven, K. (2004, December). Robert e. horton's perceptual model of infiltration processes. *Hydrological Processes*, *18*(17), 3447–3460. Retrieved from http://doi.wiley.com/10.1002/hyp.5740 doi: 10.1002/hyp.5740

Beven, K. (2006a). *Introduction.* (1st ed.; K. Beven, Ed.). International Association of Hydrological Sciences.

Beven, K. (2006b). A manifesto for the equifinality thesis. *Journal of Hydrology*, *320*(1-2), 18–36. doi: 10.1016/j.jhydrol.2005.07.007

Beven, K., & Binley, A. (1992, July). The future of distributed models: Model calibration and uncertainty prediction. *Hydrological Processes*, *6*(3), 279–298. Retrieved 2019-01-22, from http://doi.wiley.com/10.1002/hyp.3360060305 doi: 10.1002/hyp.3360060305

Beven, K., & Binley, A. (2014). GLUE: 20 years on. *Hydrological Processes*, *28*(24), 5897–5918. doi: 10.1002/hyp.10082

Beven, K. J. (1989). Changing Ideas in Hydrology: The Case of Physically Based Models. *Journal of Hydrology*, 157 – 172. doi: 10.1016/0022-1694(89)90101-7

Beven, K. J., & Kirkby, M. J. (1979). A physically based, variable contributing area model of basin hydrology / un modèle à base physique de zone d'appel variable de l'hydrologie du bassin versant. *Hydrological Sciences Bulletin*, *24*(1), 43–69. Retrieved 2019-02-10, from http://www.tandfonline.com/doi/abs/10.1080/02626667909491834 doi: 10.1080/02626667909491834

Beven, K. J., Wood, E. F., & Sivapalan, M. (1988, July). On hydrological heterogeneity - catchment morphology and catchment response. *Journal of Hydrology*, *100*(1-3), 353–375. doi: 10.1016/0022-1694(88)90192-8

Bhaskar, A. S., Beesley, L., Burns, M. J., Fletcher, T. D., Hamel, P., Oldham, C. E., & Roy, A. H. (2016). Will it rise or will it fall? managing the complex effects of urbanization on base flow. *Freshwater Science*, *35*(1), 293–310. doi: 10.1086/685084

Bhaskar, A. S., Hogan, D. M., & Archfield, S. A. (2016, August). Urban base flow with low impact development. *Hydrological Processes*, *30*(18), 3156–3171. doi: 10.1002/hyp.10808

Bhaskar, A. S., & Welty, C. (2015). Analysis of subsurface storage and streamflow generation in urban watersheds. *Water Resources Research*, *51*(3), 1493–1513. Retrieved 2019-03-29, from http://doi.wiley.com/10.1002/2014WR015607 doi: 10.1002/2014wr015607

Bhaskar, A. S., Welty, C., Maxwell, R. M., & Miller, A. J. (2015). Untangling the effects of urban development on subsurface storage in baltimore. *Water Resources Research*, *51*(2), 1158–1181. Retrieved 2017-11-15, from http://doi.wiley.com/10.1002/2014WR016039 doi: 10.1002/2014wr016039

Blecken, G.-T., Zingerb, Y., Deletic, A., Fletcherb, T. D., & Viklander, M. (2008). Influence of intermittent wetting and drying conditions on heavy metal removal by stormwater biofilters. *Water Research*, *43*, 4590–4598.

Blöschl, G. (2005, October). Rainfall-Runoff Modeling of Ungauged Catchments. In *Encyclopedia of hydrological sciences* (p. hsa140). Chichester, UK: John Wiley & Sons, Ltd. Retrieved from http://doi.wiley.com/10.1002/0470848944.hsa140 doi: 10.1002/0470848944.hsa140

Blöschl, G., & Sivapalan, M. (1995). Scale issues in hydrological modelling: A review. *Hydrological Processes*, *9*(3-4), 251–290. doi: 10.1002/hyp.3360090305

Blöschl, G., & Sivapalan, M. (1995). Scale issues in hydrological modelling: A review. *Hydrological Processes*, *9*(3), 251–290. Retrieved 2019-03-03, from http://doi.wiley.com/10.1002/hyp.3360090305 doi: 10.1002/hyp.3360090305

Booth, D. B., & Jackson, C. R. (1997). Urbanization of aquatic systems: degradation thresholds, stormwater detection, and the limits of mitigation. *JAWRA Journal of the American Water Resources Association*, *33*(5), 1077–1090.

Borgström, S. T., Elmqvist, T., Angelstam, P., & Alfsen-Norodom, C. (2006). Scale mismatches in management of urban landscapes. *Ecology and Society*, *11*(2). doi: 10.5751/es-01819-110216

Boutaghane, H., & Ouerdachi, L. (2012). Integration of pervious area stream flow in urban hydrological model. *Energy Procedia*, *18*, 1573–1582. doi: 10.1016/j.egypro.2012.05.173

Bouwer, H. (1969-12). Infiltration of water into nonuniform soil. *Journal of Irrigation and Drainage Engineering*. Retrieved 2020-05-15, from https://trid.trb.org/view/127380

Bouwer, H. (1976). Infiltration into increasingly permeable soils. *Journal of the Irrigation and Drainage Division*, *102*(1), 127–136. Retrieved 2020-05-15, from https://cedb.asce.org/CEDBsearch/record.jsp?dockey=0006526 (Publisher: ASCE)

Boyd, M. J., Bufill, M. C., & Knee, R. M. (1993, December). Pervious and impervious runoff in urban catchments. *Hydrological Sciences Journal*, *38*(6), 463–478. Retrieved from http://www.tandfonline.com/doi/abs/10.1080/02626669309492699 doi: 10.1080/02626669309492699

Bracken, L., & Croke, J. (2007). The concept of hydrological connectivity and its contribution to understanding runoff-dominated geomorphic systems. *Hydrological Processes*, *21*(13), 1749–1763. Retrieved from https://onlinelibrary.wiley.com/doi/abs/10.1002/hyp.6313 doi: 10.1002/hyp.6313

Bracken, L., Wainwright, J., Ali, G., Tetzlaff, D., Smith, M., Reaney, S., & Roy, A. (2013). Concepts of hydrological connectivity: Research approaches, pathways and future agendas. *Earth-Science Reviews*, *119*, 17–34. Retrieved 2019-02-12, from https://linkinghub.elsevier.com/retrieve/pii/S0012825213000202 doi: 10.1016/j.earscirev.2013.02.001

Bradford, S. F., & Sanders, B. F. (2002, March). Finite-Volume Model for Shallow-Water Flooding of Arbitrary Topography. *Journal of Hydraulic Engineering*, *128*(3), 289–298. doi: 10.1061/(asce)0733-9429(2002)128:3(289)

Breiman, L., Friedman, J. H., Olshen, R. A., & Stone, C. J. (1984). *Classification {And} {Regression} {Trees}*. Monterey: Brooks/Cole Publishing.

Brink, P., & TenBroek, M. (1995). Characteristic width and infiltration for continuous SWMM. *Journal of Water Management Modeling*. doi: 10.14796/JWMM.Rl83-17

Brown, R. A., & Hunt, W. F. (2011). Impacts of Media Depth on Effluent Water Quality and Hydrologic Performance of Undersized Bioretention Cells. *Journal of Irrigation and Drainage Engineering*, *137*(3), 132–143. doi: 10.1061/(asce)ir.1943-4774.0000167

Brown, R. A., O'Connor, T. P., & Borst, M. (2015). Divergent vegetation growth patterns relative to bioinfiltration unit size and plant placement. *Journal of Sustainable Water in the Built Environment*, *1*(3), 04015001.

Brutsaert, W. (2005). *Hydrology: an introduction*. Cambridge: Cambridge University Press. Retrieved from http://uclibs.org/PID/153381

Buchanan, B., Auerbach, D. A., Knighton, J., Evensen, D., Fuka, D. R., Easton, Z., ... Walter, T. (2018). Estimating dominant runoff modes across the conterminous united states. *Hydrological Processes*, *32*(26), 3881–3890. Retrieved 2020-04-20, from https://onlinelibrary.wiley.com/doi/abs/10.1002/hyp.13296 doi: 10.1002/hyp.13296

Buchanan, B., Easton, Z. M., Schneider, R., & Walter, M. T. (2012). Incorporating variable source area hydrology into a spatially distributed direct runoff model1: Incorporating variable source area hydrology into a spatially distributed direct runoff model. *JAWRA Journal of the American Water Resources Association*, *48*(1), 43–60. Retrieved 2019-02-08, from http://doi.wiley.com/10.1111/j.1752-1688.2011.00594.x doi: 10.1111/j.1752-1688.2011.00594.x

Budyko, M. I. (1977). On present-day climatic changes. *Tellus*, *29*(3), 193–204. Retrieved 2020-04-21, from http://tellusa.net/index.php/tellusa/article/view/11347 doi: 10.1111/j.2153-3490.1977.tb00725.x

Bullard, R. D. (1994). The Legacy of American Apartheid and Environmental Racism. *Journal of Civil Rights and Economic Development*, *9*(2), 1–30. doi: 10.3868/s050-004-015-0003-8

Burian, S. J., Nix, S. J., Durrans, S. R., Pitt, R. E., Fan, C.-Y., & Field, R. (1999). Historical development of wet-weather flow management. *Journal of Water Resources Planning and Management*, *125*(1), 3–13. Retrieved 2018-12-27, from http://ascelibrary.org/doi/10.1061/%28ASCE%290733-9496%281999%29125%3A1%283%29 doi: 10.1061/(asce)0733-9496(1999)125:1(3)

Burns, M. J., Fletcher, T. D., Hatt, B., Ladson, A. R., & Walsh, C. J. (2010). Can allotment-scale rainwater harvesting manage urban flood risk and protect stream health? *Novatech 2010*.

Burns, M. J., Fletcher, T. D., Walsh, C. J., Ladson, A. R., & Hatt, B. E. (2012, April). Hydrologic shortcomings of conventional urban stormwater management and opportunities for reform. *Landscape and Urban Planning*, *105*(3), 230–240. Retrieved from http://dx.doi.org/10.1016/j.landurbplan.2011.12.012http://linkinghub.elsevier.com/retrieve/pii/S016920461100363Xhttp://www.sciencedirect.com/science/article/pii/S016920461100363X doi: 10.1016/j.landurbplan.2011.12.012

Burns, M. J., Schubert, J. E., Fletcher, T. D., & Sanders, B. F. (2015). Testing the impact of at-source stormwater management on urban flooding through a coupling of network and overland flow models. *Wiley Interdisciplinary Reviews: Water*, *2*(4), 291–300. doi: 10.1002/wat2.1078

Buttle, J. M., Vonk, A. M., & Taylor, C. H. (1995, February). Applicability of isotopic hydrograph separation in a suburban basin during snowmelt. *Hydrological Processes*, *9*(2), 197–211. Retrieved from http://doi.wiley.com/10.1002/hyp.3360090206 doi: 10.1002/hyp.3360090206

Carpenter, T. M., & Georgakakos, K. P. (2006a). Intercomparison of lumped versus distributed hydrologic model ensemble simulations on operational forecast scales. *Journal of Hydrology*, *329*(1), 174–185. Retrieved 2019-01-21, from https://linkinghub.elsevier.com/retrieve/pii/S0022169406000898 doi: 10.1016/j.jhydrol.2006.02.013

Carpenter, T. M., & Georgakakos, K. P. (2006b, September). Intercomparison of lumped versus distributed hydrologic model ensemble simulations on operational forecast scales. *Journal of Hydrology*, *329*(1-2), 174–185. Retrieved from https://linkinghub.elsevier.com/retrieve/pii/S0022169406000898 doi: 10.1016/j.jhydrol.2006.02.013

Case, J. L., Wood, L. T., Blaes, J. L., White, K. D., Hain, C. R., & Schultz, C. J. (2021, jan). Soil Moisture Responses Associated with Significant Tropical Cyclone Rainfall Events. *Journal of Operational Meteorology*, 1–17. Retrieved from https://objects-us-east-1.dream.io/nwafiles/jom/articles/2021/2021-JOM1/2021-JOM1.pdf doi: 10.15191/nwajom.2021.0901

Catalog, D. O. D. (2020). *Denver open data catalog.* Retrieved 2020-05-18, from http://data.denvergov.org

Chaubey, I., Haan, C. T., Grunwald, S., & Salisbury, J. M. (1999, June). Uncertainty in the model parameters due to spatial variability of rainfall. *Journal of Hydrology*, *220*(1-2), 48–61. doi: 10.1016/s0022-1694(99)00063-3

Checker, M. (2011, December). Wiped out by the "Greenwave": Environmental gentrification and the paradoxical politics of urban sustainability. *City and Society*, *23*(2), 210–229. Retrieved from http://doi.wiley.com/10.1111/j.1548-744X.2011.01063.x doi: 10.1111/j.1548-744X.2011.01063.x

Cherry, L., Mollendor, D., Eisenstein, B., Hogue, T., Peterman, K., & McCray, J. (2019). Predicting parcel-scale redevelopment using linear and logistic regression—the berkeley neighborhood denver, colorado case study. *Sustainability*, *11*(7), 1882. Retrieved 2020-05-15, from https://www.mdpi.com/2071-1050/11/7/1882 doi: 10.3390/su11071882

Childs, E. C., & Bybordi, M. (1969). The vertical movement water in stratified porous material: 1. infiltration. *Water Resources Research*, *5*(2), 446–459. Retrieved 2020-05-15, from http://agupubs.onlinelibrary.wiley.com/doi/abs/10.1029/WR005i002p00446 doi: 10.1029/WR005i002p00446

Christian, L. N., Banner, J. L., & Mack, L. E. (2011). Sr isotopes as tracers of anthropogenic influences on stream water in the austin, texas, area. *Chemical Geology*, *282*(3-4), 84–97. Retrieved from https://linkinghub.elsevier.com/retrieve/pii/S000925411100026X doi: 10.1016/j.chemgeo.2011.01.011

Chu, S. T. (1978). Infiltration during an unsteady rain. *Water Resources Research*, *14*(3), 461–466. Retrieved 2020-05-15, from https://agupubs.onlinelibrary.wiley.com/doi/abs/10.1029/WR014i003p00461 doi: 10.1029/WR014i003p00461

Clark, S. E., & Pitt, R. (2007). Influencing Factors and a Proposed Evaluation Methodology for Predicting Groundwater Contamination Potential from Stormwater Infiltration Activities. *Water Environment Research*, *79*(1), 29–36. doi: 10.2175/106143006x143173

Clarke, R. T. (2007). Hydrological prediction in a non-stationary world. *Hydrology and Earth System Sciences*, *11*(1), 408–414. doi: 10.5194/hess-11-408-2007

Claydon, G., Thompson, S. E., Shanafield, M., & Manero, A. (2020). *Guiding urban water management in areas that experience seasonal groundwater: Expert panel report* (Tech. Rep.). Cooperative Research Centre for Water Sensitive Cities. Retrieved from www.watersensitivecities.org.au

Cobby, D., Morris, S., Parkes, A., & Robinson, V. (2009). Groundwater flood risk management: Advances towards meeting the requirements of the eu floods directive. *Journal of Flood Risk Management*, *2*(2), 111–119. doi: 10.1111/j.1753-318X.2009.01025.x

Cristiano, E., Veldhuis, M. C. T., & Van De Giesen, N. (2017). Spatial and temporal variability of rainfall and their effects on hydrological response in urban areas - a review. *Hydrology and Earth System Sciences*, *21*(7), 3859–3878. Retrieved from https://www.hydrol-earth-syst-sci.net/21/3859/2017/ doi: 10.5194/hess-21-3859-2017

Crompton, O., Sytsma, A., & Thompson, S. (2019). Emulation of the saint venant equations enables rapid and accurate predictions of infiltration and overland flow velocity on spatially heterogeneous surfaces. *Water Resources Research*. Retrieved 2019-09-30, from https://onlinelibrary.wiley.com/doi/abs/10.1029/2019WR025146 doi: 10.1029/2019wr025146

Cumming, G. S., Cumming, D. H., & Redman, C. L. (2006). Scale mismatches in social-ecological systems: Causes, consequences, and solutions. *Ecology and Society*, *11*(1). doi: 10.5751/es-01569-110114

D. Bullard, R., Bullard, R. D., & Wright, B. (2019, June). Race, Place, and the Environment in Post-Katrina New Orleans. In *Race, place, and environmental justice after hurricane katrina* (pp. 17–48). Routledge. doi: 10.4324/9780429497858-1

Damodaram, C., Giacomoni, M. H., Prakash Khedun, C., Holmes, H., Ryan, A., Saour, W., & Zechman, E. M. (2010, July). Simulation of combined best management practices and low impact development for sustainable stormwater management. *Journal of the American Water Resources Association*, *46*(5), 907–918. Retrieved from http://doi.wiley.com/10.1111/j.1752-1688.2010.00462.x doi: 10.1111/j.1752-1688.2010.00462.x

Davis, A. P. (2008). Field Performance of Bioretention: Hydrology Impacts. *Journal of Hydrologic Engineering*, *13*(2), 90–95. doi: 10.1061/(asce)1084-0699(2008)13:2(90)

Day, D. G. (1983). Drainage density variability and drainage basin outputs. *Journal of Hydrology (New Zealand)*, *22*(1), 3–17. Retrieved from http://www.jstor.org/stable/43944508

Devito, K., Creed, I., Gan, T., Mendoza, C., Petrone, R., Silins, U., & Smerdon, B. (2005). A framework for broad-scale classification of hydrologic response units on the boreal plain: Is topography the last thing to consider? *Hydrological Processes*, *19*(8), 1705–1714. doi: 10.1002/hyp.5881

DHI. (2010). *Mike 21 flow model, hydrodynamic module: Scientific documentation.* DHI Hørsholm, Denmark.

Dhi. (2017). *Mouse runoff reference manual* (Tech. Rep.). Horsolm, Denmark: DHI Software.

Di Vittorio, D., & Ahiablame, L. (2015). Spatial Translation and Scaling Up of Low Impact Development Designs in an Urban Watershed. *Journal of Water Management Modeling*. Retrieved from https://www.chijournal.org/C388 doi: 10.14796/jwmm.c388

Dietz, M. E., & Clausen, J. C. (2008, June). Stormwater runoff and export changes with development in a traditional and low impact subdivision. *Journal of Environmental Management*, *87*(4), 560–566. Retrieved from http://linkinghub.elsevier.com/retrieve/pii/S030147970700103X doi: 10.1016/j.jenvman.2007.03.026

Dietze, M. C., Fox, A., Beck-Johnson, L. M., Betancourt, J. L., Hooten, M. B., Jarnevich, C. S., ... White, E. P. (2018). Iterative near-term ecological forecasting: Needs, opportunities, and challenges. *Proceedings of the National Academy of Sciences of the United States of America*, *115*(7), 1424–1432. doi: 10.1073/pnas.1710231115

Dunne, T. (1990). Hydrology mechanics, and geomorphic implications of erosion by subsurface flow. *Special Paper of the Geological Society of America*, *252*(October), 1–28. doi: 10.1130/SPE252-p1

Dunne, T., & Black, R. D. (1970, October). Partial area contributions to storm runoff in a small new england watershed. *Water Resources Research*, *6*(5), 1296–1311. Retrieved from http://dx.doi.org/10.1029/WR006i005p01296 doi: 10.1029/WR006i005p01296

Dunne, T., & Leopold, L. (1978). *Water in environmental planning*. W.H. Freeman and Company.

Dupas, R., Abbott, B. W., Minaudo, C., & Fovet, O. (2019). Distribution of landscape units within catchments influences nutrient export dynamics. *Frontiers in Environmental Science*, *7*(APR), 1–8. doi: 10.3389/fenvs.2019.00043

Easton, Z. M., Gérard-Marchant, P., Walter, M. T., Petrovic, A. M., & Steenhuis, T. S. (2007). Hydrologic assessment of an urban variable source watershed in the northeast united states: HYDROLOGIC ASSESSMENT OF a VSA WATERSHED. *Water Resources Research*, *43*(3). Retrieved 2017-11-15, from http://doi.wiley.com/10.1029/2006WR005076 doi: 10.1029/2006wr005076

Ebrahimian, A., Gulliver, J. S., & Wilson, B. N. (2016, September). Effective impervious area for runoff in urban watersheds. *Hydrological Processes*, *30*(20), 3717–3729. Retrieved from http://doi.wiley.com/10.1002/hyp.10839 doi: 10.1002/hyp.10839

Ebrahimian, A., Wilson, B. N., & Gulliver, J. S. (2016). Improved methods to estimate the effective impervious area in urban catchments using rainfall-runoff data. *Journal of Hydrology*, *536*, 109–118. Retrieved 2019-09-18, from https://linkinghub.elsevier.com/retrieve/pii/S0022169416300567 doi: 10.1016/j.jhydrol.2016.02.023

Ehret, U., Gupta, H. V., Sivapalan, M., Weijs, S. V., Schymanski, S. J., Blöschl, G., ... Winsemius, H. C. (2014). Advancing catchment hydrology to deal with predictions under change. *Hydrology and Earth System Sciences*, *18*(2), 649–671. doi: 10.5194/hess-18-649-2014

Elliott, A. H., & Trowsdale, S. A. (2007, March). A review of models for low impact urban stormwater drainage. *Environmental Modelling and Software*, *22*(3), 394–405. Retrieved from https://linkinghub.elsevier.com/retrieve/pii/S1364815206000053 doi: 10.1016/j.envsoft.2005.12.005

Emerson, C. H., Welty, C., & Traver, R. G. (2005). Watershed-scale evaluation of a system of storm water detention basins. *Journal of Hydrologic Engineering*, *10*(3), 237–242.

Endreny, T., & Collins, V. (2009). Implications of bioretention basin spatial arrangements on stormwater recharge and groundwater mounding. *Ecological Engineering*, *35*(5), 670–677. doi: 10.1016/j.ecoleng.2008.10.017

Epps, S., Ph D., & Hathaway, J. M. (2018, May). Establishing a Framework for the Spatial Identification of Effective Impervious Areas in Gauged Basins: Review and Case Study. *Journal of Sustainable Water in the Built Environment*, *4*(2), 05018001. Retrieved from http://ascelibrary.org/doi/10.1061/JSWBAY.0000853 doi: 10.1061/jswbay.0000853

Epps, T. H., & Hathaway, J. M. (2019). Using spatially-identified effective impervious area to target green infrastructure retrofits: A modeling study in knoxville, TN. *Journal of Hydrology*, *575*, 442–453. Retrieved 2019-10-06, from http://www.sciencedirect.com/science/article/pii/S0022169419305074 doi: 10.1016/j.jhydrol.2019.05.062

ESRI. (2020). *World Cities.* Retrieved from https://hub.arcgis.com/datasets/6996f03a1b364dbab4008d99380370ed_0

Evans, C., Schumacher, R. S., & Galarneau, T. J. (2011). Sensitivity in the overland reintensification of Tropical Cyclone Erin (2007) to near-surface soil moisture characteristics. *Monthly Weather Review*, *139*(12), 3848–3870. doi: 10.1175/2011MWR3593.1

Fleckenstein, J. H., Krause, S., Hannah, D. M., & Boano, F. (2010). Groundwater-surface water interactions: New methods and models to improve understanding of processes and dynamics. *Advances in Water Resources*, *33*(11), 1291–1295.

Fletcher, T. D., Andrieu, H., & Hamel, P. (2013). Understanding, management and modelling of urban hydrology and its consequences for receiving waters: A state of the art. *Advances in Water Resources*, *51*, 261 – 279. Retrieved from http://www.sciencedirect.com/science/article/pii/S0309170812002412 doi: https://doi.org/10.1016/j.advwatres.2012.09.001

Folke, C., Pritchard, L., Berkes, F., Colding, J., & Svedin, U. (2007). The problem of fit between ecosystems and institutions: Ten years later. *Ecology and Society*, *12*(1). doi: 10.5751/es-02064-120130

Foufoula-Georgiou, E., Takbiri, Z., Czuba, J. A., & Schwenk, J. (1969a). The change of nature and the nature of change in agricultural landscapes: Hydrologic regime shifts modulate ecological transitions. *Water Resources Research*, *5*(3), 2–2. doi: 10.1111/j.1752-1688.1969.tb04897.x

Foufoula-Georgiou, E., Takbiri, Z., Czuba, J. A., & Schwenk, J. (1969b). Water Resources Research. *Journal of the American Water Resources Association*, *5*(3), 2–2. doi: 10.1111/j.1752-1688.1969.tb04897.x

Fovet, O., Ruiz, L., Faucheux, M., Molénat, J., Sekhar, M., Vertès, F., ... Durand, P. (2015). Using long time series of agricultural-derived nitrates for estimating catchment transit times. *Journal of Hydrology*, *522*, 603–617. Retrieved from http://dx.doi.org/10.1016/j.jhydrol.2015.01.030 doi: 10.1016/j.jhydrol.2015.01.030

Fries, K. J., & Kerkez, B. (2018). Using Sensor Data to Dynamically Map Large-Scale Models to Site-Scale Forecasts: A Case Study Using the National Water Model. *Water Resources Research*, *54*(8), 5636–5653. doi: 10.1029/2017WR022498

Froehlich, D. C. (2016). Return period-dependent rational formula coefficients for two locations in texas. *Journal of Irrigation and Drainage Engineering*, *142*(9), 4016035. Retrieved from http://ascelibrary.org/doi/10.1061/{%}28ASCE{%}29IR.1943-4774.0001054 doi: 10.1061/(asce)ir.1943-4774.0001054

Fry, T. J., & Maxwell, R. M. (2017). Evaluation of distributed BMPs in an urban watershed-high resolution modeling for stormwater management. *Hydrological Processes*, *31*(15), 2700–2712. Retrieved 2017-11-15, from http://doi.wiley.com/10.1002/hyp.11177 doi: 10.1002/hyp.11177

Fry, T. J., & Maxwell, R. M. (2018). Using a distributed hydrologic model to improve the green infrastructure parameterization used in a lumped model. *Water (Switzerland)*, *10*(12). Retrieved from www.mdpi.com/journal/water doi: 10.3390/w10121756

Fürst, J., Bichler, A., & Konecny, F. (2015). Regional frequency analysis of extreme groundwater levels. *Groundwater*, *53*(3), 414–423. doi: 10.1111/gwat.12223

Gagrani, V., Diemer, J. A., Karl, J. J., & Allan, C. J. (2014). Assessing the Hydrologic and Water Quality Benefits of a Network of Stormwater Control Measures in a SE U.S. Piedmont Watershed. *Journal of the American Water Resources Association*, *50*(1), 128–142. doi: 10.1111/jawr.12121

Gan, T. Y., Dlamini, E. M., & Biftu, G. F. (1997). Effects of model complexity and structure, data quality, and objective functions on hydrologic modeling. *Journal of Hydrology*, *192*(1-4), 81–103. doi: 10.1016/S0022-1694(96)03114-9

Gharari, S., Hrachowitz, M., Fenicia, F., & Savenije, H. H. (2013). An approach to identify time consistent model parameters: Sub-period calibration. *Hydrology and Earth System Sciences*, *17*(1), 149–161. doi: 10.5194/hess-17-149-2013

Gillies, R. R., Brim Box, J., Symanzik, J., & Rodemaker, E. J. (2003, August). Effects of urbanization on the aquatic fauna of the Line Creek watershed, Atlanta - A

satellite perspective. *Remote Sensing of Environment*, *86*(3), 411–422. Retrieved from http://linkinghub.elsevier.com/retrieve/pii/S0034425703000828 doi: 10.1016/s0034-4257(03)00082-8

Gober, P., Kirkwood, C. W., Balling, R. C., Ellis, A. W., & Deitrick, S. (2010, April). Water planning under climatic uncertainty in phoenix: Why we need a new paradigm. *Annals of the Association of American Geographers*, *100*(2), 356–372. Retrieved from https://www.tandfonline.com/doi/abs/10.1080/00045601003595420 doi: 10.1080/00045601003595420

Godsey, S., Elsenbeer, H., & Stallard, R. (2004). Overland flow generation in two lithologically distinct rainforest catchments. *Journal of Hydrology*, *295*(1-4), 276–290. doi: 10.1016/j.jhydrol.2004.03.014

Godsey, S. E., Kirchner, J. W., & Clow, D. W. (2009, June). Concentration-discharge relationships reflect chemostatic characteristics of US catchments. *Hydrological Processes*, *23*(13), 1844–1864. Retrieved from http://jamsb.austms.org.au/courses/CSC2408/semester3/resources/ldp/abs-guide.pdfhttp://doi.wiley.com/10.1002/hyp.7315 doi: 10.1002/hyp.7315

Golden, H. E., & Hoghooghi, N. (2018). Green infrastructure and its catchment-scale effects: an emerging science: Green infrastructure and its catchment-scale effects. *Wiley Interdisciplinary Reviews: Water*, *5*(1), e1254. Retrieved 2018-11-26, from http://doi.wiley.com/10.1002/wat2.1254 doi: 10.1002/wat2.1254

Gorski, G., & Zimmer, M. (2020). Hydrologic regimes drive nutrient export behavior in human impacted watersheds. *Hydrology and Earth System Sciences Discussions*, *500*, 1–24. doi: 10.5194/hess-2020-562

Graham, C. B., Woods, R. A., & McDonnell, J. J. (2010). Hillslope threshold response to rainfall: (1) a field based forensic approach. *Journal of Hydrology*, *393*(1-2), 65–76. Retrieved from http://dx.doi.org/10.1016/j.jhydrol.2009.12.015 doi: 10.1016/j.jhydrol.2009.12.015

Grayson, R., & Blöschl, G. (2001). *Spatial Patterns in Catchment Hydrology: Observations and Modelling*. United Kingdom: Cambridge University Press.

Green, C., Wilson, T., Masterson, T., & Boothby, N. (2006, 01). *An assessment of the additional flood losses associated with groundwater flooding: a report to hampshire county council and winchester city council* (Tech. Rep.).

Green, H. W., & Ampt, G. A. (1911, May). Studies on soil phyics. *The Journal of Agricultural Science*, *4*(1), 1–24. Retrieved from https://www.cambridge.org/core/product/identifier/S0021859600001441/type/journal{%5F}article doi: 10.1017/s0021859600001441

Gribovszki, Z., Szilágyi, J., & Kalicz, P. (2010). Diurnal fluctuations in shallow groundwater levels and streamflow rates and their interpretation - a review. *Journal of Hydrology*, *385*(1-4), 371–383. Retrieved from http://dx.doi.org/10.1016/j.jhydrol.2010.02.001 doi: 10.1016/j.jhydrol.2010.02.001

Groffman, P. M., Law, N. L., Belt, K. T., Band, L. E., & Fisher, G. T. (2004, June). Nitrogen fluxes and retention in urban watershed ecosystems. *Ecosystems*, *7*(4), 393–403. Retrieved from https://doi.org/10.1007/s10021-003-0039-x doi: 10.1007/s10021-003-0039-x

Guo, J. C. (2008). Volume-Based Imperviousness for Storm Water Designs. *Journal of Irrigation and Drainage Engineering*, *134*(2), 193–196. doi: 10.1061/(asce)0733-9437(2008)134:2(193)

Guo, J. C., & Urbonas, B. (2009, 8). Conversion of natural watershed to kinematic wave cascading plane. *Journal of Hydrologic Engineering*, *14*, 839–846. doi: 10.1061/(asce)he.1943-5584.0000045

Gupta, H., Sorooshian, V. ., Hogue, T. S. ., & Boyle, D. P. (1996). Advances in Automatic Calibration of Watershed Models. In Q. Duan, H. Gupta, S. Sorooshian, A. Rousseau, & R. Turcotte (Eds.), *Water science and application* (6th ed., pp. 9–28). American Geophysical Union.

Hahm, W. J., Rempe, D. M., Dralle, D. N., Dawson, T. E., Lovill, S. M., Bryk, A. B., ... Dietrich, W. E. (2019). Lithologically controlled subsurface critical zone thickness and water storage capacity determine regional plant community composition. *Water Resources Research*, *55*(4), 3028–3055. doi: 10.1029/2018wr023760

Hamel, P., Daly, E., & Fletcher, T. D. (2013). Source-control stormwater management for mitigating the impacts of urbanisation on baseflow: A review. *Journal of Hydrology*, *485*, 201–211. Retrieved 2019-02-18, from https://linkinghub.elsevier.com/retrieve/pii/S0022169413000292 doi: 10.1016/j.jhydrol.2013.01.001

Han, W. S., & Burian, S. J. (2009a). Determining effective impervious area for urban hydrologic modeling. *Journal of Hydrologic Engineering*, *14*(2), 111–120.

Han, W. S., & Burian, S. J. (2009b). Determining effective impervious area for urban hydrologic modeling. *Journal of Hydrologic Engineering*, *14*(2), 111–120. doi: 10.1061/(asce)1084-0699(2009)14:2(111)

Hardie, M. A., Doyle, R. B., Cotching, W. E., & Lisson, S. (2012). Subsurface lateral flow in texture-contrast (duplex) soils and catchments with shallow bedrock. *Applied and Environmental Soil Science*, *2012*, 11–16. doi: 10.1155/2012/861358

Harr, R. D. (1977). Water flux in soil and subsoil on a steep forested slope. *Journal of Hydrology*, *33*(1-2), 37–58. doi: 10.1016/0022-1694(77)90097-x

Hartmann, G., & Bárdossy, A. (2005). Investigation of the transferability of hydrological models and a method to improve model calibration. *Advances in Geosciences*, *5*, 83–87. doi: 10.5194/adgeo-5-83-2005

Herman, J., & Usher, W. (2017, January). SALib: An open-source python library for sensitivity analysis. *The Journal of Open Source Software*, *2*(9). Retrieved from https://doi.org/10.21105/joss.00097 doi: 10.21105/joss.00097

Hewlett, J. D., & Hibbert, Alden, R. (1966). Factors affecting the response of small watersheds to precipitation in humid areas. *Int. Symp. Forest Hydrol. Proc. Nat. Sci. Found Adv. Sci Univ.*, 275–290. doi: 10.1016/s0040-4039(00)86233-4

Hill, P., Mein, R., & Siriwardena, L. (1998). *How much rainfall becomes runoff?: Loss modelling for flood estimation* (Tech. Rep.). Clayton, Victoria, Australia: Monash University.

Hoke, J. E., & Anthes, R. A. (1976, dec). The Initialization of Numerical Models by a Dynamic-Initialization Technique. *Monthly Weather Review*, *104*(12), 1551–1556. Retrieved from http://journals.ametsoc.org/doi/10.1175/1520-0493(1976)104%3C1551:TIONMB%3E2.0.CO;2 doi: 10.1175/1520-0493(1976)104⟨1551:TIONMB⟩2.0.CO;2

Hopkins, K. G., Bhaskar, A. S., Woznicki, S. A., & Fanelli, R. M. (2020). Changes in event-based streamflow magnitude and timing after suburban development with infiltration-based stormwater management. *Hydrological Processes*, *34*(2), 387–403. doi: 10.1002/hyp.13593

Hopp, L., & McDonnell, J. (2009). Connectivity at the hillslope scale: Identifying interactions between storm size, bedrock permeability, slope angle and soil depth. *Journal of Hydrology*, *376*(3), 378–391. Retrieved 2019-07-26, from https://linkinghub.elsevier.com/retrieve/pii/S002216940900448X doi: 10.1016/j.jhydrol.2009.07.047

Hornberger, G. M., Wiberg, P., Raffensperger, J., & D'Odorico, P. (2014). *Elements of physical hydrology, 2nd edition* (2nd ed.). Baltimore, Maryland: Johns Hopkins University Press. doi: 10.1111/gwat.12343

Horton, R. E. (1933). The rôle of infiltration in the hydrologic cycle. *Transactions, American Geophysical Union*, *14*(1), 446. Retrieved 2018-08-26, from http://doi.wiley.com/10.1029/TR014i001p00446 doi: 10.1029/TR014i001p00446

Horton, R. E. (1939). Analysis of runoff-plat experiments with varying infiltration-capacity. *Transactions, American Geophysical Union*, *20*(4), 693. Retrieved 2019-02-25, from http://doi.wiley.com/10.1029/TR020i004p00693 doi: 10.1029/TR020i004p00693

Huber, W. C. (2001). New options for overland flow routing in SWMM. In *Urban drainage modeling* (pp. 22–29). American Society of Civil Engineers. Retrieved

2019-07-22, from http://ascelibrary.org/doi/abs/10.1061/40583%28275%293 doi: 10.1061/40583(275)3

Hughes, A. G., Vounaki, T., Peach, D. W., Ireson, A. M., Jackson, C. R., Butler, A. P., ... Wheater, H. S. (2011). Flood risk from groundwater: Examples from a chalk catchment in southern england. *Journal of Flood Risk Management*, *4*(3), 143–155. doi: 10.1111/j.1753-318X.2011.01095.x

Hunt, W. F., Jarrett, A. R., Smith, J. T., & Sharkey, L. J. (2006). Evaluating bioretention hydrology and nutrient removal at three field sites in North Carolina. *Journal of Irrigation and Drainage Engineering*, *132*(6), 600–608. Retrieved from http://ascelibrary.org/doi/10.1061/%28ASCE%290733-9437%282006%29132%3A6%28600%29 doi: 10.1061/(ASCE)0733-9437(2006)132:6(600)

Hursh, C. R., & Brater, E. F. (1941). Separating storm-hydrographs from small drainage-areas into surface- and subsurface-flow. *Transactions, AGU*, *22*, 863–870.

Hutton, C. J., Kapelan, Z., Vamvakeridou-Lyroudia, L., & Savić, D. (2014). Real-time data assimilation in urban rainfall-runoff models. *Procedia Engineering*, *70*, 843–852. doi: 10.1016/j.proeng.2014.02.092

Hwang, J., Rhee, D. S., & Seo, Y. (2017). Implication of directly connected impervious areas to the mitigation of peak flows in urban catchments. *Water*, *9*(9), 696. Retrieved 2018-01-22, from http://www.mdpi.com/2073-4441/9/9/696 doi: 10.3390/w9090696

IEWEA. (2016). *Specification for separation distances for groundwater-controlled urban development* (Tech. Rep. No. February). Western Australia: Institute of Public Works Engineering Australasia.

Innovyze. (2014). *Infoworks icm help v5.0.*

Iorgulescu, I., & Beven, K. J. (2004). Nonparametric direct mapping of rainfall-runoff relationships: An alternative approach to data analysis and modeling?: MAPPING OF RAINFALL-RUNOFF RELATIONSHIPS. *Water Resources Research*, *40*(8). Retrieved 2019-12-03, from http://doi.wiley.com/10.1029/2004WR003094 doi: 10.1029/2004wr003094

Jackisch, N., & Weiler, M. (2017). The hydrologic outcome of a Low Impact Development (LID) site including superposition with streamflow peaks. *Urban Water Journal*, *14*(2), 143–159. Retrieved from http://dx.doi.org/10.1080/1573062X.2015.1080735 doi: 10.1080/1573062X.2015.1080735

Jakeman, A. J., & Hornberger, G. M. (1993). How much complexity is warranted in a rainfall-runoff model? *Water Resources Research*, *29*(8), 2637–2649. doi: 10.1029/93wr00877

James, W., Rossman, L. A., Robert, W., & James, C. (2010a). *User's guide to swmm5* (Tech. Rep. No. November). CHI Press. Retrieved from https://www.chiwater.com/Files/UsersGuideToSWMM5Edn13.pdf

James, W., Rossman, L. A., Robert, W., & James, C. (2010b). *User's guide to SWMM5* (Tech. Rep. No. November). CHI Press. Retrieved from https://www.chiwater.com/Files/UsersGuideToSWMM5Edn13.pdf

Jang, S., Cho, M., Yoon, J., Yoon, Y., Kim, S., Kim, G., ... Aksoy, H. (2007). Using SWMM as a tool for hydrologic impact assessment. *Desalination*, *212*(1-3), 344–356. doi: 10.1016/j.desal.2007.05.005

Janke, B., Gulliver, J., & Wilson, B. (2011). *Development of techniques to quantify effective impervious cover* (Tech. Rep. No. Cts-11-20). University of Minnesota.

Jarden, K. M., Jefferson, A. J., & Grieser, J. M. (2016a). Assessing the effects of catchment-scale urban green infrastructure retrofits on hydrograph characteristics. *Hydrological Processes*, *30*(10), 1536–1550. doi: 10.1002/hyp.10736

Jarden, K. M., Jefferson, A. J., & Grieser, J. M. (2016b). Assessing the effects of catchment-scale urban green infrastructure retrofits on hydrograph characteristics: Hydrologic effects of catchment-scale green infrastructure retrofits. *Hydrological Processes*, *30*(10), 1536–1550. Retrieved 2019-02-07, from http://doi.wiley.com/10.1002/hyp.10736 doi: 10.1002/hyp.10736

Jefferson, A. J., Bell, C. D., Clinton, S. M., & Mcmillan, S. K. (2015, December). Application of isotope hydrograph separation to understand contributions of stormwater control measures to urban headwater streams. *Hydrological Processes*, *29*(25), 5290–5306. Retrieved 2018-01-11, from http://doi.wiley.com/10.1002/hyp.10680 doi: 10.1002/hyp.10680

Jefferson, A. J., Bhaskar, A. S., Hopkins, K. G., Fanelli, R., Avellaneda, P. M., & McMillan, S. K. (2017, November). Stormwater management network effectiveness and implications for urban watershed function: A critical review. *Hydrological Processes*, *31*(23), 4056–4080. Retrieved from http://onlinelibrary.wiley.com/doi/abs/10.1002/hyp.11347http://doi.wiley.com/10.1002/hyp.11347 doi: 10.1002/hyp.11347

Jencso, K. G., & McGlynn, B. L. (2011). Hierarchical controls on runoff generation: Topographically driven hydrologic connectivity, geology, and vegetation. *Water Resources Research*, *47*(11), 1–16. doi: 10.1029/2011wr010666

Jensen, J. R. (2000). *Remote sensing of the environment an earth resource perspective*. Upper Saddle River, NJ : Pearson Prentice Hall, ©2007.

Johannessen, B. G., Hamouz, V., Gragne, A. S., & Muthanna, T. M. (2019). The transferability of SWMM model parameters between green roofs with similar build-up. *Journal of Hydrology*, *569*(October 2018), 816–828. doi: 10.1016/j.jhydrol.2019.01.004

Karvonen, A. (2011). *Politics of urban runoff - nature, technology, and the sustainable city*. Retrieved from https://ebookcentral.proquest.com/lib/berkeley-ebooks/detail.action?docID=3339323

Kaspersen, P. S., Fensholt, R., & Drews, M. (2015). Using landsat vegetation indices to estimate impervious surface fractions for european cities. *Remote Sensing*, *7*(6), 8224–8249.

Khatami, S., Peel, M. C., Peterson, T. J., & Western, A. W. (2019). Equifinality and flux mapping: A new approach to model evaluation and process representation under uncertainty. *Water Resources Research*, *55*(11), 8922–8941. doi: 10.1029/2018wr023750

Kinal, J., & Stoneman, G. (2012). Disconnection of groundwater from surface water causes a fundamental change in hydrology in a forested catchment in south-western australia. *Journal of Hydrology*, *472*, 14–24.

Klemeš, V. (1983, August). Conceptualization and scale in hydrology. *Journal of Hydrology*, *65*(1-3), 1–23. Retrieved from http://linkinghub.elsevier.com/retrieve/pii/0022169483902081 doi: 10.1016/0022-1694(83)90208-1

KlemeŠ, V. (1986). Operational testing of hydrological simulation models. *Hydrological Sciences Journal*, *31*(1), 13–24. doi: 10.1080/02626668609491024

Klemeš, V. (1986). Dilettantism in hydrology: Transition or destiny? *Water Resources Research*, *22*(9s), 177s-188s. Retrieved from https://agupubs.onlinelibrary.wiley.com/doi/abs/10.1029/WR022i09Sp0177S doi: 10.1029/WR022i09Sp0177S

Knight, J., & Voth, M. (2010). Mapping impervious cover using multi-temporal modis ndvi data. *Ieee journal of selected topics in applied earth observations and remote sensing*, *4*(2), 303–309.

Koutsoyiannis, D. (2006). Nonstationarity versus scaling in hydrology. *Journal of Hydrology*, *324*(1-4), 239–254. doi: 10.1016/j.jhydrol.2005.09.022

Kuczera, G., Lambert, M., Heneker, T., Jennings, S., Frost, A., & Coombes, P. (2006). Joint probability and design storms at the crossroads. *Australasian Journal of Water Resources*, *10*(1), 63–79. doi: 10.1080/13241583.2006.11465282

Kuichling, E. (1889). The relation between the rainfall and the discharge of sewers in populous districts. *Transactions of the American Society of Civil Engineers*, *20*(1), 1–56. Retrieved from http://cedb.asce.org/CEDBsearch/record.jsp?dockey=0254503

Lapides, D., Sytsma, A., & Thompson, S. (2021). Implications of distinct methodological interpretations and runoff coefficient usage for rational method predictions. *In review at Journal of American Water Resources Association*.

Lawrence, R. L., & Wright, A. (2001). Rule-based classification systems using classification and regression tree (CART) analysis. *Photogrammetric Engineering*, 6.

Lee, J. G., & Heaney, J. P. (2003a). Estimation of urban imperviousness and its impacts on storm water systems. *Journal of Water Resources Planning and Management*, *129*(5), 419–426. Retrieved from https://ascelibrary.org/doi/abs/10.1061/%28ASCE%290733-9496%282003%29129%3A5%28419%29 doi: 10.1061/(asce)0733-9496(2003)129:5(419)

Lee, J. G., & Heaney, J. P. (2003b). Estimation of urban imperviousness and its impacts on storm water systems. *Journal of Water Resources Planning and Management*, *129*(5), 419–426. Retrieved from https://ascelibrary.org/doi/abs/10.1061/{%}28ASCE{%}290733-9496{%}282003{%}29129{%}3A5{%}28419{%}29http://ascelibrary.org/doi/abs/10.1061/(ASCE)0733-9496(2003)129:5(419) doi: 10.1061/(asce)0733-9496(2003)129:5(419)

Leopold, L. B. (1968, December). *Hydrology for urban land planning - a guidebook on the hydrologic effects of urban land use* (Vol. 554; Circular). Washington: US Department of the Interior. Retrieved from http://enviro.lclark.edu/resources/Tryon/Water/Hydrology.pdf

Lerner, D. N. (1990). Groundwater recharge in urban areas. *Atmospheric Environment. Part B. Urban Atmosphere*, *24*(1), 29–33.

Lexartza-Artza, I., & Wainwright, J. (2009). Hydrological connectivity: Linking concepts with practical implications. *Catena*, *79*(2), 146–152. Retrieved 2019-03-27, from https://linkinghub.elsevier.com/retrieve/pii/S0341816209001453 doi: 10.1016/j.catena.2009.07.001

Li, C., Wang, W., Xiong, J., & Chen, P. (2014). Sensitivity analysis for urban drainage modeling using mutual information. *Entropy*, *16*(11), 5738–5752. Retrieved 2019-07-09, from http://www.mdpi.com/1099-4300/16/11/5738 doi: 10.3390/e16115738

Li, C. Z., Zhang, L., Wang, H., Zhang, Y. Q., Yu, F. L., & Yan, D. H. (2012). The transferability of hydrological models under nonstationary climatic conditions. *Hydrology and Earth System Sciences*, *16*(4), 1239–1254. doi: 10.5194/hess-16-1239-2012

Li, H.-Y., Sivapalan, M., Tian, F., & Harman, C. (2014). Functional approach to exploring climatic and landscape controls of runoff generation: 1. behavioral constraints on runoff volume. *Water Resources Research*, *50*(12), 9300–9322. Retrieved 2020-04-20, from http://doi.wiley.com/10.1002/2014WR016307 doi: 10.1002/2014wr016307

Lim, T. C. (2016). Predictors of urban variable source area: a cross-sectional analysis of urbanized catchments in the united states: Predictors of urban variable source area. *Hydrological Processes*, *30*(25), 4799–4814. Retrieved 2018-11-05, from http://doi.wiley.com/10.1002/hyp.10943 doi: 10.1002/hyp.10943

Lim, T. C., & Welty, C. (2017). Effects of spatial configuration of imperviousness and green infrastructure networks on hydrologic response in a residential sewershed. *Water Resources Research*, *53*(9), 8084–8104. doi: 10.1002/2017wr020631

Liu, Z., He, C., Zhou, Y., & Wu, J. (2014). How much of the world's land has been urbanized, really? A hierarchical framework for avoiding confusion. *Landscape Ecology*, *29*(5), 763–771. doi: 10.1007/s10980-014-0034-y

Lovell, S. T., & Taylor, J. R. (2013, October). Supplying urban ecosystem services through multifunctional green infrastructure in the United States. *Landscape Ecology*, *28*(8), 1447–1463. Retrieved from http://link.springer.com/10.1007/s10980-013-9912-y doi: 10.1007/s10980-013-9912-y

Lyon, S. W., McHale, M. R., Walter, M. T., & Steenhuis, T. S. (2006). The impact of runoff generation mechanisms on the location of critical source areas 1. *JAWRA Journal of the American Water Resources Association*, *42*(3), 793–804.

Machusick, M., Welker, A., & Traver, R. (2011, March). Groundwater mounding at a stormwater infiltration bmp. *Journal of Irrigation and Drainage Engineering*, *137*(3), 154–160. Retrieved from https://ascelibrary.org/doi/abs/10.1061/{%}28ASCE{%}29IR.1943-4774.0000184 doi: 10.1061/(asce)ir.1943-4774.0000184

Makido, Y., Hellman, D., & Shandas, V. (2019, May). Nature-Based Designs to Mitigate Urban Heat: The Efficacy of Green Infrastructure Treatments in Portland, Oregon. *Atmosphere*, *10*(5), 282. Retrieved from https://www.mdpi.com/2073-4433/10/5/282 doi: 10.3390/atmos10050282

Mansell, M., & Rollet, F. (2006). Water balance and the behaviour of different paving surfaces. *Water and Environment Journal*, *20*(1), 7–10. Retrieved 2020-01-03, from https://onlinelibrary.wiley.com/doi/abs/10.1111/j.1747-6593.2005.00015.x doi: 10.1111/j.1747-6593.2005.00015.x

Mapping, S. V., & LiDAR Program, U. o. M., NASA Grant NNX13AP69G. (2016). *Sonoma vegetation mapping and lidar products.* Retrieved from "http://sonomavegmap.org/data-downloads/"

Maréchal, J. C., Ladouche, B., & Dörfliger, N. (2008). Karst flash flooding in a Mediterranean karst, the example of Fontaine de Nîmes. *Engineering Geology*, *99*(3-4), 138–146. doi: 10.1016/j.enggeo.2007.11.013

Martin, K. L., Hwang, T., Vose, J. M., Coulston, J. W., Wear, D. N., Miles, B., & Band, L. E. (2017, October). Watershed impacts of climate and land use changes depend on magnitude and land use context. *Ecohydrology*, *10*(7), e1870. Retrieved from http://doi.wiley.com/10.1002/eco.1870 doi: 10.1002/eco.1870

Maxwell, R., & Miller, N. (2005). Development of a Coupled Land Surface and Groundwater Model. Journal of Hydrometeorology. *Journal of Hydrometeorology*, *6*(3), 233–247. doi: doi:10.1175/JHM422.1

Mayor, Á. G., Bautista, S., Small, E. E., Dixon, M., & Bellot, J. (2008). Measurement of the connectivity of runoff source areas as determined by vegetation pattern and topography: A tool for assessing potential water and soil losses in drylands. *Water Resources Research*, *44*(10), 1–13. doi: 10.1029/2007wr006367

McDonnell, B., Tryby, M., Ratliff, K., & Wu, J. (2020). *Pyswmm v0.6.0.* Retrieved from https://pyswmm.readthedocs.io/en/v0.6.0/

McDonnell, J. J. (2003). Where does water go when it rains? moving beyond the variable source area concept of rainfall-runoff response. *Hydrological Processes*, *17*(9), 1869–1875. Retrieved 2019-02-16, from http://doi.wiley.com/10.1002/hyp.5132 doi: 10.1002/hyp.5132

McGlynn, B. L., McDonnel, J. J., & Brammer, D. D. (2002, February). A review of the evolving perceptual model of hillslope flowpaths at the maimai catchments, new zealand. *Journal of Hydrology*, *257*(1-4), 1–26. Retrieved from http://linkinghub.elsevier.com/retrieve/pii/S0022169401005595 doi: 10.1016/s0022-1694(01)00559-5

McGrane, S. J. (2016). Impacts of urbanisation on hydrological and water quality dynamics, and urban water management: a review. *Hydrological Sciences Journal*, *61*(13), 2295–2311. Retrieved 2019-04-05, from https://www.tandfonline.com/doi/full/10.1080/02626667.2015.1128084 doi: 10.1080/02626667.2015.1128084

McMillan, H. (2020). Linking hydrologic signatures to hydrologic processes: A review. *Hydrological Processes*, *34*(6), 1393–1409. doi: 10.1002/hyp.13632

McNamee, Porter & Seeley, Inc., Sangal, S., Bonema, S. R., & McNamee, Porter & Seeley, Inc. (1994). A methodology for calibrating SWMM models. *Journal of Water Management Modeling*. Retrieved 2019-10-01, from https://www.chijournal.org/R176-24 doi: 10.14796/jwmm.r176-24

McPherson, M. (1969, January). *Some notes on the rational method of storm drain design* (Tech. Rep. No. 6). New York, NY: ASCE Urban Water Resources Research Program. Retrieved from http://ascelibrary.org/doi/10.1061/9780784408438.ch11 doi: 10.1061/9780784408438.ch11

McPhillips, L. E., Earl, S. R., Hale, R. L., & Grimm, N. B. (2019). Urbanization in arid central arizona watersheds results in decreased stream flashiness. *Water Resources Research*, *55*(11), 9436–9453. doi: 10.1029/2019wr025835

Mein, R., & Larson, C. (1973). Modeling infiltration during a Steady Rain. *Water Resources Research*, *9*(2), 384–394.

Merz, R., Parajka, J., & Blöschl, G. (2011). Time stability of catchment model parameters: Implications for climate impact analyses. *Water Resources Research*, *47*(2), 1–17. doi: 10.1029/2010WR009505

Miles, B., & Band, L. E. (2015, April). Green infrastructure stormwater management at the watershed scale: urban variable source area and watershed capacitance: INVITED COMMENTARY. *Hydrological Processes*, *29*(9), 2268–2274. Retrieved 2017-11-15, from http://doi.wiley.com/10.1002/hyp.10448 doi: 10.1002/hyp.10448

Miller, R. A. (1978). The Hydraulically Effective Impervious Area Of An Urban Basin, Broward County, Florida.. Retrieved 2020-04-14, from https://trid.trb.org/view/80994 (Number: Conf Paper)

Milly, P. C., Betancourt, J., Falkenmark, M., Hirsch, R. M., Kundzewicz, Z. W., Lettenmaier, D. P., & Stouffer, R. J. (2008). Climate change: Stationarity is dead: Whither water management? *Science*, *319*(5863), 573–574. doi: 10.1126/science.1151915

Minet, J., Laloy, E., Lambot, S., & Vanclooster, M. (2011). Effect of high-resolution spatial soil moisture variability on simulated runoff response using a distributed hydrologic model. *Hydrology and Earth System Sciences*, *15*(4), 1323–1328. doi: 10.5194/hess-15-1323-2011

Mittman, T., Band, L. E., Hwang, T., & Smith, M. L. (2012). Distributed Hydrologic Modeling in the Suburban Landscape: Assessing Parameter Transferability from Gauged Reference Catchments. *Journal of the American Water Resources Association*, *48*(3), 546–557. doi: 10.1111/j.1752-1688.2011.00636.x

Moftakhari, H. R., AghaKouchak, A., Sanders, B. F., & Matthew, R. A. (2017). Cumulative hazard: The case of nuisance flooding. *Earth's Future*, *5*(2), 214–223. doi: 10.1002/2016ef000494

Montgomery, D. R., Dietrich, W. E., Torres, R., Anderson, S. P., Heffner, J. T., & Loague, K. (1997). Hydrologic response of a steep, unchanneled valley to natural and applied rainfall. *Water Resources Research*, *33*(1), 91–109. doi: 10.1029/96wr02985

Montgomery D.R., & Dietrich W.E. (1988). Where do channels begin? *Nature*, *336*(17), 232–234.

Mosley, M. P. (1979, August). Streamflow generation in a forested watershed, new zealand. *Water Resources Research*, *15*(4), 795–806. Retrieved from http://doi.wiley.com/10.1029/WR015i004p00795 doi: 10.1029/WR015i004p00795

Newcomer, M. E., Gurdak, J. J., Sklar, L. S., & Nanus, L. (2014, February). Urban recharge beneath low impact development and effects of climate variability and change. *Water Resources Research*, *50*(2), 1716–1734. Retrieved from http://doi.wiley.com/10.1002/2013WR014282https://agupubs-onlinelibrary-wiley-com.libproxy.berkeley.edu/doi/10.1002/2013WR014282 doi: 10.1002/2013WR014282

Niazi, M., Nietch, C., Maghrebi, M., Jackson, N., Bennett, B. R., Tryby, M., & Massoudieh, A. (2017, may). Storm Water Management Model: Performance Review and Gap Analysis. *Journal of Sustainable Water in the Built Environment*, *3*(2), 04017002. Retrieved from http://ascelibrary.org/doi/10.1061/JSWBAY.0000817 doi: 10.1061/JSWBAY.0000817

Niel, H., Paturel, J.-E. E., Servat, E., Niel, H. N., Paturel, J.-E. E., & Servat, E. (2003, 7). Study of parameter stability of a lumped hydrologic model in a context of climatic variability. *Journal of Hydrology*, *278*(1-4), 213–230. Retrieved from www.elsevier.com/locate/jhydrol doi: 10.1016/s0022-1694(03)00158-6

Norton, B. A., Coutts, A. M., Livesley, S. J., Harris, R. J., Hunter, A. M., & Williams, N. S. (2015, February). Planning for cooler cities: A framework to prioritise green infrastructure to mitigate high temperatures in urban landscapes. *Landscape and Urban Planning*, *134*, 127–138. Retrieved from http://linkinghub.elsevier.com/retrieve/pii/S0169204614002503 doi: 10.1016/j.landurbplan.2014.10.018

Nossent, J., Elsen, P., & Bauwens, W. (2011). Sobol' sensitivity analysis of a complex environmental model. *Environmental Modelling and Software*, *26*(12), 1515–1525. doi: 10.1016/j.envsoft.2011.08.010

Ocampo, C., Rennie, B., & Oldham, C. (2017). *Performance of two urban stormwater biofilters in an area with seasonally high groundwater* (Tech. Rep.). Melbourne, Australia: Cooperative Research Centre for Water Sensitive Cities.

Ocampo, C. J., Oldham, C. E., et al. (2013). The impact of urbanisation on hydrology in areas with significant groundwater surface water interations: Three case studies. *Water Sensitive Urban Design 2013: WSUD 2013*, 503.

Oke, T. R. (1973, August). City size and the urban heat island. *Atmospheric Environment (1967)*, *7*(8), 769–779. doi: 10.1016/0004-6981(73)90140-6

Palla, A., & Gnecco, I. (2015, September). Hydrologic modeling of Low Impact Development systems at the urban catchment scale. *Journal of Hydrology*, *528*, 361–368. Retrieved from http://linkinghub.elsevier.com/retrieve/pii/S0022169415004631http://www.sciencedirect.com/science/article/pii/S0022169415004631 doi: 10.1016/j.jhydrol.2015.06.050

Panos, C. L., Hogue, T. S., Gilliom, R. L., & McCray, J. E. (2018). High-resolution modeling of infill development impact on stormwater dynamics in denver, colorado. *Journal of Sustainable Water in the Built Environment*, *4*(4), 04018009. Retrieved 2019-02-02, from http://ascelibrary.org/doi/10.1061/JSWBAY.0000863 doi: 10.1061/jswbay.0000863

Panos, C. L., Hogue, T. S., Gilliom, R. L., & McCray, J. E. (2018, nov). High-Resolution Modeling of Infill Development Impact on Stormwater Dynamics in Denver, Colorado. *Journal of Sustainable Water in the Built Environment*, *4*(4), 04018009. Retrieved from http://ascelibrary.org/doi/10.1061/JSWBAY.0000863 doi: 10.1061/JSWBAY.0000863

Panos, C. L., Wolfand, J. M., & Hogue, T. S. (2020). SWMM sensitivity to LID siting and routing parameters: Implications for stormwater regulatory compliance. *JAWRA Journal of the American Water Resources Association*, 1752–1688.12867. Retrieved 2020-07-27, from https://onlinelibrary.wiley.com/doi/abs/10.1111/1752-1688.12867 doi: 10.1111/1752-1688.12867

Panos, C. L., Wolfand, J. M., & Hogue, T. S. (2021). Assessing resilience of a dual drainage urban system to redevelopment and climate change. *Journal of Hydrology*, *596*(June 2020), 126101. Retrieved from https://doi.org/10.1016/j.jhydrol.2021.126101 doi: 10.1016/j.jhydrol.2021.126101

Pappas, E., Smith, D., Huang, C., Shuster, W., & Bonta, J. (2008). Impervious surface impacts to runoff and sediment discharge under laboratory rainfall simulation. *Catena*, *72*(1), 146–152. Retrieved 2019-09-06, from https://linkinghub.elsevier.com/retrieve/pii/S0341816207000811 doi: 10.1016/j.catena.2007.05.001

Patterson, J. J., Smith, C., & Bellamy, J. (2013, October). Understanding enabling capacities for managing the 'wicked problem' of nonpoint source water pollution in catchments: A conceptual framework. *Journal of Environmental Management*, *128*, 441–452. Retrieved from https://linkinghub.elsevier.com/retrieve/pii/S0301479713003629 doi: 10.1016/j.jenvman.2013.05.033

Pellerin, B. A., Wollheim, W. M., Feng, X., & Vörörsmarty, C. J. (2008, June). The application of electrical conductivity as a tracer for hydrograph separation in urban catchments. *Hydrological Processes*, *22*(12), 1810–1818. Retrieved from http://doi.wiley.com/10.1002/hyp.6786 doi: 10.1002/hyp.6786

Penna, D., Tromp-Van Meerveld, H. J., Gobbi, A., Borga, M., & Dalla Fontana, G. (2011). The influence of soil moisture on threshold runoff generation processes in an alpine headwater catchment. *Hydrology and Earth System Sciences*, *15*(3), 689–702. doi: 10.5194/hess-15-689-2011

Penny, G., Srinivasan, V., Apoorva, R., Jeremiah, K., Peschel, J., Young, S., & Thompson, S. (2020a). A process-based approach to attribution of historical streamflow decline in a data-scarce and human-dominated watershed. *Hydrological Processes*, *34*(8), 1981–1995. doi: 10.1002/hyp.13707

Penny, G., Srinivasan, V., Apoorva, R., Jeremiah, K., Peschel, J., Young, S., & Thompson, S. (2020b, April). A process-based approach to attribution of historical streamflow decline in

a data-scarce and human-dominated watershed. *Hydrological Processes*, *34*(8), 1981–1995. Retrieved from https://onlinelibrary.wiley.com/doi/abs/10.1002/hyp.13707 doi: 10.1002/hyp.13707

Petrucci, G., & Bonhomme, C. (2014). The dilemma of spatial representation for urban hydrology semi-distributed modelling: Trade-offs among complexity, calibration and geographical data. *Journal of Hydrology*, *517*, 997–1007. Retrieved from http://dx.doi.org/10.1016/j.jhydrol.2014.06.019 doi: 10.1016/j.jhydrol.2014.06.019

Petrucci, G., Rioust, E., Deroubaix, J.-F., & Tassin, B. (2013, April). Do stormwater source control policies deliver the right hydrologic outcomes? *Journal of Hydrology*, *485*, 188–200. Retrieved 2017-11-15, from http://linkinghub.elsevier.com/retrieve/pii/S0022169412005021 doi: 10.1016/j.jhydrol.2012.06.018

Philip, J. R. (1969). Hydrostatics and hydrodynamics in swelling soils. *Water Resources Research*, *5*(5), 1070–1077. doi: 10.1029/WR005i005p01070

Pitt, R. E., Williamson, D., Voorhees, J., & Clark, S. (2005). *Review of Historical Street Dust and Dirt Accumulation and Washoff Data* (Vol. 6062). doi: 10.14796/jwmm.r223-12

Poff, N. L., Allan, J. D., Bain, M. B., Karr, J. R., Prestegaard, K. L., Richter, B. D., ... Stromberg, J. C. (1997). The natural flow regime. *BioScience*, *47*(11), 769–784. Retrieved 2017-11-15, from https://academic.oup.com/bioscience/article-lookup/doi/10.2307/1313099 doi: 10.2307/1313099

Porporato, A., Daly, E., & Rodriguez-Iturbe, I. (2004). Soil water balance and ecosystem response to climate change. *American Naturalist*, *164*(5), 625–632. doi: 10.1086/424970

Prasad, A. M., Iverson, L. R., & Liaw, A. (2006). Newer classification and regression tree techniques: Bagging and random forests for ecological prediction. *Ecosystems*, *9*(2), 181–199. Retrieved 2019-11-06, from https://doi.org/10.1007/s10021-005-0054-1 doi: 10.1007/s10021-005-0054-1

Ramier, D., Berthier, E., & Andrieu, H. (2004). An urban lysimeter to assess runoff losses on asphalt concrete plates. *Physics and Chemistry of the Earth, Parts A/B/C*, *29*(11), 839–847. Retrieved 2020-01-03, from http://www.sciencedirect.com/science/article/pii/S1474706504001160 doi: 10.1016/j.pce.2004.05.011

Rawls, W. J., Brakensiek, D. L., & Miller, N. (1983). Green-ampt infiltration parameters from soils data. *Journal of Hydraulic Engineering*, *109*(1), 62–70. Retrieved 2019-07-31, from http://ascelibrary.org/doi/10.1061/%28ASCE%290733-9429%281983%29109%3A1%2862%29 doi: 10.1061/(asce)0733-9429(1983)109:1(62)

Redfern, T. W., Macdonald, N., Kjeldsen, T. R., Miller, J. D., & Reynard, N. (2016). Current understanding of hydrological processes on common urban surfaces. *Progress in Physical*

Geography, *40*(5), 699–713. Retrieved 2017-11-15, from http://journals.sagepub.com/doi/10.1177/0309133316652819 doi: 10.1177/0309133316652819

Reed, S., Koren, V., Smith, M., Zhang, Z., Moreda, F., & Seo, D. J. (2004). Overall distributed model intercomparison project results. *Journal of Hydrology*, *298*(1-4), 27–60. doi: 10.1016/j.jhydrol.2004.03.031

Reid, C. E., Jerrett, M., Petersen, M. L., Pfister, G. G., Morefield, P. E., Tager, I. B., ... Balmes, J. R. (2015). Spatiotemporal prediction of fine particulate matter during the 2008 northern california wildfires using machine learning. *Environmental Science & Technology*, *49*(6), 3887–3896. Retrieved 2019-11-10, from https://pubs.acs.org/doi/10.1021/es505846r doi: 10.1021/es505846r

Rempe, D. M., & Dietrich, W. E. (2018). Direct observations of rock moisture, a hidden component of the hydrologic cycle. *Proceedings of the National Academy of Sciences of the United States of America*, *115*(11), 2664–2669. doi: 10.1073/pnas.1800141115

Richts, A., Struckmeier, W. F., & Zaepke, M. (2011). WHYMAP and the Groundwater Resources Map of the World 1:25,000,000. In *Sustaining groundwater resources* (pp. 159–173). Dordrecht: Springer Netherlands. Retrieved from http://link.springer.com/10.1007/978-90-481-3426-7_10 doi: 10.1007/978-90-481-3426-7_10

Rittel, H. W., & Webber, M. M. (1973, June). Dilemmas in a general theory of planning. *Policy Sciences*, *4*(2), 155–169. Retrieved from https://link-springer-com.libproxy.berkeley.edu/article/10.1007/BF01405730 doi: 10.1007/bf01405730

Robinson, J. S., & Sivapalan, M. (1997). Temporal scales and hydrological regimes : Implications for flood frequency scaling interactions can help identify different hydrological using the theoretical regimes are characterized by low values of the coefficient of variation , peaks , while fast re. *Water Resources Research*, *33*(12), 2981–2999.

Rolls, R. J., Leigh, C., & Sheldon, F. (2012). Mechanistic effects of low-flow hydrology on riverine ecosystems: Ecological principles and consequences of alteration. *Freshwater Science*, *31*(4), 1163–1186. doi: 10.1899/12-002.1

Rosa, D. J., Clausen, J. C., & Dietz, M. E. (2015, June). Calibration and Verification of SWMM for Low Impact Development. *Journal of the American Water Resources Association*, *51*(3), 746–757. Retrieved from http://doi.wiley.com/10.1111/jawr.12272 doi: 10.1111/jawr.12272

Rossman, L. A. (2015, August). *Comment on "Green-Ampt initial deficit in continuous simulation"*. Retrieved 2019-12-20, from https://www.openswmm.org/Topic/4834/green-ampt-initial-deficit-in-continuous-simulation

Rossman, L. A., & Huber, W. C. (2016). *Storm Water Management Model Reference Manual Volume I – Hydrology (revised)(EPA/600/R-15/162A)* (Vol. I; Tech. Rep. No. January). Washington, DC, EPA/600/R-15/162A: US EPA Office of Research and Development. Retrieved from https://nepis.epa.gov/Exe/ZyPDF.cgi?Dockey=P100NYRA.txt

Roy, A. H., & Shuster, W. D. (2009). Assessing impervious surface connectivity and applications for watershed management. *JAWRA Journal of the American Water Resources Association*, *45*(1), 198–209.

Roy, A. H., Wenger, S. J., Fletcher, T. D., Walsh, C. J., Ladson, A. R., Shuster, W. D., ... Brown, R. R. (2008, August). Impediments and solutions to sustainable, watershed-scale urban stormwater management: Lessons from australia and the united states. *Environmental Management*, *42*(2), 344–359. Retrieved from https://doi.org/10.1007/s00267-008-9119-1http://link.springer.com/10.1007/s00267-008-9119-1 doi: 10.1007/s00267-008-9119-1

Saadi, M., Oudin, L., & Ribstein, P. (2020). Beyond imperviousness: the role of antecedent wetness in runoff generation in urbanized catchments. *Water Resources Research*, *56*(11), e2020WR028060.

Saltelli, A. (2002). Making best use of model evaluations to compute sensitivity indices. *Computer Physics Communications*, *145*(2), 280–297. doi: 10.1016/s0010-4655(02)00280-1

Saltelli, A., Aleksankina, K., Becker, W., Fennell, P., Ferretti, F., Holst, N., ... Wu, Q. (2019, April). Why so many published sensitivity analyses are false: A systematic review of sensitivity analysis practices. *Environmental Modelling and Software*, *114*, 29–39. doi: 10.1016/j.envsoft.2019.01.012

Saltelli, A., Annoni, P., Azzini, I., Campolongo, F., Ratto, M., & Tarantola, S. (2010). Variance based sensitivity analysis of model output. Design and estimator for the total sensitivity index. *Computer Physics Communications*, *181*(2), 259–270. Retrieved from http://dx.doi.org/10.1016/j.cpc.2009.09.018 doi: 10.1016/j.cpc.2009.09.018

Salvadore, E., Bronders, J., & Batelaan, O. (2015). Hydrological modelling of urbanized catchments: A review and future directions. *Journal of Hydrology*, *529*(P1), 62–81. Retrieved from http://dx.doi.org/10.1016/j.jhydrol.2015.06.028 doi: 10.1016/j.jhydrol.2015.06.028

Samuels, P., Klijn, F., & Dijkman, J. (2006). An analysis of the current practice of policies on river flood risk management in different countries. *Irrigation and Drainage*, *55*(SUPPL. 1), 25–27. doi: 10.1002/ird.257

Savenije, H. H. (2009). HESS opinions: "The art of hydrology". *Hydrology and Earth System Sciences*, *13*(2), 157–161. doi: 10.5194/hess-13-157-2009

Savenije, H. H. G. (2001). Equifinality, a blessing in disguise? *Hydrological Processes*, *15*(14), 2835–2838. Retrieved 2018-11-26, from http://doi.wiley.com/10.1002/hyp.494 doi: 10.1002/hyp.494

Schaefli, B. (2016, October). Snow hydrology signatures for model identification within a limits-of-acceptability approach. *Hydrological Processes*, *30*(22), 4019–4035. Retrieved from http://doi.wiley.com/10.1002/hyp.10972 doi: 10.1002/hyp.10972

Scheffer, M., & Carpenter, S. R. (2003). Catastrophic regime shifts in ecosystems: Linking theory to observation. *Trends in Ecology and Evolution*, *18*(12), 648–656. doi: 10.1016/j.tree.2003.09.002

Schneiderman, E. M., Steenhuis, T. S., Thongs, D. J., Easton, Z. M., Zion, M. S., Neal, A. L., ... Walter, M. T. (2007). Incorporating variable source area hydrology into a curve-number-based watershed model. *Hydrological Processes*, *21*(25), 3420–3430. Retrieved from http://dx.doi.org/10.1002/hyp.6556 doi: 10.1002/hyp.6556

Schwartz, S. S., & Smith, B. (2014). Slowflow fingerprints of urban hydrology. *Journal of Hydrology*, *515*, 116–128. Retrieved 2019-02-02, from https://linkinghub.elsevier.com/retrieve/pii/S0022169414002935 doi: 10.1016/j.jhydrol.2014.04.019

Sebilo, M., Mayer, B., Nicolardot, B., Pinay, G., & Mariotti, A. (2013). Long-term fate of nitrate fertilizer in agricultural soils. *Proceedings of the National Academy of Sciences of the United States of America*, *110*(45), 18185–18189. doi: 10.1073/pnas.1305372110

Seo, Y., Choi, N.-J., & Schmidt, A. R. (2013). Contribution of directly connected and isolated impervious areas to urban drainage network hydrographs. *Hydrology and Earth System Sciences*, *17*(9), 3473–3483. Retrieved 2019-10-14, from https://www.hydrol-earth-syst-sci.net/17/3473/2013/ doi: 10.5194/hess-17-3473-2013

Shangguan, W., Hengl, T., Mendes de Jesus, J., Yuan, H., & Dai, Y. (2017). Mapping the global depth to bedrock for land surface modeling. *Journal of Advances in Modeling Earth Systems*, *9*(1), 65–88. Retrieved from https://agupubs.onlinelibrary.wiley.com/doi/abs/10.1002/2016MS000686 doi: 10.1002/2016MS000686

Shields, C., & Tague, C. (2015, January). Ecohydrology in semiarid urban ecosystems: Modeling the relationship between connected impervious area and ecosystem productivity. *Water Resources Research*, *51*(1), 302–319. Retrieved from http://doi.wiley.com/10.1002/2014WR016108 doi: 10.1002/2014wr016108

Shields, C. A., & Tague, C. L. (2012, May). Assessing the Role of Parameter and Input Uncertainty in Ecohydrologic Modeling: Implications for a Semi-arid and Urbanizing Coastal California Catchment. *Ecosystems*, *15*(5), 775–791. Retrieved from https://link-springer-com.libproxy.berkeley.edu/article/10.1007/s10021-012-9545-z doi: 10.1007/s10021-012-9545-z

Shin, M. J., Guillaume, J. H., Croke, B. F., & Jakeman, A. J. (2013). Addressing ten questions about conceptual rainfall-runoff models with global sensitivity analyses in R. *Journal of Hydrology*, *503*, 135–152. Retrieved from http://dx.doi.org/10.1016/j.jhydrol.2013.08.047 doi: 10.1016/j.jhydrol.2013.08.047

Shrestha, S., Fang, X., & Li, J. (2013). Mapping the 95th percentile daily rainfall in the contiguous u.s. In *World environmental and water resources congress 2013* (pp. 219–229). American Society of Civil Engineers. Retrieved 2019-10-03, from http://ascelibrary.org/doi/10.1061/9780784412947.021 doi: 10.1061/9780784412947.021

Shuster, W., & Rhea, L. (2013, April). Catchment-scale hydrologic implications of parcel-level stormwater management (Ohio USA). *Journal of Hydrology*, *485*, 177–187. Retrieved from http://www.sciencedirect.com/science/article/pii/S0022169412009432https://linkinghub.elsevier.com/retrieve/pii/S0022169412009432 doi: 10.1016/j.jhydrol.2012.10.043

Shuster, W. D., Pappas, E., & Zhang, Y. (2008, September). Laboratory-Scale Simulation of Runoff Response from Pervious-Impervious Systems. *Journal of Hydrologic Engineering*, *13*(9), 886–893. Retrieved from https://ascelibrary.org/doi/abs/10.1061/{%}28ASCE{%}291084-0699{%}282008{%}2913{%}3A9{%}28886{%}29 doi: 10.1061/(asce)1084-0699(2008)13:9(886)

Sidle, R. C., Tsuboyama, Y., Noguchi, S., Hosoda, I., Fujieda, M., & Shimizu, T. (2000). Stormflow generation in steep forested headwaters: A linked hydrogeomorphic paradigm. *Hydrological Processes*, *14*(3), 369–385. doi: 10.1002/(sici)1099-1085(20000228)14:3⟨369::aid-hyp943⟩3.0.co;2-p

Sidle, W., & Lee, P. (2006, September). Urban stormwater tracing with the naturally occurring deuterium isotope. *Water Environment Research*, *71*(6), 1251–1256. Retrieved from http://doi.wiley.com/10.2175/106143096X122357 doi: 10.2175/106143096x122357

Simmons, D. L., & Reynolds, R. J. (1982). Effects Of Urbanization On Base Flow Of Selected South-shore Streams, Long Island, New York. *JAWRA Journal of the American Water Resources Association*, *18*(5), 797–805.

Singh, V. P. (1997, October). Effect of spatial and temporal variability in rainfall and watershed characteristics on stream flow hydrograph. *Hydrological Processes*, *11*(12), 1649–1669. Retrieved from https://onlinelibrary.wiley.com/doi/full/10.1002/{%}28SICI{%}291099-1085{%}2819971015{%}2911{%}3A12{%}3C1649{%}3A{%}3AAID-HYP495{%}3E3.0.CO{%}3B2-1https://onlinelibrary.wiley.com/doi/abs/10.1002/{%}28SICI{%}291099-1085{%}2819971015{%}2911{%}3A12{%}3C1649{%}3A{%}3AAID-HYP495{%}3E3.0.CO{%}3B2-1https://onlinelibrary.wiley.com/doi/10.1002/(SICI)1099-1085(19971015)11:12{%}3C1649::AID-HYP495{%}3E3.0.CO;2-1 doi: 10.1002/(sici)1099-1085(19971015)11:12⟨1649::aid-hyp495⟩3.0.co;2-1

Singh, V. P. (2013). *Extremes in a changing climate: Detection, analysis and uncertainty* (A. AghaKouchak, K. Hsu, S. Sorooshian, D. Easterling, & S. Schubert, Eds.). Springer. Retrieved from http://dx.doi.org/10.1016/j.cirp.2016.06.001%0Ahttp://dx.doi.org/10.1016/j.powtec.2016.12.055%0Ahttps://doi.org/10.1016/j.ijfatigue.2019.02.006%0Ahttps://doi.org/10.1016/j.matlet.2019.04.024%0Ahttps://doi.org/10.1016/j.matlet.2019.127252%0Ahttp://dx.doi.o doi: 10.1088/1751-8113/44/8/085201

Sivapalan, M. (2003). Process complexity at hillslope scale, process simplicity at the watershed scale: is there a connection? *Hydrological Processes*, *17*(5), 1037–1041. doi: 10.1002/hyp.5109

Sklash, M. G., & Farvolden, R. N. (1979). The role of groundwater in storm runoff. *Journal of Hydrology*, *43*(1), 45–65.

Sklash, M. G., Stewart, M. K., & Pearce, A. J. (1986, August). Storm runoff generation in humid headwater catchments: 2. a case study of hillslope and low-order stream response. *Water Resources Research*, *22*(8), 1273–1282. Retrieved from http://doi.wiley.com/10.1029/WR022i008p01273 doi: 10.1029/WR022i008p01273

Smith, R., Goodrich, D., Woolhiser, D., Unkrich, C., et al. (1995). Kineros-a kinematic runoff and erosion model. *Computer models of watershed hydrology.*, 697–732.

Sobol', I. (1990). On sensitivity estimation for nonlinear mathematical models. *Matematicheskoe Modelirovanie*, 112–118.

Sorooshian, S., & Gupta, V. K. (1995). Chapter 2. Model Calibration. In V. P. Singh (Ed.), *Computer models of watershed hydrology* (Rev. ed. ed.). Highlands Ranch, Colo. :. Retrieved from http://hdl.handle.net/2027/mdp.39015041316129

Sorooshian, S., Gupta, V. K., & Fulton, J. L. (1983). Evaluation of maximum likelihood parameter estimation techniques for conceptual rainfall-runoff models: Influence of calibration data variability and length on model credibility. *Water Resources Research*, *19*(1), 251–259. doi: 10.1029/WR019i001p00251

Spahr, K. M., Bell, C. D., McCray, J. E., & Hogue, T. S. (2020, February). Greening up stormwater infrastructure: Measuring vegetation to establish context and promote cobenefits in a diverse set of US cities. *Urban Forestry and Urban Greening*, *48*, 126548. Retrieved from http://www.sciencedirect.com/science/article/pii/S1618866719301657 doi: 10.1016/j.ufug.2019.126548

Steenhuis, T. S., Winchell, M., Rossing, J., Zollweg, J. A., & Walter, M. F. (1995). *Scs runoff equation revisited for variable-source runoff areas* (Vol. 121) (No. 3). doi: 10.1061/(asce)0733-9437(1995)121:3(234)

Stewart, R. D., Bhaskar, A. S., Parolari, A. J., Herrmann, D. L., Jian, J., Schifman, L. A., & Shuster, W. D. (2019). An analytical approach to ascertain saturation-excess versus infiltration-excess overland flow in urban and reference landscapes. *Hydrological Processes*, *33*(26), 3349–3363. Retrieved 2020-06-16, from https://onlinelibrary.wiley.com/doi/abs/10.1002/hyp.13562 doi: 10.1002/hyp.13562

Struthers, I., & Sivapalan, M. (2007). A conceptual investigation of process controls upon flood frequency: Role of thresholds. *Hydrology and Earth System Sciences*, *11*(4), 1405–1416. doi: 10.5194/hess-11-1405-2007

Sun, N., Hong, B., & Hall, M. (2014). Assessment of the SWMM model uncertainties within the generalized likelihood uncertainty estimation (GLUE) framework for a high-resolution urban sewershed. *Hydrological Processes*, *28*(6), 3018–3034. doi: 10.1002/hyp.9869

Sutherland, R. (1995). *Methods for Estimating the Effective Impervious Area of Urban Watersheds* (Technical Note from Watershed Protection Techniques). Watershed Protection Techniques.

Sytsma, A., Bell, C., Eisenstein, W., Hogue, T., & Kondolf, G. M. (2020, September). A geospatial approach for estimating hydrological connectivity of impervious surfaces. *Journal of Hydrology*, 30. Retrieved from https://linkinghub.elsevier.com/retrieve/pii/S0022169420310052 doi: 10.1016/j.jhydrol.2020.125545

Sytsma, A., Crompton, O., Panos, C., Thompson, S., & Kondolf, G. (2021). Implications of non-stationarity for calibration of lumped urban runoff models. *Unpublished*.

Tague, C. L., & Band, L. E. (2004). RHESSys: Regional Hydro-Ecologic Simulation System—An ObjectOriented Approach to Spatially Distributed Modeling of Carbon, Water, and Nutrient Cycling. *Earth Interactions*, *8*(19).

Tegegne, G., & Kim, Y.-O. (2018). Modelling ungauged catchments using the catchment runoff response similarity. *Journal of Hydrology*, *564*, 452–466. Retrieved 2020-05-15, from https://linkinghub.elsevier.com/retrieve/pii/S0022169418305535 doi: 10.1016/j.jhydrol.2018.07.042

Thomas, I. A., Jordan, P., Mellander, P. E., Fenton, O., Shine, O., Ó hUallacháin, D., ... Murphy, P. N. (2016, June). Improving the identification of hydrologically sensitive areas using lidar dems for the delineation and mitigation of critical source areas of diffuse pollution. *Science of the Total Environment*, *556*, 276–290. Retrieved from https://linkinghub.elsevier.com/retrieve/pii/S0048969716303941http://www.sciencedirect.com/science/article/pii/S0048969716303941http://dx.doi.org/10.1016/j.scitotenv.2016.02.183 doi: 10.1016/j.scitotenv.2016.02.183

Thompson, S. E., Basu, N. B., Lascurain, J., Aubeneau, A., & Rao, P. S. (2011). Relative dominance of hydrologic versus biogeochemical factors on solute export across impact gradients. *Water Resources Research*, *47*(7), 1–20. doi: 10.1029/2010WR009605

Thompson, S. E., Sivapalan, M., Harman, C. J., Srinivasan, V., Hipsey, M. R., Reed, P., ... Blöschl, G. (2013). Developing predictive insight into changing water systems: use-inspired hydrologic science for the anthropocene. *Hydrology and Earth System Sciences*, *17*(12), 5013–5039. Retrieved 2020-07-09, from https://www.hydrol-earth-syst-sci.net/17/5013/2013/ doi: 10.5194/hess-17-5013-2013

Tilahun, S. A., Ayana, E. K., Guzman, C. D., Dagnew, D. C., Zegeye, A. D., Tebebu, T. Y., ... Steenhuis, T. S. (2016). Revisiting storm runoff processes in the upper blue nile basin: The debre mawi watershed. *Catena*, *143*, 47–56.

Toth, J. (1963). A theoretical analysis of groundwater flow in small drainage basins. *Journal of Geophysical Research*, *68*(16), 4795–4812.

Tromp-Van Meerveld, H. J., & McDonnell, J. J. (2006). Threshold relations in subsurface stormflow: 1. a 147-storm analysis of the panola hillslope. *Water Resources Research*, *42*(2), 1–11. doi: 10.1029/2004wr003778

Tu, M.-c., Caplan, J. S., Eisenman, S. W., & Wadzuk, B. M. (2020). When green infrastructure turns grey: Plant water stress as a consequence of overdesign in a tree trench system. *Water*, *12*(2), 573.

Tuomela, C., Sillanpää, N., & Koivusalo, H. (2019). Assessment of stormwater pollutant loads and source area contributions with storm water management model (SWMM). *Journal of Environmental Management*, *233*(July 2018), 719–727. Retrieved from https://doi.org/10.1016/j.jenvman.2018.12.061 doi: 10.1016/j.jenvman.2018.12.061

Tyralis, H., Papacharalampous, G., & Langousis, A. (2019). A brief review of random forests for water scientists and practitioners and their recent history in water resources. *Water*, *11*(5), 910. Retrieved 2019-10-06, from https://www.mdpi.com/2073-4441/11/5/910 doi: 10.3390/w11050910

United Nations. (2018). *World urbanization prospects: The 2018 revision* (Tech. Rep.).

United States Environmental Protection Agency. (2018). *EPA SWMM 5.1.013 Code Viewer.* OpenSWMM. Retrieved from https://www.openswmm.org/SWMM51013?query=green

Urbonas, B. (2000). Chapter 7: Assessment of Stormwater Best Management Practice Effectiveness. In *Innovative urban wet-weather flow management systems* (pp. 7.1–7.46).

U.S. Geological Survey. (2017). *1 meter digital elevation models (DEMs) - USGS national map 3dep downloadable data collection.* Retrieved from https://nationalmap.gov/3DEP/

Usda. (1986). *Urban hydrology for small watersheds TR-55* (Tech. Rep. No. Technical Release 55). Retrieved 2019-11-01, from https://www.nrcs.usda.gov/Internet/FSE_DOCUMENTS/stelprdb1044171.pdf

Valeo, C., & Moin, S. M. (2000, February). Variable source area modelling in urbanizing watersheds. *Journal of Hydrology*, *228*(1-2), 68–81. Retrieved from http://linkinghub.elsevier.com/retrieve/pii/S0022169400001530 doi: 10.1016/s0022-1694(00)00153-0

Valeo, C., & Moin, S. M. (2001, August). Hortonian and variable source area modeling in urbanizing basins. *Journal of Hydrologic Engineering*, *6*(4), 328–335. Retrieved from http://ascelibrary.org/doi/10.1061/{%}28ASCE{%}291084-0699{%}282001{%}296{%}3A4{%}28328{%}29 doi: 10.1061/(asce)1084-0699(2001)6:4(328)

Vaze, J., Post, D. A., Chiew, F. H., Perraud, J. M., Viney, N. R., & Teng, J. (2010). Climate non-stationarity - Validity of calibrated rainfall-runoff models for use in climate change studies. *Journal of Hydrology*, *394*(3-4), 447–457. Retrieved from http://dx.doi.org/10.1016/j.jhydrol.2010.09.018 doi: 10.1016/j.jhydrol.2010.09.018

Vezzaro, L., Eriksson, E., Ledin, A., & Mikkelsen, P. S. (2012, December). Quantification of uncertainty in modelled partitioning and removal of heavy metals (Cu, Zn) in a stormwater retention pond and a biofilter. *Water Research*, *46*(20), 6891–6903. Retrieved from http://www.sciencedirect.com/science/article/pii/S0043135411004957 doi: 10.1016/j.watres.2011.08.047

Viessman, W., & Lewis, G. (2011). *Introduction to Hydrology* (5th ed. ed.). Prentice Hall/Pearson Education.

Voter, C. B., & Loheide, S. P. (2018). Urban residential surface and subsurface hydrology: Synergistic effects of low-impact features at the parcel scale. *Water Resources Research*, *54*(10), 8216–8233. doi: 10.1029/2018wr022534

Wagener, T. (2003). Evaluation of catchment models. *Hydrological Processes*, *17*(16), 3375–3378. doi: 10.1002/hyp.5158

Wagener, T., Sivapalan, M., Troch, P. A., McGlynn, B. L., Harman, C. J., Gupta, H. V., ... Wilson, J. S. (2010, May). The future of hydrology: An evolving science for a changing world. *Water Resources Research*, *46*(5), 1–10. Retrieved from http://doi.wiley.com/10.1029/2009WR008906 doi: 10.1029/2009wr008906

Walker, G., & Burningham, K. (2011). Flood risk, vulnerability and environmental justice: Evidence and evaluation of inequality in a UK context. *Critical Social Policy*, *31*(2), 216–240. doi: 10.1177/0261018310396149

Walsh, C. J., Roy, A. H., Feminella, J. W., Cottingham, P. D., Groffman, P. M., & Morgan II, R. P. (2005). The urban stream syndrome: current knowledge and the search for a cure. *Journal of the North American Benthological Society*, *24*(3), 706–723.

Walter, M. T., & Shaw, S. B. (2005, December). Discussion - "curve number hydrology in water quality modeling: Uses, abuses, and future directions," by david c. garen and daniel s. moore. *Journal of the American Water Resources Association*, *41*(6), 1491–1492. Retrieved from http://doi.wiley.com/10.1111/j.1752-1688.2005.tb03815.x doi: 10.1111/j.1752-1688.2005.tb03815.x

Walter, M. T., Walter, M. F., Brooks, E. S., Steenhuis, T. S., Boll, J., & Weiler, K. (2000). Hydrologically sensitive areas: Variable source area hydrology implications for water quality risk assessment. *Journal of Soil and Water Conservation*, *55*(3), 277–284.

Washington State Department of Ecology. (2019). *2019 Stormwater Management Manual for Western Washington.* Western Washington. doi: PublicationNo.19-10-021

Waters, D., Watt, W. E., Marsalek, J., & Anderson, B. C. (2003). Adaptation of a storm drainage system to accomodate increased rainfall resulting from climate change. *Journal of Environmental Planning and Management*, *46*(5), 755–770. doi: 10.1080/0964056032000138472

Weiler, M., & McDonnell, J. (2004). Virtual experiments: a new approach for improving process conceptualization in hillslope hydrology. *Journal of Hydrology*, *285*(1), 3–18. Retrieved 2019-07-29, from https://linkinghub.elsevier.com/retrieve/pii/S0022169403002713 doi: 10.1016/s0022-1694(03)00271-3

Western, A. W., Grayson, R. B., Blöschl, G., Willgoose, G. R., & McMahon, T. A. (1999). Observed spatial organization of soil moisture and its relation to terrain indices. *Water Resources Research*, *35*(3), 797–810. doi: 10.1029/1998wr900065

Westra, S., Thyer, M., Leonard, M., Kavetski, D., Lambert, M., Cha, Y., ... Stow, C. A. (2014, June). A strategy for diagnosing and interpreting hydrological model nonstationarity. *Water Resources Research*, *50*(6), 5375–5377. Retrieved from http://doi.wiley.com/10.1002/2013WR014719 doi: 10.1002/2013WR014979.Reply

Whipkey, R. Z. (1965). Subsurface Stormflow From Forested Slopes. *International Association of Scientific Hydrology. Bulletin*, *10*(2), 74–85. Retrieved 2019-02-18, from http://www.tandfonline.com/doi/abs/10.1080/02626666509493392 doi: 10.1080/02626666509493392

Whiting, J. A., & Godsey, S. E. (2016). Discontinuous headwater stream networks with stable flowheads, salmon river basin, idaho. *Hydrological Processes*, *30*(13), 2305–2316. doi: 10.1002/hyp.10790

Wilby, R. L., Beven, K. J., & Reynard, N. S. (2008, July). *Climate change and fluvial flood risk in the uk: More of the same?* (Vol. 22) (No. 14). doi: 10.1002/hyp.6847

Wong, B. P., & Kerkez, B. (2016). Real-time environmental sensor data: An application to water quality using web services. *Environmental Modelling and Software*, *84*, 505–517. Retrieved from http://dx.doi.org/10.1016/j.envsoft.2016.07.020 doi: 10.1016/j.envsoft.2016.07.020

Wong, B. P., & Kerkez, B. (2018). Real-Time Control of Urban Headwater Catchments Through Linear Feedback: Performance, Analysis, and Site Selection. *Water Resources Research*, *54*(10), 7309–7330. doi: 10.1029/2018WR022657

Wood, E. F., Sivapalan, M., Beven, K., & Band, L. (1988, September). Effects of spatial variability and scale with implications to hydrologic modeling. *Journal of Hydrology*, *102*(1-4), 29–47. Retrieved from http://linkinghub.elsevier.com/retrieve/pii/002216948890090X doi: 10.1016/0022-1694(88)90090-x

Woods, R. A., & Rowe, L. K. (1996). The changing spatial variability of subsurface flow across a hillside. *Journal of Hydrology, New Zealand*, *35*.

Woodward, S. J., Wöhling, T., & Stenger, R. (2016). Uncertainty in the modelling of spatial and temporal patterns of shallow groundwater flow paths: The role of geological and hydrological site information. *Journal of Hydrology*, *534*, 680–694. Retrieved from http://dx.doi.org/10.1016/j.jhydrol.2016.01.045 doi: 10.1016/j.jhydrol.2016.01.045

Worqlul, A. W., Ayana, E. K., Yen, H., Jeong, J., MacAlister, C., Taylor, R., ... Steenhuis, T. S. (2018). Evaluating hydrologic responses to soil characteristics using swat model in a paired-watersheds in the upper blue nile basin. *CATENA*, *163*, 332-341. Retrieved from https://www.sciencedirect.com/science/article/pii/S0341816217304423 doi: https://doi.org/10.1016/j.catena.2017.12.040

Xiong, Y., & Melching, C. S. (2005). Comparison of kinematic-wave and nonlinear reservoir routing of urban watershed runoff. *Journal of Hydrologic Engineering*, *10*(1), 39–49. Retrieved 2020-05-15, from http://ascelibrary.org/doi/10.1061/%28ASCE%291084-0699%282005%2910%3A1%2839%29 doi: 10.1061/(asce)1084-0699(2005)10:1(39)

Yen, H., Jeong, J., Tseng, W.-H., Kim, M.-K., Records, R. M., & Arabi, M. (2015). Computational procedure for evaluating sampling techniques on watershed model calibration. *Journal of Hydrologic Engineering*, *20*(7), 04014080. doi: 10.1061/(ASCE)HE.1943-5584.0001095

Yevjevich, V. (1968). Misconceptions in hydrology and their consequences. *Water Resources Research*, *4*(2), 225–232. Retrieved from https://agupubs.onlinelibrary.wiley.com/doi/abs/10.1029/WR004i002p00225 doi: 10.1029/WR004i002p00225

Zha, Y., Gao, J., & Ni, S. (2003, January). Use of normalized difference built-up index in automatically mapping urban areas from TM imagery. *International Journal of Remote Sensing*, *24*(3), 583–594. Retrieved from http://www.tandfonline.com/doi/abs/10.1080/01431160304987 doi: 10.1080/01431160304987

Zhang, K., & Chui, T. F. M. (2019). A review on implementing infiltration-based green infrastructure in shallow groundwater environments: Challenges, approaches, and progress. *Journal of Hydrology*, *579*(April), 124089. Retrieved from https://doi.org/10.1016/j.jhydrol.2019.124089 doi: 10.1016/j.jhydrol.2019.124089

Zhang, K., & Chui, T. F. M. (2020). Assessing the impact of spatial allocation of bioretention cells on shallow groundwater – an integrated surface-subsurface catchment-scale analysis with swmm-modflow. *Journal of Hydrology*, *586*(August 2019), 124910. Retrieved from https://doi.org/10.1016/j.jhydrol.2020.124910 doi: 10.1016/j.jhydrol.2020.124910

Zhang, Y., & Shuster, W. (2014). Impacts of spatial distribution of impervious areas on runoff response of hillslope catchments: Simulation study. *Journal of Hydrologic Engineering*, *19*(6), 1089–1100. Retrieved 2019-10-14, from http://ascelibrary.org/doi/10.1061/%28ASCE%29HE.1943-5584.0000905 doi: 10.1061/(asce)he.1943-5584.0000905

Zimmer, M. A., & McGlynn, B. L. (2017). Ephemeral and intermittent runoff generation processes in a low relief, highly weathered catchment. *Water Resources Research*, *53*(8), 7055–7077. doi: 10.1002/2016wr019742

Zipper, S. C., Motew, M., Booth, E. G., Chen, X., Qiu, J., Kucharik, C. J., ... Loheide, S. P. (2018). Continuous separation of land use and climate effects on the past and future water balance. *Journal of Hydrology*, *565*(May), 106–122. Retrieved from https://doi.org/10.1016/j.jhydrol.2018.08.022 doi: 10.1016/j.jhydrol.2018.08.022